

ISSN:2454-1311



International Journal of Advanced Engineering Management and Science

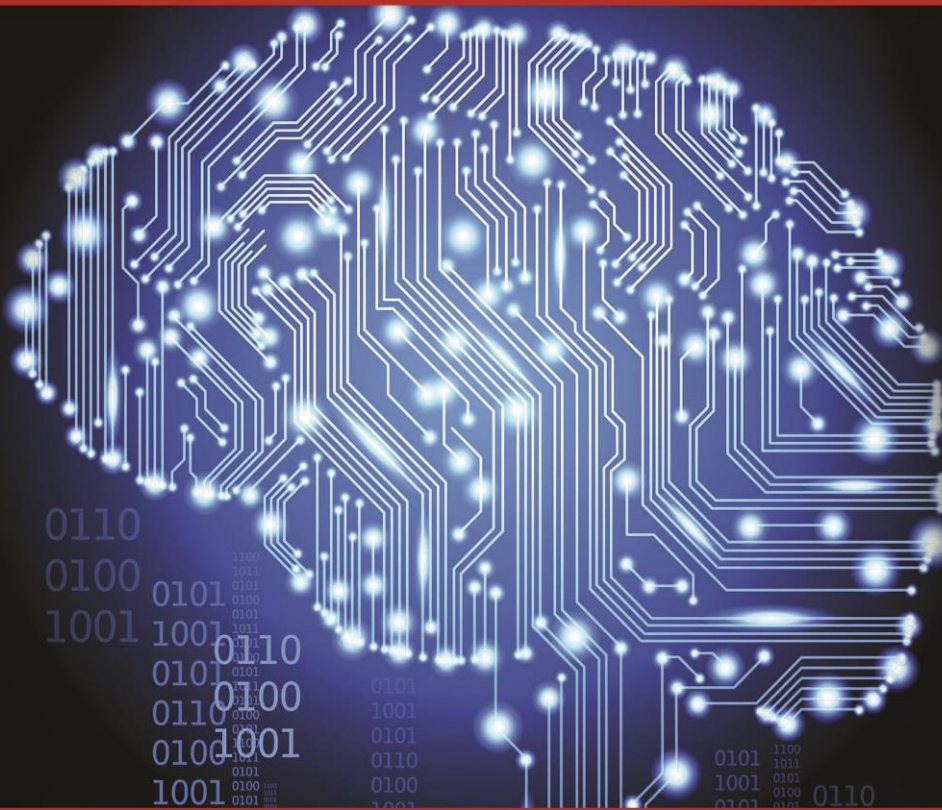
(IJAEMS)

An Open Access Peer Reviewed International Journal

Vol.-4

Issue - 1

Jan, 2018



Journal DOI: 10.24001/ijaems

Issue DOI: 10.24001/ijaems.4.1



<http://www.ijaems.com/> | editor@ijaems.com

Editorial Board

Dr. Zafer Omer Ozdemir

Energy Systems Engineering Kırklareli, Kırklareli University, Turkey

Dr. H.Saremi

Vice- chancellor For Administrative & Finance Affairs, Islamic Azad university of Iran, Quchan branch, Quchan-Iran

Dr. Ahmed Kadhim Hussein

Department of Mechanical Engineering, College of Engineering, University of Babylon, Republic of Iraq

Mohammad Reza Kabaranzad Ghadim

Associated Prof., Department of Management, Industrial Management, Central Tehran Branch, Islamic Azad University, Tehran, Iran

Prof. Ramel D. Tomaquin

Prof. 6 in the College of Business and Management, Surigao del Sur State University (SDSSU), Tandag City, Surigao Del Sur, Philippines

Dr. Ram Karan Singh

BE.(Civil Engineering), M.Tech.(Hydraulics Engineering), PhD(Hydraulics & Water Resources Engineering),BITS- Pilani, Professor, Department of Civil Engineering, King Khalid University, Saudi Arabia.

Dr. Asheesh Kumar Shah

*IIM Calcutta, Wharton School of Business, DAVV INDORE, SGSITS, Indore
Country Head at CrafsOL Technology Pvt.Ltd, Country Coordinator at French Embassy, Project Coordinator at IIT Delhi, INDIA*

Dr. Uma Choudhary

Specialization in Software Engineering Associate Professor, Department of Computer Science Mody University, Lakshmangarh, India

Dr. Ebrahim Nohani

Ph.D.(hydraulic Structures), Department of hydraulic Structures, Islamic Azad University, Dezful, IRAN.

Dr.Dinh Tran Ngoc Huy

Specialization Banking and Finance, Professor, Department Banking and Finance, Viet Nam

Dr. Shuai Li

Computer Science and Engineering, University of Cambridge, England, Great Britain

Dr. Ahmadad Nabih ZakiRashed

Specialization Optical Communication System, Professor, Department of Electronic Engineering, Menoufia University

Dr.Alok Kumar Bharadwaj

BE(AMU), ME(IIT, Roorkee), Ph.D (AMU),Professor, Department of Electrical Engineering, INDIA

Dr. M. Kannan

Specialization in Software Engineering and Data mining, Ph.D, Professor, Computer Science,SCSVMV University, Kanchipuram, India

Dr.Sambit Kumar Mishra

Specialization Database Management Systems, BE, ME, Ph.D,Professor, Computer Science Engineering Gandhi Institute for Education and Technology, Baniatangi, Khordha, India

Dr. M. Venkata Ramana

Specialization in Nano Crystal Technology, Ph.D,Professor, Physics,Andhara Pradesh, INDIA

Dr.Swapnesh Taterh

Ph.d with Specialization in Information System Security, Associate Professor, Department of Computer Science Engineering Amity University, INDIA

Dr. Rabindra Kayastha

Associate Professor, Department of Natural Sciences, School of Science, Kathmandu University, Nepal

Amir Azizi

Assistant Professor, Department of Industrial Engineering, Science and Research Branch-Islamic Azad University, Tehran, Iran

Dr. A. Heidari

Faculty of Chemistry, California South University (CSU), Irvine, California, USA

DR. C. M. Velu

Prof.& HOD, CSE, Datta Kala Group of Institutions, Pune, India

Dr. Sameh El-Sayed Mohamed Yehia

Assistant Professor, Civil Engineering(Structural), Higher Institute of Engineering -El-Shorouk Academy, Cairo, Egypt

Dr. Hou, Cheng-I

Specialization in Software Engineering, Artificial Intelligence, Wisdom Tourism, Leisure Agriculture and Farm Planning, Associate Professor, Department of Tourism and MICE, Chung Hua University, Hsinchu Taiwan

Branga Adrian Nicolae

Associate Professor, Teaching and research work in Numerical Analysis, Approximation Theory and Spline Functions, Lucian Blaga University of Sibiu, Romania

Dr. Amit Rathi

Department of ECE, SEEC, Manipal University Jaipur, Rajasthan, India

Dr. Elsanosy M. Elamin

Dept. of Electrical Engineering, Faculty of Engineering. University of Kordofan, P.O. Box: 160, Elobeid, Sudan

FOREWORD

I am pleased to put into the hands of readers Volume-4; Issue-1: Jan, 2018 of “**International Journal of Advanced Engineering, Management and Science (IJAEMS) (ISSN: 2354-1311)**”, an international journal which publishes peer reviewed quality research papers on a wide variety of topics related to Science, Technology, Management and Humanities. Looking to the keen interest shown by the authors and readers, the editorial board has decided to release print issue also, but this decision the journal issue will be available in various library also in print and online version. This will motivate authors for quick publication of their research papers. Even with these changes our objective remains the same, that is, to encourage young researchers and academicians to think innovatively and share their research findings with others for the betterment of mankind. This journal has DOI (Digital Object Identifier) also, this will improve citation of research papers.

I thank all the authors of the research papers for contributing their scholarly articles. Despite many challenges, the entire editorial board has worked tirelessly and helped me to bring out this issue of the journal well in time. They all deserve my heartfelt thanks.

Finally, I hope the readers will make good use of this valuable research material and continue to contribute their research finding for publication in this journal. Constructive comments and suggestions from our readers are welcome for further improvement of the quality and usefulness of the journal.

With warm regards.

Dr. Uma Choudhary

Editor-in-Chief

Date: Jan, 2018

Vol-4, Issue-1, January, 2018

Sr No.	Title
1	<p><u>Numerical simulation of biodiversity: comparison of changing initial conditions and fixed length of growing season</u> <i>Author: Atsu J. U., Ekaka-a E.N.</i>  DOI: 10.22161/ijaems.4.1.1</p> <p style="text-align: right;"><i>Page No: 001-003</i></p>
2	<p><u>Numerical and Statistical Quantifications of Biodiversity: Two-At-A-Time Equal Variations</u> <i>Author: Ekaka-a E.N., Osahogulu D.J., Atsu J. U., Isibor L. A.</i>  DOI: 10.22161/ijaems.4.1.2</p> <p style="text-align: right;"><i>Page No: 004-009</i></p>
3	<p><u>Modelling the effects of decreasing the inter-competition coefficients on biodiversity loss</u> <i>Author: Ekaka-a E. N., Eke Nwagrade, Atsu J. U.</i>  DOI: 10.22161/ijaems.4.1.3</p> <p style="text-align: right;"><i>Page No: 010-013</i></p>
4	<p><u>Simulation modelling of the effect of a random disturbance on biodiversity of a mathematical model of mutualism between two interacting yeast species</u> <i>Author: Eke Nwagrade, Atsu J. U., Ekaka-a E. N</i>  DOI: 10.22161/ijaems.4.1.4</p> <p style="text-align: right;"><i>Page No: 014-018</i></p>
5	<p><u>Study of a Laboratory-based Gamma Spectrometry for Food and Environmental Samples</u> <i>Author: M. N. Islam, H. Akhter, M. Begum, Y. Mawla, M. Kamal</i>  DOI: 10.22161/ijaems.4.1.5</p> <p style="text-align: right;"><i>Page No: 019-023</i></p>
6	<p><u>Deterministic Stabilization of a Dynamical System using a Computational Approach</u> <i>Author: Isobeye George, Jeremiah U. Atsu, Enu-Obari N. Ekaka-a</i>  DOI: 10.22161/ijaems.4.1.6</p> <p style="text-align: right;"><i>Page No: 024-028</i></p>
7	<p><u>Simulation modeling of the sensitivity analysis of differential effects of the intrinsic growth rate of a fish population: its implication for the selection of a local minimum</u> <i>Author: Nwachukwu Eucharia C., Ekaka-a Enu-Obari N., Atsu Jeremiah U.</i>  DOI: 10.22161/ijaems.4.1.7</p> <p style="text-align: right;"><i>Page No: 029-034</i></p>
8	<p><u>Rates of Soft Ground Tunneling in Vicinity of Existing Structures</u> <i>Author: Ayman S. Shehata, Adel M. El-Kelesh, Al-Sayed E. El-kasaby, Mustafa Mansour</i>  DOI: 10.22161/ijaems.4.1.8</p> <p style="text-align: right;"><i>Page No: 035-045</i></p>

9	<p><u>Packing Improvement by using of Quality Function Deployment Method: A Case Study in Spare Part Automotive Industry in Indonesia</u> Author: Humiras Hardi Purba, Adi Fitra , Gidionton Saritua Siagian, Widodo Dumadi  DOI: 10.22161/ijaems.4.1.9</p> <p style="text-align: right;">Page No: 046-053</p>
10	<p><u>Gravitational Model to Predict the Megalopolis Mobility of the Center of Mexico</u> Author: Juan Bacilio Guerrero Escamilla, Sócrates López Pérez, Yamile Rangel Martínez, Silvia Mendoza Mendoza  DOI: 10.22161/ijaems.4.1.10</p> <p style="text-align: right;">Page No: 054-065</p>
11	<p><u>Artificial Neural Network Controller for Reducing the Total Harmonic Distortion (THD) in HVDC</u> Author: Dr. Ali Nathem Hamoodi, Rasha Abdul-nafaa Mohammed  DOI: 10.22161/ijaems.4.1.11</p> <p style="text-align: right;">Page No: 066-073</p>
12	<p><u>Quantic Analysis of Formation of a Biomaterial of Latex, Retinol, and Chitosan for Biomedical Applications</u> Author: Karina García-Aguilar, Iliana Herrera-Cantú, Erick Pedraza-Gress, Lillhian Arely Flores-Gonzalez, Manuel Aparicio-Razo, Oscar Sánchez-Parada, Emmanuel Vázquez-López, Juan Jesús García-Mar, Manuel González-Pérez  DOI: 10.22161/ijaems.4.1.12</p> <p style="text-align: right;">Page No: 074-079</p>

Numerical simulation of biodiversity: comparison of changing initial conditions and fixed length of growing season

Atsu, J. U.¹; Ekaka-a, E.N.²

¹Department of Mathematics/Statistics, Cross River University of Technology, Calabar, Nigeria

²Department of Mathematics, Rivers State University, Nkpolu, Port – Harcourt, Nigeria

Abstract— This study examined the effect of varying the initial value of industrialization for a fixed length of growing season on the prediction of biodiversity loss. We have found that when the initial value of industrialization is 0.1 under a shorter length of growing season, a relative low due of biodiversity loss can be maintained. The biodiversity loss value can be further lowered by maintaining the same length of growing season but with a reduced initial value of industrialization to 0.01 or 0.02. We would expect this alternative result to provide a further insight into our fight against biodiversity loss which has both human and sustainable development devastating effects.

Keywords— varying initial data, industrialization, numerical simulation, growing season, quantitative technique, forestry resources biomass.

I. INTRODUCTION

The vulnerability of the forest resource biomass to the ecological risk of biodiversity loss is one of the major concerns for experts working on the mitigation measures of forest conservation and sustainable development. In order to circumvent this ongoing environmental problem, we have proposed to study the effect of the synergistic variation of the initial data value of industrialization and a fixed length of the growing season that has previously predicted a high volume of biodiversity loss. Atsu and Ekaka-a (2017) in modeling the intervention with respect to biodiversity loss, considered changing length of growing season for a forestry resource biomass. Their result showed that a longer length of growing season dominantly predicts a biodiversity gain and vice versa. Hooper et al (2012) examined a global synthesis which reveals biodiversity loss over time as a major driver of the accompanying ecosystem change. In their study, global environmental changes over time were considered with no consideration given to initial data of species resources biomass. In the same context, Isbell et al (2015) showed that biodiversity increases the resistance of ecosystem productivity to climate extremes. This was however

without recourse to the underlying factors that sustain biodiversity and even quantitatively.

Tilman et al (2014) undertook a study which showed that species diversity is a major determinant of ecosystem productivity, stability, invasibility and nutrient dynamics. This paper did not consider a quantitative technique that can be used to maintain species diversity. Aerts and Honnay (2011) did research on forest restoration, biodiversity and ecosystem function. Their result qualitatively showed that restoring multiple forest functions requires multiple species.

Naeem et al (1999) did a biological essay that suggests that biodiversity and ecosystem functioning are necessary drivers of natural life support processes. It is pertinent to point out that in all these papers, quantitative examination of the factors responsible for biodiversity richness and ecosystem functioning was left out. Reich et al (2012) showed qualitatively that the impacts of biodiversity loss escalate through time as redundancy fades but without a quantitative technique.

This research idea is therefore expected to quantitatively select the relatively best-fit initial value of industrialization that will indicate a decrease in biodiversity loss. We will use a computationally efficient numerical scheme called Ruge-Kutta ordinary differential equation of order 4-5 (ODE 45) to tackle this challenging environmental problem when the length of the growing season is five (5) months with a varying trend.

II. MATHEMATICAL FORMULATIONS

The method that we have proposed to analyse our research problem has considered the following simplifying assumptions:

- i. The growth of forestry resources biomass and human population is governed by a logistic type equation.
- ii. The growth rate of population pressure is proportional to the density of human population.
- iii. The depletion of the forestry resources is due to human population and population related activities.

Based on these simplifying assumptions the governing equations of the model according to Ramdhani, Jaharuddin & Nugrahani (2015) are defined by

$$\frac{dB}{dt} = s \left(1 - \frac{B}{L}\right) B - s_1 B - \beta_2 NB - \beta_3 B^2 I \quad (1)$$

$$\frac{dN}{dt} = r \left(1 - \frac{N}{K}\right) N - r_0 N + \beta_1 NB \quad (2)$$

$$\frac{dP}{dt} = \lambda N - \lambda_0 P - \theta I \quad (3)$$

$$\frac{dI}{dt} = \pi \theta P + \pi_1 s_1 IB - \theta_0 I \quad (4)$$

With the initial condition $B(0) \geq 0, N(0) \geq 0, P(0) \geq 0, I(0) \geq 0$ and $0 < \pi \leq 1, 0 < \pi_1 \leq 1$

In this context, B is the density of forestry resources biomass with its intrinsic growth rate coefficient s and carrying capacity L , N represents the density of the human population, P is the population pressure density while I is the density of industrialization s_0 represents the coefficient of the natural depletion rate of resources biomass, r_0 is the coefficient of natural depletion rate of human population, r is the intrinsic growth rate of population density, K represents the carrying capacity of the population density, β_1 is the growth rate of cumulative density of human population effect of resources, β_2 is the depletion rate

coefficient of the resource biomass density due to population. We recognize λ as the growth rate coefficient of population pressure while λ_0 is its natural depletion rate coefficient, θ is its depletion rate coefficient due to industrialization, s_1 is the coefficient of depletion rate of the biomass density as a result of industrialization, the combined effect of $\pi_1 s_1$ is the growth rate of industrialization due to forestry resources, π is the growth rate of industrialization effect of population pressure, θ_0 is the coefficient of control rate of industrialization which is an applied mitigation measure by government, while β_3 is the depletion rate coefficient of forestry resources biomass due to crowding by industrialization.

Analysis

Since these system of equations does not have a closed form solution, we have proposed to use an efficient numerical simulation scheme called ODE 45 numerical scheme. The parameters used in the analysis are as follows $L = 40, k = 50, \pi = 0.001, \theta = 8, \lambda = 5, \beta_1 = 0.01, \beta_2 = 7, s_0 = 1, s_1 = 4, \pi_1 = 0.005, \lambda_0 = 4, s = 34, \theta_0 = 1, r = 11, r_0 = 10$ and $\beta_3 = 2$

III. RESULTS AND DISCUSSION

Table.1: Quantifying the impact of changing initial industrial condition data on the biodiversity when the length of the growing season is 5 months.

Example	LGS(months)	I(O)	FRB _{old} (kg)	FRB _{new} (kg)	Estimated effect (%)
1	5	0.1	38.8263	36.9474	4.84
2	5	0.2	38.8263	35.9823	7.34
3	5	0.3	38.8263	35.3065	9.07
4	5	0.4	38.8263	34.7867	10.41
5	5	0.5	38.8263	34.3616	11.51
6	5	0.6	38.8263	33.9965	12.44
7	5	0.7	38.8263	33.6797	13.26
8	5	0.8	38.8263	33.3942	13.99
9	5	0.9	38.8263	33.1372	14.65
10	5	0.95	38.8263	33.0202	14.95
11	5	1.10	38.8261	32.6851	15.82
12	5	1.20	38.8311	32.4863	16.34
13	5	1.30	38.8305	32.2957	16.83
14	5	1.80	38.8306	31.4797	18.93
15	5	2.40	38.8258	30.6902	20.95
16	5	3.40	38.8316	29.6636	23.61
17	5	4.40	38.8263	28.8117	25.79
18	5	5.40	38.8262	28.0727	27.65
19	5	8.40	38.8258	26.3744	32.07
20	5	18.40	38.8267	22.8112	41.25

What do we empirically deduce from Table 1?

We can deduce that when the initial condition value of industrialization $I(0)$ is 0.1 biodiversity loss is 4.84 percent. When the initial condition value of industrialization is increased monotonically from 0.1 to 1.10, this predicts a corresponding increase in biodiversity loss value monotonically from 4.84 percent to 15.82

percent. Furthermore, an increase in the initial condition value of industrialization to a value of 18.40 dominantly predicts a high percentage of biodiversity loss (41.25%). The following mitigation measure against biodiversity loss is suggestive.

Mitigation measures

Table.2: Quantifying the impact on biodiversity loss of decreasing the initial condition value of industrialization $I(0)$ and its implication for biodiversity control.

Example	LGS(months)	I(O)	FRB _{old} (kg)	FRB _{new} (kg)	Estimated effect (%)
1	5	0.01	38.8190	38.4158	1.04
2	5	0.02	38.8196	38.1999	1.60
3	5	0.03	38.8043	38.0053	2.06
4	5	0.04	38.7840	37.8206	2.48
5	5	0.05	38.8357	37.6515	3.05
6	5	0.08	38.8317	37.2056	4.19

What do we learn from Table 2?

A relatively decreased initial condition value of industrialization has predicted a relatively weak biodiversity loss. This can be sustained by maintaining a relatively low initial condition value of industrialization which would inturn dominantly predict a high biodiversity gain. This mitigation strategy would ensure high levels of biodiversity gain.

IV. CONCLUSION

We have used the technique of a numerical simulation to quantify the impact on biodiversity of maintaining a sustainable level of industrialization. This level of industrialization if properly managed can lead to a high biodiversity gain scenario.

V. RECOMMENDATIONS

- i. For sustainable development to occur, proper levels of industrialization should be maintained relative to biodiversity requirements.
- ii. Proper monitoring of industrialization pressures should be conducted in order to maintain a proper functioning of the ecosystem which results into improved ecosystem services.
- iii. Data on industrialization, biodiversity and ecosystem services must be updated continually to keep tract of ecosystem functioning.

REFERENCES

- [1] Aerts, R. & Honnay, O. (2011). Forest restoration, biodiversity and ecosystem functioning. *PMC Ecology*, 11(29).
- [2] Atsu, J. U. & Ekaka-a, E. N. (2017). Modeling intervention with respect to biodiversity loss: A case study of forest resource biomass undergoing changing length of growing season. *International Journal of Engineering, Management and Science*, 3(9).
- [3] Hooper, D. U., Adair, E. C., Cardinale, B. J., Byrnes, J. E. K., Hungate, B. A., Matulich, K. L., Gonzalez, A., Duffy, J. E., Gamfeldt, L. & O'Connor, M. I. (2012). *Nature*. 486: 105 – 108.
- [4] Isbell, F., Craven, D., Conolly, J., Loreau, M., Schmid, B., Beierkuhnlein, C., Bezener, T.M., Bonin, C., Bruelheide, H., DeLuca, E., Ebeling, A., Griffin, J.N., Guo, Q., Hautier, Y., Hector, A., Jentsch, A., Kreyling, J., Lanta, V. Manning, P. Mayer, S. T., Mori, A. S., Naeem, S., Niklaus, P. A., Polley, H. W. & Reich, P. B. (2015). *Nature*, 526: 514 – 577.
- [5] Naeem, S.; Chair, F. S., Chapin, III, Constanza, R.; Ehrlich, P.R., Golley, F. B., Hooper, D. U., Lawton, J. H. O'Neill, R. V., Mooney, H. A., Sala, O. E. Symstad, A. J. & Tilman, D. (1999). Biodiversity and ecosystem functioning: Maintaining Natural life support processes. *Issues in Ecology*. Number 4.
- [6] Ramdhani, V.; Jaharuddin & Nugrahani, E. H. (2015). Dynamical system of modeling the depletion of forestry resources due to crowding by industrialization. *Applied Mathematical Science*, 9(82): 4067 – 4079.
- [7] Reich, P.B., Tilman, D.U. Isbell, F., Mueller, K., Habbie, S. E., Flynn, D. F. B. & Eisenhauer, N. (2012). Impacts of biodiversity loss escalate through time as redundancy fades. *Science*, 336: Issues 589.
- [8] Tilman, D., Isbell, F. & Cowles, J. M. (2014). Biodiversity and ecosystem functioning. *Annual Review of Ecology, Evolution and Systematics*, 45: 471 – 493.

Numerical and Statistical Quantifications of Biodiversity: Two-At-A-Time Equal Variations

Ekaka-a E.N.^{1*}, Osahogulu D.J.², Atsu J. U.^{3*}, Isibor L. A.²

¹Department of Mathematics Rivers State University, Nkpolu, Port Harcourt, Nigeria

²Department of Mathematics/Statistics, Ignatius Ajuru University of Education, Rumuolumeni, Port Harcourt, Nigeria

³Department of Mathematics/Statistics, Cross River State University of Technology, Calabar, Nigeria

Abstract— The ecological concept of biodiversity is a challenging environmental problem that requires a sound mathematical reasoning. We have used the method of a numerical simulation that is indexed by a numerical scheme to predict biodiversity loss and biodiversity gain due to a decreasing and increasing variations of the intrinsic growth rates together. The novel results that we have obtained that we have not seen elsewhere, but do complement other similar numerical predictions of biodiversity are presented and discussed quantitatively.

Keywords— Ecological concept, environmental problem, biodiversity, numerical simulation, intrinsic growth rate, ecosystem stability.

I. INTRODUCTION

The ongoing debate between biodiversity, ecosystem stability, and its implications, Atsu and Ekaka-a (2017)¹ makes it imperative to examine the effects of varying the intrinsic growth rates together on biodiversity loss and biodiversity gain by using a computationally efficient numerical scheme called Matlab function ordinary differential equation of order 45 (ODE 45). Other related contributions on the link between biodiversity and ecosystem stability have been adequately sighted. ([2] – [26]).

II. MATERIALS AND METHODS

If a variation of a model parameter value produces a new biomass which is smaller than the old biomass for any interacting legumes, such as cowpea and groundnut, then a biodiversity loss has occurred and can be quantified as we have done in this study.

On the other hand, if a variation of a model parameter value produces a new biomass which outweighs the old biomass irrespective of the type of legumes, then a biodiversity gain has occurred and can be similarly quantified.

Following Ekaka-a et al (2009), we have considered the following continuous dynamical system of nonlinear first order ordinary differential equation

$$\frac{dC(t)}{dt} = \alpha_1 C(t) - \beta_1 C^2(t) - r_1 C(t)G(t)$$

$$\frac{dG(t)}{dt} = \alpha_2 G(t) - \beta_2 G^2(t) - r_2 C(t)G(t)$$

With $C(0) = 0.12$ and $G(0) = 0.14$

For the purpose of clarity, the variables and the parameter values for these model equations are defined as follows

- $C_b(t)$ and $G_b(t)$ are called the biomass of cowpea and groundnut at time (t) in the unit of weeks
- α_1 and α_2 are called the intrinsic growth rates for populations $C_b(t)$ and $G_b(t)$ in the absence of self-interaction and inter-competition interaction
- β_1 and β_2 are called the intra-competition coefficients
- r_1 and r_2 are called the inter-competition coefficients to analyze our propose problem,

$\alpha_1 = 0.0225, \alpha_2 = 0.0446; \beta_1 = 0.0069, \beta_2 = 0.0133; r_1 = 0.0018, r_2 = 0.0012.$

The core numerical method that we have used in this present analysis is called ODE 45.

III. RESULTS AND DISCUSSIONS

The results of this study are displayed and discussed quantitatively in Tables 1.1, 1.2, 1.3, 1.4, 1.5, 2.1, 2.2, 2.3, 2.4 and 2.5.

Table.1.1: Evaluating the effect of varying the intrinsic growth rates together by 10% on biodiversity loss using ODE 45 numerical scheme.

$C_b(t)$	$C_{bm}(t)$	BL(%)	$G_b(t)$	$G_{bm}(t)$	BL(%)
0.1200	0.1200	0	0.1200	0.1200	0
0.1226	0.1201	2.0034	0.1253	0.1203	3.9312
0.1253	0.1203	3.9641	0.1307	0.1207	7.7015
0.1280	0.1204	5.8831	0.1364	0.1210	11.3173
0.1307	0.1206	7.7611	0.1424	0.1213	14.7850
0.1335	0.1207	9.5991	0.1485	0.1216	18.1105
0.1364	0.1209	11.3979	0.1550	0.1220	21.2998
0.1393	0.1210	13.1582	0.1617	0.1223	24.3584
0.1423	0.1212	14.8809	0.1686	0.1226	27.2915

0.1454	0.1213	16.5668	0.1759	0.1230	30.1044
0.1485	0.1214	18.2166	0.1835	0.1233	32.8018
0.1517	0.1216	19.8310	0.1913	0.1236	35.3886
0.1549	0.1217	21.4108	0.1995	0.1239	37.8693
0.1582	0.1219	22.9568	0.2080	0.1243	40.2481
0.1616	0.1220	24.4695	0.2168	0.1246	42.5293
0.1650	0.1222	25.9497	0.2260	0.1249	44.7168
0.1685	0.1223	27.3980	0.2355	0.1253	46.8144
0.1720	0.1225	28.8152	0.2454	0.1256	48.8258
0.1757	0.1226	30.2018	0.2557	0.1259	50.7546
0.1793	0.1227	31.5585	0.2664	0.1263	52.6041

0.1485	0.1228	17.2972	0.1835	0.1260	31.2995
0.1517	0.1231	18.8398	0.1913	0.1267	33.7993
0.1549	0.1234	20.3509	0.1995	0.1273	36.2017
0.1582	0.1237	21.8312	0.2080	0.1279	38.5104
0.1616	0.1239	23.2813	0.2168	0.1285	40.7289
0.1650	0.1242	24.7017	0.2260	0.1291	42.8609
0.1685	0.1245	26.0930	0.2355	0.1298	44.9095
0.1720	0.1248	27.4558	0.2454	0.1304	46.8781
0.1757	0.1251	28.7906	0.2557	0.1310	48.7696
0.1793	0.1254	30.0981	0.2664	0.1316	50.5872

From Table 1.1, when all the model parameter values are fixed, the cowpea biomass data denoted $C_b(t)$ when the length of the growing season is twenty one weeks range from a low value of 0.12grams/area to 0.1793grams/area whereas $C_{bm}(t)$ data range from a low value 0.12 grams/area to 0.1227 grams/area due to a 10% variation of the intrinsic growth rates together. On the basis of this calculation, the new simulated cowpea data due to a joint variation of the intrinsic growth rates dominantly predicts a depletion which mimics biodiversity loss. The extent of biodiversity loss has been quantified to range from zero to 31.6 approximately providing an average of 16.8 which re-classifies the vulnerability of the cowpea biomass to biodiversity loss. A similar observation can be made from the groundnut biomass component. In summary, the groundnut biomass is about 1.67 approximately more vulnerable to biodiversity loss than the cowpea biomass. Statistically, the average of biomass vulnerability to biodiversity loss with respect to the groundnut legume is 29.57% approximately.

From Table 1.2, when all the model parameter values are fixed, the cowpea biomass data denoted $C_b(t)$ when the length of the growing season is twenty one weeks range from a low value of 0.12 grams/area to 0.1793 grams/area whereas $C_{bm}(t)$ data range from a low value 0.12 grams/area to 0.1254 grams/area due to a 15% variation of the intrinsic growth rates together. On the basis of this calculation, the new simulated cowpea data due to a joint variation of the intrinsic growth rates dominantly predicts a depletion which mimics biodiversity loss. The extent of biodiversity loss has been quantified to range from zero to 30.1 approximately providing an average of 15.97 which re-classifies the vulnerability of the cowpea biomass to biodiversity loss. A similar observation can be made from the groundnut biomass component. In summary, the groundnut biomass is about 1.68 approximately more vulnerable to biodiversity loss than the cowpea biomass. Statistically, the average of biomass vulnerability to biodiversity loss with respect to the groundnut legume is 28.28% approximately.

Table.1.2: Evaluating the effect of varying the intrinsic growth rates together by 15% on biodiversity loss using ODE 45 numerical scheme.

$C_b(t)$	$C_{bm}(t)$	BL(%)	$G_b(t)$	$G_{bm}(t)$	BL(%)
0.1200	0.1200	0	0.1200	0.1200	0
0.1226	0.1203	1.8931	0.1253	0.1206	3.7169
0.1253	0.1206	3.7480	0.1307	0.1212	7.2896
0.1280	0.1208	5.5655	0.1364	0.1218	10.7235
0.1307	0.1211	7.3462	0.1424	0.1224	14.0240
0.1335	0.1214	9.0908	0.1485	0.1230	17.1963
0.1364	0.1217	10.8001	0.1550	0.1236	20.2451
0.1393	0.1220	12.4747	0.1617	0.1242	23.1754
0.1423	0.1222	14.1153	0.1686	0.1248	25.9917
0.1454	0.1225	15.7226	0.1759	0.1254	28.6983

Table.1.3: Evaluating the effect of varying the intrinsic growth rates together by 20% on biodiversity loss using ODE 45 numerical scheme.

$C_b(t)$	$C_{bm}(t)$	BL(%)	$G_b(t)$	$G_{bm}(t)$	BL(%)
0.1200	0.1200	0	0.1200	0.1200	0
0.1226	0.1204	1.7828	0.1253	0.1209	3.5022
0.1253	0.1208	3.5315	0.1307	0.1217	6.8759
0.1280	0.1212	5.2468	0.1364	0.1226	10.1258
0.1307	0.1217	6.9293	0.1424	0.1235	13.2563
0.1335	0.1221	8.5796	0.1485	0.1244	16.2718
0.1364	0.1225	10.1982	0.1550	0.1253	19.1764
0.1393	0.1229	11.7858	0.1617	0.1261	21.9741
0.1423	0.1233	13.3429	0.1686	0.1270	24.6688
0.1454	0.1238	14.8699	0.1759	0.1279	27.2641
0.1485	0.1242	16.3676	0.1835	0.1289	29.7638

0.1517	0.1246	17.8364	0.1913	0.1298	32.1712
0.1549	0.1250	19.2768	0.1995	0.1307	34.4897
0.1582	0.1255	20.6893	0.2080	0.1316	36.7225
0.1616	0.1259	22.0745	0.2168	0.1325	38.8727
0.1650	0.1263	23.4328	0.2260	0.1335	40.9432
0.1685	0.1267	24.7647	0.2355	0.1344	42.9371
0.1720	0.1272	26.0707	0.2454	0.1353	44.8570
0.1757	0.1276	27.3513	0.2557	0.1363	46.7055
0.1793	0.1280	28.6068	0.2664	0.1372	48.4854

0.1582	0.1273	19.5309	0.2080	0.1354	34.8830
0.1616	0.1279	20.8489	0.2168	0.1367	36.9588
0.1650	0.1284	22.1427	0.2260	0.1379	38.9619
0.1685	0.1290	23.4128	0.2355	0.1392	40.8947
0.1720	0.1296	24.6594	0.2454	0.1405	42.7597
0.1757	0.1302	25.8831	0.2557	0.1418	44.5592
0.1793	0.1308	27.0841	0.2664	0.1431	46.2954

Table.1.5: Evaluating the effect of varying the intrinsic growth rates together by 95% on biodiversity loss using ODE 45 numerical scheme.

From Table 1.3, when all the model parameter values are fixed, the cowpea biomass data $C_b(t)$ when the length of the growing season is twenty one weeks range from a low value of 0.12 grams/area to 0.1793 grams/area whereas $C_{bm}(t)$ data range from a low value 0.12 grams/area to 0.1280 grams/area due to a 20% variation of the intrinsic growth rates together. On the basis of this calculation, the new simulated cowpea data due to a joint variation of the intrinsic growth rates dominantly predicts a depletion which mimics biodiversity loss. The extent of biodiversity loss has been quantified to range from zero to 28.6 approximately providing an average of 15.14 which re-classifies the vulnerability of the cowpea biomass to biodiversity loss. A similar observation can be made from the groundnut biomass component. In summary, the groundnut biomass is about 1.69 approximately more vulnerable to biodiversity loss than the cowpea biomass. Statistically, the average of biomass vulnerability to biodiversity loss with respect to the groundnut legume is 26.95% approximately.

$C_b(t)$	$C_{bm}(t)BL(\%)$	$G_b(t)$	$G_{bm}(t)$	BL(%)	
0.1200	0.1200	0	0.1200	0.1200	0
0.1226	0.1225	0.1124	0.1253	0.1250	0.2226
0.1253	0.1250	0.2245	0.1307	0.1301	0.4442
0.1280	0.1275	0.3363	0.1364	0.1355	0.6650
0.1307	0.1301	0.4478	0.1424	0.1411	0.8847
0.1335	0.1328	0.5590	0.1485	0.1469	1.1035
0.1364	0.1355	0.6699	0.1550	0.1529	1.3213
0.1393	0.1383	0.7805	0.1617	0.1592	1.5381
0.1423	0.1411	0.8908	0.1686	0.1657	1.7537
0.1454	0.1439	1.0007	0.1759	0.1724	1.9682
0.1485	0.1468	1.1103	0.1835	0.1795	2.1815
0.1517	0.1498	1.2195	0.1913	0.1867	2.3936
0.1549	0.1528	1.3284	0.1995	0.1943	2.6045
0.1582	0.1559	1.4369	0.2080	0.2021	2.8141
0.1616	0.1591	1.5450	0.2168	0.2103	3.0223
0.1650	0.1623	1.6527	0.2260	0.2187	3.2291
0.1685	0.1655	1.7600	0.2355	0.2274	3.4344
0.1720	0.1688	1.8668	0.2454	0.2365	3.6383
0.1757	0.1722	1.9733	0.2557	0.2459	3.8406
0.1793	0.1756	2.0792	0.2664	0.2556	4.0412

Table.1.4: Evaluating the effect of varying the intrinsic growth rates together by 25% on biodiversity loss using ODE 45 numerical scheme.

$C_b(t)$	$C_{bm}(t)BL(\%)$	$G_b(t)$	$G_{bm}(t)$	BL(%)	
0.1200	0.1200	0	0.1200	0.1200	0
0.1226	0.1206	1.6723	0.1253	0.1211	3.2869
0.1253	0.1211	3.3145	0.1307	0.1223	6.4603
0.1280	0.1217	4.9271	0.1364	0.1234	9.5240
0.1307	0.1222	6.5106	0.1424	0.1246	12.4818
0.1335	0.1228	8.0656	0.1485	0.1258	15.3370
0.1364	0.1233	9.5924	0.1550	0.1269	18.0933
0.1393	0.1239	11.0915	0.1617	0.1281	20.7540
0.1423	0.1245	12.5635	0.1686	0.1293	23.3223
0.1454	0.1250	14.0087	0.1759	0.1305	25.8013
0.1485	0.1256	15.4276	0.1835	0.1317	28.1940
0.1517	0.1262	16.8207	0.1913	0.1330	30.5033
0.1549	0.1267	18.1883	0.1995	0.1342	32.7321

Table.2.1: Evaluating the effect of varying the intrinsic growth rates together by 105% on biodiversity gain using ODE 45 numerical scheme.

$C_b(t)$	$C_{bm}(t)BG(\%)$	$G_b(t)$	$G_{bm}(t)$	BG(%)	
0.1200	0.1200	0	0.1200	0.1200	0
0.1226	0.1227	0.1125	0.1253	0.1255	0.2231
0.1253	0.1255	0.2250	0.1307	0.1313	0.4462
0.1280	0.1284	0.3374	0.1364	0.1373	0.6694
0.1307	0.1313	0.4498	0.1424	0.1436	0.8926
0.1335	0.1343	0.5621	0.1485	0.1502	1.1158
0.1364	0.1373	0.6744	0.1550	0.1570	1.3389

0.1393	0.1404	0.7866	0.1617	0.1642	1.5620
0.1423	0.1436	0.8987	0.1686	0.1717	1.7848
0.1454	0.1469	1.0108	0.1759	0.1794	2.0074
0.1485	0.1502	1.1227	0.1835	0.1875	2.2298
0.1517	0.1535	1.2345	0.1913	0.1960	2.4518
0.1549	0.1570	1.3461	0.1995	0.2048	2.6735
0.1582	0.1605	1.4576	0.2080	0.2140	2.8947
0.1616	0.1641	1.5690	0.2168	0.2236	3.1153
0.1650	0.1678	1.6801	0.2260	0.2335	3.3354
0.1685	0.1715	1.7911	0.2355	0.2439	3.5548
0.1720	0.1753	1.9018	0.2454	0.2547	3.7734
0.1757	0.1792	2.0124	0.2557	0.2659	3.9912
0.1793	0.1832	2.1226	0.2664	0.2776	4.2080

Table.2.2: Evaluating the effect of varying the intrinsic growth rates together by 110% on biodiversity gain using ODE 45 numerical scheme.

C _b (t)	C _{bm} (t)BG(%)	G _b (t)	G _{bm} (t)	BG(%)	
0.1200	0.1200	0	0.1200	0.1200	0
0.1226	0.1229	0.2251	0.1253	0.1258	0.4466
0.1253	0.1258	0.4504	0.1307	0.1319	0.8944
0.1280	0.1288	0.6759	0.1364	0.1383	1.3433
0.1307	0.1319	0.9016	0.1424	0.1449	1.7932
0.1335	0.1350	1.1274	0.1485	0.1519	2.2441
0.1364	0.1383	1.3533	0.1550	0.1592	2.6958
0.1393	0.1415	1.5794	0.1617	0.1668	3.1482
0.1423	0.1449	1.8055	0.1686	0.1747	3.6013
0.1454	0.1483	2.0317	0.1759	0.1830	4.0549
0.1485	0.1518	2.2578	0.1835	0.1917	4.5089
0.1517	0.1554	2.4840	0.1913	0.2008	4.9632
0.1549	0.1591	2.7102	0.1995	0.2103	5.4177
0.1582	0.1628	2.9363	0.2080	0.2202	5.8722
0.1616	0.1667	3.1623	0.2168	0.2305	6.3265
0.1650	0.1706	3.3881	0.2260	0.2413	6.7804
0.1685	0.1746	3.6138	0.2355	0.2526	7.2339
0.1720	0.1786	3.8393	0.2454	0.2643	7.6867
0.1757	0.1828	4.0646	0.2557	0.2765	8.1387
0.1793	0.1870	4.2895	0.2664	0.2893	8.5895

Table.2.3: Evaluating the effect of varying the intrinsic growth rates together by 115% on biodiversity gain using ODE 45 numerical scheme.

C _b (t)	C _{bm} (t)BG(%)	G _b (t)	G _{bm} (t)	BG(%)	
0.1200	0.1200	0	0.1200	0.1200	0
0.1226	0.1230	0.3379	0.1253	0.1261	0.6707
0.1253	0.1261	0.6764	0.1307	0.1325	1.3446
0.1280	0.1293	1.0156	0.1364	0.1392	2.0217
0.1307	0.1325	1.3554	0.1424	0.1462	2.7018
0.1335	0.1358	1.6959	0.1485	0.1536	3.3848
0.1364	0.1392	2.0368	0.1550	0.1613	4.0707
0.1393	0.1427	2.3784	0.1617	0.1694	4.7591
0.1423	0.1462	2.7204	0.1686	0.1778	5.4500
0.1454	0.1498	3.0628	0.1759	0.1867	6.1432
0.1485	0.1536	3.4057	0.1835	0.1960	6.8385
0.1517	0.1574	3.7489	0.1913	0.2057	7.5357
0.1549	0.1612	4.0924	0.1995	0.2159	8.2345
0.1582	0.1652	4.4362	0.2080	0.2266	8.9348
0.1616	0.1693	4.7803	0.2168	0.2377	9.6363
0.1650	0.1734	5.1244	0.2260	0.2494	10.3387
0.1685	0.1777	5.4687	0.2355	0.2615	11.0417
0.1720	0.1820	5.8130	0.2454	0.2743	11.7451
0.1757	0.1865	6.1573	0.2557	0.2875	12.4484
0.1793	0.1910	6.5016	0.2664	0.3014	13.1514

Table.2.4: Evaluating the effect of varying the intrinsic growth rates together by 120% on biodiversity gain using ODE 45 numerical scheme.

C _b (t)	C _{bm} (t)BG(%)	G _b (t)	G _{bm} (t)	BG(%)	
0.1200	0.1200	0	0.1200	0.1200	0
0.1226	0.1232	0.4507	0.1253	0.1264	0.8952
0.1253	0.1264	0.9029	0.1307	0.1331	1.7968
0.1280	0.1297	1.3564	0.1364	0.1401	2.7046
0.1307	0.1331	1.8113	0.1424	0.1475	3.6185
0.1335	0.1366	2.2675	0.1485	0.1553	4.5383
0.1364	0.1401	2.7249	0.1550	0.1634	5.4639
0.1393	0.1438	3.1836	0.1617	0.1720	6.3950
0.1423	0.1475	3.6434	0.1686	0.1810	7.3315
0.1454	0.1514	4.1043	0.1759	0.1905	8.2731
0.1485	0.1553	4.5663	0.1835	0.2004	9.2195
0.1517	0.1593	5.0292	0.1913	0.2108	10.1706
0.1549	0.1634	5.4931	0.1995	0.2217	11.1258
0.1582	0.1676	5.9578	0.2080	0.2331	12.0850
0.1616	0.1719	6.4233	0.2168	0.2451	13.0478

0.1650	0.1763	6.8895	0.2260	0.2577	14.0138
0.1685	0.1809	7.3564	0.2355	0.2708	14.9825
0.1720	0.1855	7.8237	0.2454	0.2846	15.9536
0.1757	0.1902	8.2915	0.2557	0.2990	16.9265
0.1793	0.1951	8.7597	0.2664	0.3141	17.9007

Table.2.5: Evaluating the effect of varying the intrinsic growth rates together by 125% on biodiversity gain using ODE 45 numerical scheme.

C _b (t)	C _{bm} (t)	BG(%)	G _b (t)	G _{bm} (t)	BG(%)
0.1200	0.1200	0	0.1200	0.1200	0
0.1226	0.1233	0.5637	0.1253	0.1267	1.1203
0.1253	0.1267	1.1299	0.1307	0.1337	2.2510
0.1280	0.1301	1.6984	0.1364	0.1410	3.3921
0.1307	0.1337	2.2692	0.1424	0.1488	4.5433
0.1335	0.1373	2.8423	0.1485	0.1570	5.7046
0.1364	0.1411	3.4176	0.1550	0.1656	6.8757
0.1393	0.1449	3.9951	0.1617	0.1747	8.0564
0.1423	0.1488	4.5747	0.1686	0.1842	9.2464
0.1454	0.1529	5.1563	0.1759	0.1943	10.4454
0.1485	0.1570	5.7398	0.1835	0.2048	11.6532
0.1517	0.1613	6.3253	0.1913	0.2159	12.8694
0.1549	0.1656	6.9125	0.1995	0.2276	14.0935
0.1582	0.1701	7.5014	0.2080	0.2399	15.3253
0.1616	0.1746	8.0919	0.2168	0.2527	16.5641
0.1650	0.1793	8.6839	0.2260	0.2662	17.8095
0.1685	0.1841	9.2773	0.2355	0.2804	19.0609
0.1720	0.1890	9.8720	0.2454	0.2953	20.3177
0.1757	0.1940	10.4678	0.2557	0.3109	21.5792
0.1793	0.1992	11.0647	0.2664	0.3273	22.8448

Statistical measure by Table	BL ₁ (Average)	BL ₂ (Average)
Table 1.1	16.801	29.5726
Table 1.2	15.9748	28.2803
Table 1.3	15.1369	26.9532
Table 1.4	14.2872	25.5902
Table 1.5	1.0497	2.0550
Statistical measure by Table	BG ₁ (Average)	BG ₁ (Average)
Table 2.1	1.0648	2.1134
Table 2.2	2.1448	4.2870
Table 2.3	3.2404	6.5226
Table 2.4	4.3518	8.8221
Table 2.5	5.4792	11.1876

IV. CONCLUSION

By using ODE 45 we have found out that a biodiversity loss can be obtained due to a decreasing variation of the intrinsic growth rates together, whereas a dominant biodiversity gain can be obtained due to an increasing variation of the intrinsic growth rates together. On the basis of this analysis, the decreasing variation of the intrinsic growth rates together has generally indicated a decrease in the yields of these two crops, whereas an increasing variation of the same parameter values has indicated an improvement in the yields of both cowpea and groundnut. In this context, an alarming rate of biodiversity loss of these quantified magnitude are a strong signal on lower food production, endemic poverty and a weak sustainable development scenario, whereas a biodiversity gain has the potential to alleviate poverty and sustain development. These two components of biodiversity as predicted in this work have their policy implications.

This present numerical idea can be extended to examine the effects of varying the intra and inter competition coefficients together in our future investigation.

REFERENCES

- [1] Atsu, J. U. & Ekaka-a, E. N. (2017). Modeling the policy implications of biodiversity loss: A case study of the Cross River national park, south – south Nigeria. International Journal of Pure and Applied Science, Cambridge Research and Publications. vol 10 No. 1; pp 30-37.
- [2] Atsu, J. U. & Ekaka-a, E. N. (2017). Quantifying the impact of changing intrinsic growth rate on the biodiversity of the forest resource biomass: implications for the Cross River State forest resource at the Cross River National Park, South – South, Nigeria: African Scholar Journal of Pure and Applied Science, 7(1); 117 – 130.
- [3] De Mazancourt, C., Isbell, F., Larocque, A., Berendse, F., De Luca, E., Grace, J.B et al. (2013). Predicting ecosystem stability from community composition and biodiversity. Ecology Letters,, DOI: 10.1111/ele.12088.
- [4] Doak, D.F., Bigger, D., Harding, E.K., Marvier, M.A., O’Malley, R.E. & Thomson, D. (1998). The statistical inevitability of stability-diversity relationships in community ecology. Am. Nat., 151, 264–276.
- [5] Ernest, S.K.M. & Brown, J.H. (2001). Homeostasis and compensation: the role of species and resources in ecosystem stability. Ecology, 82, 2118–2132. Fowler, M.S. (2009). Increasing community size and connectance can increase stability in competitive communities. J. Theor. Biol., 258, 179–188.
- [6] Fowler, M.S., Laakso, J., Kaitala, V., Ruokolainen, L. & Ranta, E. (2012). Species dynamics alter community

- diversity-biomass stability relationships. *Ecol. Lett.*, 15, 1387–1396.
- [7] Gonzalez, A. & Descamps-Julien, B. (2004). Population and community variability in randomly fluctuating environments. *Oikos*, 106, 105–116.
- [8] Gonzalez, A. & Loreau, M. (2009). The causes and consequences of compensatory dynamics in ecological communities. *Annu. Rev. Ecol. Evol. Syst.*, 40, 393–414.
- [9] Grman, E., Lau, J.A., Donald, R., Schoolmaster, J. & Gross, K.L. (2010). Mechanisms contributing to stability in ecosystem function depend on the environmental context. *Ecol. Lett.*, 13, 1400–1410.
- [10] Hector, A., Hautier, Y., Saner, P., Wacker, L., Bagchi, R., Joshi, J. et al. (2010). General stabilizing effects of plant diversity on grassland productivity through population asynchrony and over yielding. *Ecology*, 91, 2213–2220.
- [11] Loreau, M. & de Mazancourt, C. (2013). Biodiversity and ecosystem stability: a synthesis of underlying mechanisms. *Ecol. Lett.*, DOI: 10.1111/ele.12073.
- [12] Loreau, M. & Hector, A. (2001). Partitioning selection and complementarity in biodiversity experiments. *Nature*, 412, 72–76.
- [13] MacArthur, R. (1955). Fluctuations of Animal Populations, and a Measure of Community Stability. *Ecology*, 36, 533–536.
- [14] Marquard, E., Weigelt, A., Roscher, C., Gubsch, M., Lipowsky, A. & Schmid, B. (2009). Positive biodiversity-productivity relationship due to increased plant density. *J. Ecol.*, 97, 696–704.
- [15] May, R.M. (1973). Stability and complexity in model ecosystems. 2001, Princeton Landmarks in Biology edn. Princeton University Press, Princeton. McCann, K.S. (2000). The diversity-stability debate. *Nature*, 405, 228–233.
- [16] McNaughton, S.J. (1977). Diversity and stability of ecological communities: a comment on the role of empiricism in ecology. *Am. Nat.*, 111, 515–525.
- [17] Mutshinda, C.M., O'Hara, R.B. & Woivod, I.P. (2009). What drives community dynamics? *Proc. Biol. Sci.*, 276, 2923–2929.
- [18] Proulx, R., Wirth, C., Voigt, W., Weigelt, A., Roscher, C., Attinger, S. et al. (2010). Diversity Promotes Temporal Stability across Levels of Ecosystem Organization in Experimental Grasslands. *PLoS ONE*, 5, e13382.
- [19] Roscher, C., Weigelt, A., Proulx, R., Marquard, E., Schumacher, J., Weisser, W.W. et al. (2011). Identifying population- and community-level mechanisms of diversity–stability relationships in experimental grasslands. *J. Ecol.*, 99, 1460–1469.
- [20] Van Ruijven, J. & Berendse, F. (2007). Contrasting effects of diversity on the temporal stability of plant populations. *Oikos*, 116, 1323–1330.
- [21] Solomon, S., D. Qin, M. Manning, Z. Chen, M. Marquis, K.B. Averyt, M. Tignor and H.L. Miller (eds.). Cambridge University Press, Cambridge, United Kingdom and New York, NY, USA, 996pp.
- [22] Rahmstorf, S., Cazenave, A., Church, J.A., Hansen, J.E., Keeling, R.F., Parker, D.E., and R.C.J. Somerville, 2007: Recent climate observations compared to projections. *Science* 316 (5825):709-709.
- [23] Domingues, C.M, Church, J.A., White, N.J., Gleckler, P.J, Wijffels, S.E., Barker, P.M. and J.R.Dunn, 2008: Improved estimates of upper-ocean warming and multi-decadal sea-level rise. *Nature* 453:1090-1094.

Modelling the effects of decreasing the inter-competition coefficients on biodiversity loss

Ekaka-a, E. N.¹; Eke, Nwagrade²; Atsu, J. U.³

¹Department of Mathematics, Rivers State University Nkporlu–Oroworukwo, Port Harcourt, Rivers State

²Department of Mathematics/Statistics, Ignatius Ajuru University of Education, Port Harcourt, Rivers State

³Department of Mathematics/Statistics, Cross River University of Technology, Calabar, Nigeria.

Abstract— The notion of a biodiversity loss has been identified as a major devastating biological phenomenon which needs to be mitigated against. In the short term, we have utilised a Matlab numerical scheme to quantify the effects of decreasing and increasing the inter – competition coefficients on biodiversity loss and biodiversity gain. On the simplifying assumption of a fixed initial condition(4, 10), two enhancing factors of intrinsic growth rates, two inhibiting growth rates of intra – competition coefficients and two inhibiting growth rates of inter – competition coefficients. The novel results that we have obtained; which we have not seen elsewhere complement our recent contribution to knowledge in the context of applying a numerical scheme to predict both biodiversity loss and biodiversity gain.

Keywords— Competition coefficients, biodiversity loss, biodiversity gain, numerical scheme, initial condition, intrinsic growth rate.

I. INTRODUCTION

Following the recent application of a numerical simulation to model biodiversity (Atsu and Ekaka-a 2017), we have come to observe that the mathematical technique of a numerical simulation which is rarely been applied to interpret the extent of biodiversity loss and biodiversity gain is an important short term and long term quantitative scientific process. We will expect the application of a numerical simulation to model biodiversity to contribute to other previous research outputs.

II. MATERIALS AND METHODS

The core method of ODE 45 numerical scheme has been coded to analyze a Lotka – Volterra mathematical structure dynamical system of non – linear first order differential equation with the following parameter values: The intrinsic growth rate of the first species is estimated to be 0.1; the intrinsic growth rate of the second yeast species is estimated to be 0.08; the intra – competition coefficients due to the self-interaction between the first yeast species and itself is estimated to be 0.0014; the intra – competition coefficients due to the self-interaction between the second yeast species and itself is estimated to be 0.001; the intra – competition coefficients which is another set of inhibiting factors are estimated to be 0.0012 and 0.0009 respectively. The aim of this present analysis is to vary the inter – competition coefficient together and quantify the effect of this variation on biodiversity loss and biodiversity gain in which the initial condition is specified by (4,10) for a shorter length of growing season of twenty (20) days

III. RESULTS

The results of these numerical simulation analyses are presented in Table 1, Table 2, and Table 3

IV. DISCUSSION OF RESULTS

The results are presented and discussed as follows.

Table.1: Evaluating the effect of $r_1 = 0.00012$ and $r_2 = 0.00009$ together on $x(t)$ and $y(t)$ using ODE 45 numerical scheme

Example	$x(t)$	$x_m(t)$	BL(%)	$y(t)$	$y_m(t)$	BL(%)
1	4.0000	4.0000	0	10.0000	10.0000	0
2	4.4497	4.4003	1.1113	10.7618	10.7253	0.3398
3	4.9514	4.8381	2.2864	11.5776	11.4950	0.7130
4	5.5111	5.3167	3.5262	12.4505	12.3107	1.1229
5	6.1356	5.8391	4.8318	13.3844	13.1739	1.5728
6	6.8325	6.4086	6.2034	14.3829	14.0857	2.0663
7	7.6102	7.0287	7.6410	15.4502	15.0473	2.6074
8	8.4778	7.7026	9.1439	16.5906	16.0597	3.2001

Example	$x(t)$	$x_m(t)$	BL(%)	$y(t)$	$y_m(t)$	BL(%)
9	9.4456	8.4339	10.7107	17.8090	17.1235	3.8490
10	10.5247	9.2260	12.3396	19.1103	18.2391	4.5587
11	11.7273	10.0822	14.0278	20.5002	19.4067	5.3340
12	13.0666	11.0058	15.7718	21.9847	20.6261	6.1799
13	14.5569	11.9997	17.5674	23.5705	21.8966	7.1015
14	16.2134	13.0664	19.4097	25.2650	23.2175	8.1041
15	18.0522	14.2084	21.2929	27.0765	24.5875	9.1927
16	20.0902	15.4272	23.2106	29.0141	26.0047	10.3721
17	22.3450	16.7240	25.1557	31.0880	27.4672	11.6469
18	24.8344	18.0991	27.1208	33.3096	28.9723	13.0212
19	27.5763	19.5521	29.0981	35.6920	30.5173	14.4981
20	30.5884	21.0817	31.0794	38.2492	32.0987	16.0800

Table.2: Evaluating the effect of $r_1 = 0.00018$ and $r_2 = 0.000135$ together on $x(t)$ and $y(t)$ using ODE 45 numerical scheme

Example	$x(t)$	$x_m(t)$	BL(%)	$y(t)$	$y_m(t)$	BL(%)
1	4.0000	4.0000	0	10.0000	10.0000	0
2	4.4497	4.4030	1.0500	10.7618	10.7273	0.3210
3	4.9514	4.8443	2.1611	11.5776	11.4995	0.6740
4	5.5111	5.3273	3.3346	12.4505	12.3183	1.0619
5	6.1356	5.8551	4.5715	13.3844	13.1852	1.4881
6	6.8325	6.4313	5.8722	14.3829	14.1015	1.9561
7	7.6102	7.0594	7.2370	15.4502	15.0686	2.4698
8	8.4778	7.7432	8.6654	16.5906	16.0874	3.0332
9	9.4456	8.4862	10.1565	17.8090	17.1588	3.6507
10	10.5247	9.2924	11.7085	19.1103	18.2834	4.3269
11	11.7273	10.1653	13.3193	20.5002	19.4616	5.0665
12	13.0666	11.1085	14.9857	21.9847	20.6932	5.8748
13	14.5569	12.1253	16.7041	23.5705	21.9779	6.7566
14	16.2134	13.2188	18.4699	25.2650	23.3152	7.7174
15	18.0522	14.3916	20.2780	27.0765	24.7040	8.7623
16	20.0902	15.6458	22.1224	29.0141	26.1427	9.8963
17	22.3450	16.9830	23.9966	31.0880	27.6297	11.1241
18	24.8344	18.4039	25.8936	33.3096	29.1626	12.4501
19	27.5763	19.9084	27.8060	35.6920	30.7388	13.8776
20	30.5884	21.4956	29.7263	38.2492	32.3552	15.4095

Table.3: Evaluating the effect of $r_1 = 0.001176$ and $r_2 = 0.000882$ together on $x(t)$ and $y(t)$ using ODE 45 numerical scheme

Example	$x(t)$	$x_m(t)$	BL(%)	$y(t)$	$y_m(t)$	BL(%)
1	4.0000	4.0000	0	10.0000	10.0000	0
2	4.4497	4.4486	0.0249	10.7618	10.7610	0.0076
3	4.9514	4.9488	0.0516	11.5776	11.5757	0.0161
4	5.5111	5.5066	0.0802	12.4505	12.4473	0.0255
5	6.1356	6.1288	0.1108	13.3844	13.3795	0.0361
6	6.8325	6.8227	0.1436	14.3829	14.3760	0.0479
7	7.6102	7.5966	0.1787	15.4502	15.4407	0.0611
8	8.4778	8.4595	0.2161	16.5906	16.5781	0.0759
9	9.4456	9.4214	0.2560	17.8090	17.7925	0.0924
10	10.5247	10.4933	0.2985	19.1103	19.0891	0.1109

Example	$x(t)$	$x_m(t)$	BL(%)	$y(t)$	$y_m(t)$	BL(%)
11	11.7273	11.6870	0.3437	20.5002	20.4732	0.1316
12	13.0666	13.0155	0.3917	21.9847	21.9507	0.1549
13	14.5569	14.4925	0.4425	23.5705	23.5279	0.1809
14	16.2134	16.1329	0.4964	25.2650	25.2120	0.2101
15	18.0522	17.9523	0.5532	27.0765	27.0108	0.2429
16	20.0902	19.9670	0.6132	29.0141	28.9330	0.2795
17	22.3450	22.1939	0.6763	31.0880	30.9883	0.3206
18	24.8344	24.6499	0.7427	33.3096	33.1875	0.3666
19	27.5763	27.3523	0.8123	35.6920	35.5428	0.4180
20	30.5884	30.3176	0.8852	38.2492	38.0674	0.4753

By using ODE 45 numerical scheme, we have observed that a ten (10) percent variation of the inter-competition coefficient has predicted a monotonically increasing values for the populations ranging from 4.000 to 30.5884 approximately when all the model parameters are fixed. For the same population, due to a variation of the intrinsic growth rates, we have obtained a new population of the first yeast species called $x_1(t)$ ranging from 4.000 to 21.0817. A biodiversity loss has occurred ranging from 0 and increasing monotonically to 31.0794, quantified in percentage terms. In essence, example twenty (20) shows that the first yeast population during a shorter growing season of twenty (20) units of time is more vulnerable to the ecological risk of biodiversity loss. A similar observation is applicable to the second yeast species $y(t)$. In this case, when the model parameter values are fixed, the simulated growth rate data range from 10.0 and increased monotonically to 38.2492 compared to the range from 10.0 to 32.0987 due to a ten (10) percent variation of the intrinsic growth rates. We have also observed that biodiversity loss is quantified to range from 0 to 16.08.

In summary, by comparing these two dominant scenarios of biodiversity loss, it is very clear that the first yeast species is almost double more vulnerable to biodiversity loss than the second yeast species. Similar observations are applicable to Table 2 and Table 3. On the basis of this analysis, we have observed that a ninety – eight (98) percent variation of the inter – competition coefficient together has predicted a far lower volume of biodiversity loss as expected which can be tolerated because it is an evidence that this devastating ecological risk will soon be lost at the next level of variation such as hundred and one (101) percentage variation.

V. CONCLUSION

We have successfully utilized the technique of ODE 45 numerical scheme to model the possibility of biodiversity loss. These results have been discussed quantitatively. A small variation of the inter – competition coefficient

together is dominantly associated with a higher vulnerability to biodiversity loss whereas the inevitability of biodiversity loss which should be expected can be tolerated for a lower decreasing volume of the intrinsic growth rates together. It is therefore necessary to find some sort of mitigation measures that will recover biodiversity loss and sustain biodiversity gain. This idea will be key subject in our next investigation.

REFERENCES

- [1] Atsu, J. U. & Ekaka-a, E. N. (2017). Modeling the policy implications of biodiversity loss: A case study of the Cross River national park, south –south Nigeria. International Journal of Pure and Applied Science, Cambridge Research and Publications. vol 10 No. 1; pp 30-37.
- [2] Atsu, J. U. & Ekaka-a, E. N. (2017). Quantifying the impact of changing Intrinsic growth rate on the biodiversity of the forest resource biomass: implications for the Cross River State forest resource at the Cross River National Park, South – South, Nigeria: African Scholar Journal of Pure and Applied Science, 7(1); 117 – 130.
- [3] De Mazancourt, C., Isbell, F., Larocque, A., Berendse, F., De Luca, E., Grace, J.B et al. (2013). Predicting ecosystem stability from community composition and biodiversity. Ecology Letters., DOI: 10.1111/ele.12088.
- [4] Ernest, S.K.M. & Brown, J.H. (2001). Homeostasis and compensation: the role of species and resources in ecosystem stability. Ecology, 82, 2118–2132.
- [5] Fowler, M.S., Laakso, J., Kaitala, V., Ruokolainen, L. & Ranta, E. (2012). Species dynamics alter community diversity-biomass stability relationships. Ecol. Lett., 15, 1387–1396.
- [6] Gonzalez, A. & Descamps-Julien, B. (2004). Population and community variability in randomly fluctuating environments. Oikos, 106, 105–116.
- [7] Grman, E., Lau, J.A., Donald, R., Schoolmaster, J. & Gross, K.L. (2010). Mechanisms contributing to

- stability in ecosystem function depend on the environmental context. *Ecol. Lett.*, 13, 1400–1410.
- [8] Hector, A., Hautier, Y., Saner, P., Wacker, L., Bagchi, R., Joshi, J. et al. (2010). General stabilizing effects of plant diversity on grassland productivity through population asynchrony andoveryielding. *Ecology*, 91, 2213–2220.
- [9] Loreau, M. & de Mazancourt, C.. (2013). Biodiversity and ecosystem stability: a synthesis of underlying mechanisms. *Ecol. Lett.*, DOI: 10.1111/ele.12073.
- [10] MacArthur, R. (1955). Fluctuations of Animal Populations, and a Measure of Community Stability. *Ecology*, 36, 533–536.
- [11] Marquard, E., Weigelt, A., Roscher, C., Gubsch, M., Lipowsky, A. & Schmid, B. (2009). Positive biodiversity-productivity relationship due to increased plant density. *J. Ecol.*, 97, 696–704.
- [12] May, R.M. (1973). Stability and complexity in model ecosystems. 2001, Princeton Landmarks in Biology edn. Princeton University Press, Princeton.
- McCann, K.S. (2000). The diversity-stability debate. *Nature*, 405, 228–233.
- [13] McNaughton, S.J. (1977). Diversity and stability of ecological communities: a comment on the role of empiricism in ecology. *Am. Nat.*, 111, 515–525.
- [14] Mutshinda, C.M., O’Hara, R.B. & Woiwod, I.P. (2009). What drives community dynamics? *Proc. Biol. Sci.*, 276, 2923–2929.
- [15] Proulx, R., Wirth, C., Voigt, W., Weigelt, A., Roscher, C., Attinger, S. et al.(2010). Diversity Promotes Temporal Stability across Levels of Ecosystem Organization in Experimental Grasslands. *PLoS ONE*, 5, e13382.

Simulation modelling of the effect of a random disturbance on biodiversity of a mathematical model of mutualism between two interacting yeast species

Eke, Nwagrade¹; Atsu, J. U.²; Ekaka-a, E. N³

¹Department of Mathematics/Statistics, Ignatius Ajuru University of Education, Port Harcourt, Rivers State

²Department of Mathematics/Statistics, Cross River University of Technology, Calabar, Nigeria.

³Department of Mathematics, Rivers State University Nkporlu–Oroworukwo, Port Harcourt, Rivers State

Abstract— *The effect of a random disturbance on the ecosystem is one of the oldest scientific observations of which its effect on biodiversity is no exception. We have used ODE 45 numerical scheme to tackle this problem. The novel results that we have obtained have not been seen elsewhere; these are presented and fully discussed quantitatively.*

Keywords— *Random disturbance, numerical scheme, biodiversity, dynamical system, stochastic, deterministic dynamical system.*

I. INTRODUCTION

An ecological dynamical system is inherently stochastic in its scientific construction and definition. In this scenario, a deterministic definition of an ecological dynamical system is a special case of a stochastic ecological system that is more highly vulnerable to random disturbance which can be attributed to the other environmental and climatic factors and other characteristics of the ecosystem which we cannot go into in detailed discussion. However, there are two factors that may have a high potential to influence the performance of biodiversity gain. One of these factors could be a conducive steady environment that is less hostile to

interaction between yeast populations. The other factor could be attributed to an ecological system where human activities do not have a huge impact on the growing yeast species. These two factors put together are capable to improve the performance of yeast species in terms of their yields that can mimic strong evidence of biodiversity gain. In other words, a random noise disturbance in terms of these mentioned factors may not necessarily bring about biodiversity loss but are capable to increase the magnitude of biodiversity gain.

II. MATERIALS AND METHODS

We have considered a semi – stochastic fashion of our deterministic dynamical system in which a dynamical system with two random noise perturbation scenarios of 0.01 and 0.1 in the first instance and next for a random noise perturbation of 0.8. This method is based on the 150 percent variation of the inter-competition coefficients together.

III. RESULTS

The corresponding results of this study are presented in Table 1, Table 2, Table 3, Table 4, Table 5, and Table 6

Table.1: Quantifying the effect of a random disturbance having the intensity of 0.01 on biodiversity gain using ODE 45 numerical scheme. Scenario One

Example	$x(t)$	$x_m(t)$	BG (%)	$y(t)$	$y_m(t)$	BG (%)
1	4.0000	4.0000	0	10.0000	10.0000	0
2	4.4497	4.5132	1.4276	10.7618	10.8509	0.8273
3	4.9514	5.1133	3.2706	11.5776	11.7320	1.3340
4	5.5111	5.7691	4.6831	12.4505	12.6952	1.9650
5	6.1356	6.5317	6.4556	13.3844	13.7425	2.6755
6	6.8325	7.3519	7.6024	14.3829	14.8480	3.2337
7	7.6102	8.2747	8.7320	15.4502	16.0596	3.9444
8	8.4778	9.3598	10.4040	16.5906	17.3229	4.4139

Example	$x(t)$	$x_m(t)$	BG (%)	$y(t)$	$y_m(t)$	BG (%)
9	9.4456	10.6178	12.4105	17.8090	18.7357	5.2036
10	10.5247	12.0170	14.1789	19.1103	20.2260	5.8379
11	11.7273	13.5941	15.9187	20.5002	21.8492	6.5805
12	13.0666	15.3911	17.7895	21.9847	23.6066	7.3774
13	14.5569	17.4257	19.7075	23.5705	25.5991	8.6065
14	16.2134	19.7543	21.8394	25.2650	27.7541	9.8517
15	18.0522	22.4048	24.1112	27.0765	30.0533	10.9939
16	20.0902	25.4003	26.4313	29.0141	32.5986	12.3545
17	22.3450	28.8608	29.1598	31.0880	35.4470	14.0217
18	24.8344	32.6905	31.6343	33.3096	38.6581	16.0567
19	27.5763	37.0962	34.5221	35.6920	42.2245	18.3025
20	30.5884	42.0707	37.5382	38.2492	46.2160	20.8286

Table.2: Quantifying the effect of a random disturbance having the intensity of 0.01 on biodiversity gain using ODE 45 numerical scheme. Scenario Two

Example	$x(t)$	$x_m(t)$	BG (%)	$y(t)$	$y_m(t)$	BG (%)
1	4.0000	4.0000	0	10.0000	10.0000	0
2	4.4497	4.5237	1.6635	10.7618	10.8162	0.5054
3	4.9514	5.1350	3.7100	11.5776	11.7026	1.0797
4	5.5111	5.8552	6.2449	12.4505	12.7082	2.0699
5	6.1356	6.6134	7.7883	13.3844	13.7418	2.6703
6	6.8325	7.5144	9.9797	14.3829	14.9599	4.0116
7	7.6102	8.4799	11.4283	15.4502	16.2132	4.9386
8	8.4778	9.5569	12.7289	16.5906	17.5598	5.8418
9	9.4456	10.8277	14.6327	17.8090	19.0138	6.7651
10	10.5247	12.2314	16.2166	19.1103	20.5377	7.4689
11	11.7273	13.8468	18.0734	20.5002	22.2450	8.5111
12	13.0666	15.6921	20.0927	21.9847	24.0618	9.4480
13	14.5569	17.7736	22.0973	23.5705	26.0330	10.4475
14	16.2134	20.1278	24.1427	25.2650	28.1513	11.4237
15	18.0522	22.7965	26.2811	27.0765	30.5581	12.8584
16	20.0902	25.8497	28.6678	29.0141	33.2120	14.4686
17	22.3450	29.3634	31.4092	31.0880	36.0546	15.9761
18	24.8344	33.3098	34.1278	33.3096	39.2617	17.8690
19	27.5763	37.7921	37.0457	35.6920	42.9179	20.2453
20	30.5884	42.8728	40.1607	38.2492	46.9771	22.8184

Table.3: Quantifying the effect of a random disturbance having the intensity of 0.1 on biodiversity gain using ODE 45 numerical scheme. Scenario Three

Example	$x(t)$	$x_m(t)$	BG (%)	$y(t)$	$y_m(t)$	BG (%)
1	4.0000	4.0000	0	10.0000	10.0000	0
2	4.4497	4.5334	1.8803	10.7618	10.8330	0.6613
3	4.9514	5.0793	2.5839	11.5776	11.7789	1.7395
4	5.5111	5.7124	3.6543	12.4505	12.7405	2.3287
5	6.1356	6.4569	5.2377	13.3844	13.7864	3.0037
6	6.8325	7.2961	6.7848	14.3829	14.9548	3.9766
7	7.6102	8.2988	9.0489	15.4502	16.1720	4.6722
8	8.4778	9.3920	10.7836	16.5906	17.4731	5.3191
9	9.4456	10.6431	12.6781	17.8090	18.9168	6.2202
10	10.5247	12.0703	14.6858	19.1103	20.4365	6.9397

Example	$x(t)$	$x_m(t)$	BG(%)	$y(t)$	$y_m(t)$	BG(%)
11	11.7273	13.6683	16.5511	20.5002	22.1251	7.9260
12	13.0666	15.4880	18.5308	21.9847	23.9678	9.0203
13	14.5569	17.4978	20.2024	23.5705	25.9385	10.0464
14	16.2134	19.8987	22.7301	25.2650	28.1712	11.5028
15	18.0522	22.5636	24.9908	27.0765	30.5360	12.7766
16	20.0902	25.5495	27.1740	29.0141	33.1085	14.1121
17	22.3450	28.9518	29.5672	31.0880	36.0206	15.8668
18	24.8344	32.8223	32.1648	33.3096	39.2187	17.7398
19	27.5763	37.2030	34.9093	35.6920	42.7775	19.8519
20	30.5884	42.1760	37.8825	38.2492	46.7649	22.2637

Table.4: Quantifying the effect of a random disturbance having the intensity of 0.1 on biodiversity gain using ODE 45 numerical scheme. Scenario Four

Example	$x(t)$	$x_m(t)$	BG(%)	$y(t)$	$y_m(t)$	BG(%)
1	4.0000	4.0000	0	10.0000	10.0000	0
2	4.4497	4.4867	0.8312	10.7618	10.8039	0.3907
3	4.9514	5.0647	2.2898	11.5776	11.6835	0.9150
4	5.5111	5.6951	3.3405	12.4505	12.6824	1.8624
5	6.1356	6.5067	6.0488	13.3844	13.7450	2.6946
6	6.8325	7.3949	8.2316	14.3829	14.8654	3.3550
7	7.6102	8.3792	10.1059	15.4502	16.0553	3.9163
8	8.4778	9.4514	11.4848	16.5906	17.3531	4.5954
9	9.4456	10.7237	13.5309	17.8090	18.7569	5.3224
10	10.5247	12.1772	15.7008	19.1103	20.2479	5.9526
11	11.7273	13.7391	17.1551	20.5002	21.9514	7.0789
12	13.0666	15.5557	19.0486	21.9847	23.7044	7.8224
13	14.5569	17.6162	21.0155	23.5705	25.6845	8.9686
14	16.2134	19.9303	22.9250	25.2650	27.9186	10.5029
15	18.0522	22.5407	24.8641	27.0765	30.2741	11.8094
16	20.0902	25.5231	27.0421	29.0141	32.9389	13.5275
17	22.3450	28.9112	29.3857	31.0880	35.7840	15.1058
18	24.8344	32.8304	32.1974	33.3096	38.9832	17.0329
19	27.5763	37.2158	34.9561	35.6920	42.5658	19.2588
20	30.5884	42.1994	37.9592	38.2492	46.5714	21.7578

Table.5: Quantifying the effect of a random disturbance having the intensity of 0.8 on biodiversity gain using ODE 45 numerical scheme. Scenario Five

Example	$x(t)$	$x_m(t)$	BG(%)	$y(t)$	$y_m(t)$	BG(%)
1	4.0000	4.0000	0	10.0000	10.0000	0
2	4.4497	4.8324	8.6014	10.7618	11.4308	6.2161
3	4.9514	5.8134	17.4109	11.5776	12.7359	10.0048
4	5.5111	6.9156	25.4863	12.4505	14.2481	14.4378
5	6.1356	8.2866	35.0587	13.3844	15.5423	16.1229
6	6.8325	9.6980	41.9400	14.3829	17.1956	19.5561
7	7.6102	11.2228	47.4713	15.4502	18.8135	21.7691
8	8.4778	12.9207	52.4067	16.5906	20.7384	25.0008
9	9.4456	15.1202	60.0765	17.8090	22.8115	28.0896
10	10.5247	17.3165	64.5317	19.1103	25.0589	31.1277
11	11.7273	19.9405	70.0344	20.5002	27.5825	34.5477
12	13.0666	22.7270	73.9314	21.9847	30.4937	38.7040

Example	$x(t)$	$x_m(t)$	BG(%)	$y(t)$	$y_m(t)$	BG(%)
13	14.5569	26.0227	78.7651	23.5705	33.5233	42.2257
14	16.2134	29.7098	83.2424	25.2650	36.7004	45.2614
15	18.0522	34.0788	88.7790	27.0765	40.6045	49.9621
16	20.0902	39.0831	94.5379	29.0141	44.6849	54.0111
17	22.3450	44.9096	100.9828	31.0880	48.9859	57.5719
18	24.8344	51.3077	106.5995	33.3096	53.9942	62.0979
19	27.5763	58.3908	111.7429	35.6920	60.0885	68.3532
20	30.5884	66.7729	118.2950	38.2492	66.8022	74.6498

Table.6: Quantifying the effect of a random disturbance having the intensity of 0.8 on biodiversity gain using ODE 45 numerical scheme. Scenario Six

Example	$x(t)$	$x_m(t)$	BG(%)	$y(t)$	$y_m(t)$	BG(%)
1	4.0000	4.0000	0	10.0000	10.0000	0
2	4.4497	4.8883	9.8575	10.7618	11.1320	3.4394
3	4.9514	5.9583	20.3360	11.5776	12.4481	7.5191
4	5.5111	6.9956	26.9379	12.4505	13.8045	10.8751
5	6.1356	8.2553	34.5478	13.3844	15.3543	14.7181
6	6.8325	9.7534	42.7497	14.3829	17.0949	18.8558
7	7.6102	11.3727	49.4406	15.4502	18.7917	21.6279
8	8.4778	13.1416	55.0121	16.5906	20.8438	25.6357
9	9.4456	15.2574	61.5298	17.8090	22.9964	29.1282
10	10.5247	17.3844	65.1771	19.1103	25.2481	32.1174
11	11.7273	19.9983	70.5275	20.5002	27.7474	35.3519
12	13.0666	23.1748	77.3585	21.9847	30.5111	38.7835
13	14.5569	26.8443	84.4089	23.5705	33.4027	41.7137
14	16.2134	31.0127	91.2778	25.2650	36.8937	46.0266
15	18.0522	35.6022	97.2178	27.0765	40.4674	49.4558
16	20.0902	40.7135	102.6534	29.0141	44.7757	54.3243
17	22.3450	46.7144	109.0600	31.0880	49.3679	58.8006
18	24.8344	53.3229	114.7143	33.3096	54.9415	64.9419
19	27.5763	61.0529	121.3966	35.6920	60.9044	70.6391
20	30.5884	69.7168	127.9196	38.2492	67.8519	77.3942

IV. DISCUSSION OF RESULTS

For a random noise variation of 0.01 and 0.1 over repeated simulations as shown on Table 1 to table 4, we have observed a relatively smaller prediction of biodiversity gain whereas for a random noise variation of 0.8, we have observed a bigger prediction of biodiversity gain. On the basis of this present analysis, a random noise inclusion which may be considered as having a negative effect, has turned out in this scenario to have a positive effect on the ecological services.

V. CONCLUSION

Not all random noise driven factors do predict biodiversity loss. We have utilized the technique of a numerical simulation to predict that a higher random noise perturbation has the potential to predict bigger volumes of biodiversity gain than a lower random noise perturbation, provided the two yeast species interact

mutually on the simplifying assumption of varying the inter-competition coefficients together. This numerical result complements a popular ecological idea that in a harsh ecological environment, species tend to benefit each other (Ekaka-a 2009, Ford, Lumb, Ekaka-a 2010). The predictions of this present study are based on the one hundred and fifty (150) percent variations of the inter competition coefficients together on the simplifying assumption that the intra-competition coefficients outweigh the inter-competition coefficients. However, we have not extended this idea to the scenario of two (2) competing yeast species undergoing a random noise perturbation. This will be the subject of our next investigation.

REFERENCES

- [1] Atsu, J. U. & Ekaka-a, E. N. (2017). Modeling the policy implications of biodiversity loss: A case study

- of the Cross River national park, south – south Nigeria. International Journal of Pure and Applied Science, Cambridge Research and Publications. vol 10 No. 1; pp 30-37.
- [2] Atsu, J. U. & Ekaka-a, E. N. (2017). Quantifying the impact of changing intrinsic growth rate on the biodiversity of the forest resource biomass: implications for the Cross River State forest resource at the Cross River National Park, South – South, Nigeria: African Scholar Journal of Pure and Applied Science, 7(1); 117 – 130.
- [3] De Mazancourt, C., Isbell, F., Larocque, A., Berendse, F., De Luca, E., Grace, J.B et al. (2013). Predicting ecosystem stability from community composition and biodiversity. Ecology Letters,, DOI: 10.1111/ele.12088.
- [4] Ernest, S.K.M. & Brown, J.H. (2001). Homeostasis and compensation: the role of species and resources in ecosystem stability. Ecology, 82, 2118–2132.
- [5] Fowler, M.S., Laakso, J., Kaitala, V., Ruokolainen, L. & Ranta, E. (2012). Species dynamics alter community diversity-biomass stability relationships. Ecol. Lett., 15, 1387–1396.
- [6] Gonzalez, A. & Descamps-Julien, B. (2004). Population and community variability in randomly fluctuating environments. Oikos, 106, 105–116.
- [7] Grman, E., Lau, J.A., Donald, R., Schoolmaster, J. & Gross, K.L. (2010). Mechanisms contributing to stability in ecosystem function depend on the environmental context. Ecol. Lett., 13, 1400–1410.
- [8] Hector, A., Hautier, Y., Saner, P., Wacker, L., Bagchi, R., Joshi, J. et al. (2010). General stabilizing effects of plant diversity on grassland productivity through population asynchrony and overyielding. Ecology, 91, 2213–2220.
- [9] Loreau, M.. & de Mazancourt, C.. (2013). Biodiversity and ecosystem stability: a synthesis of underlying mechanisms. Ecol. Lett., DOI: 10.1111/ele.12073.
- [10] MacArthur, R. (1955). Fluctuations of Animal Populations, and a Measure of Community Stability. Ecology, 36, 533–536.
- [11] Marquard, E., Weigelt, A., Roscher, C., Gubsch, M., Lipowsky, A. & Schmid, B. (2009). Positive biodiversity-productivity relationship due to increased plant density. J. Ecol., 97, 696–704.
- [12] May, R.M. (1973). Stability and complexity in model ecosystems. 2001, Princeton Landmarks in Biology edn. Princeton University Press, Princeton. McCann, K.S. (2000). The diversity-stability debate. Nature, 405, 228–233.
- [13] McNaughton, S.J. (1977). Diversity and stability of ecological communities: a comment on the role of empiricism in ecology. Am. Nat., 111, 515–525.
- [14] Mutshinda, C.M., O’Hara, R.B. & Woivod, I.P. (2009). What drives community dynamics? Proc. Biol. Sci., 276, 2923–2929.
- [15] Proulx, R., Wirth, C., Voigt, W., Weigelt, A., Roscher, C., Attinger, S. et al. (2010). Diversity Promotes Temporal Stability across Levels of Ecosystem Organization in Experimental Grasslands. PLoS ONE, 5, e13382.

Study of a Laboratory-based Gamma Spectrometry for Food and Environmental Samples

M. N. Islam¹, H. Akhter², M. Begum³, Y. Mawla⁴, M. Kamal⁵

^{1,2,3,4} Electronics Division, Atomic Energy Centre, Bangladesh Atomic Energy Commission,
P.O. Box No. 164, Dhaka, Bangladesh.

⁵ Radioactivity Testing and Monitoring Laboratory, Atomic Energy Centre, Bangladesh Atomic Energy Commission,
P.O. Box No. 1352, Chittagong, Bangladesh.

Abstract— A comprehensive study on a laboratory-based Gamma Spectrometry has been presented in this paper for food and environmental samples. The system comprises of HPGe detector with proper cooling for minimizing thermal generation of charge-carriers and appropriate shielding to reduce background emission; associated processing electronics and acquisition as well as analysis software. The choice of HPGe detector for laboratory-based Gamma Spectrometry, its radiation interaction mechanism and system optimization have been presented.

Keywords—HPGe Detector, Radiotracers, Efficiency Calibration, Energy Calibration, Activity Concentration.

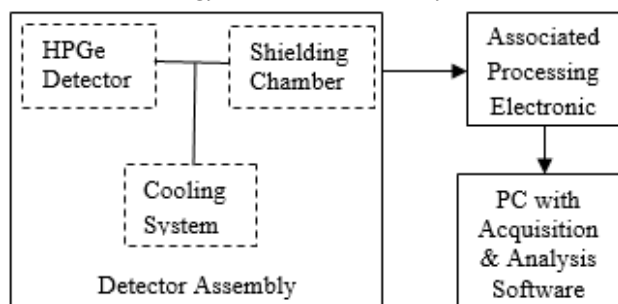


Fig.1: Block Shows the Configuration of Laboratory-based Gamma Spectrometry.

I. INTRODUCTION

Environmental Gamma Spectrometry is an essential tool for modeling spatio-temporal processes through coordination of data from different radiotracers. The two main advantages of environmental gamma spectrometry are: it is a nondestructive technique; and the measurement of different radiotracers is done simultaneously. The principal radiotracers of interest for environmental studies, measured via gamma spectrometry, are: ²¹⁰Pb, ²²⁶Ra, ¹³⁷Cs, ²⁴¹Am, ²³⁸U (²³⁴Th), ²³⁵U, ²³²Th (²²⁸Ac), ⁴⁰K, ⁷Be, ²¹²Pb, ²²²Rn, ²¹⁴Pb ²¹⁴Bi and ⁸⁸Y. [1]. Gamma-ray spectrometry has been widely used in various environmental and natural sciences by its ability to determine the concentrations of each radionuclide of the

samples, and also because of the easiness in sample preparation and measurement procedures [2]. The purpose of an HPGe detector is to convert gamma rays into electrical impulses which can be used, with suitable signal processing, to determine their energy and intensity. All HPGe radiation detectors are either coaxial HPGe, well-type HPGe or broad energy HPGe (BEGe) just large, reverse-biased diodes. The germanium material can be either "n-type" or "p-type". The type depends on the concentration of donor or acceptor atoms in the crystal. [3]. Liquid nitrogen (LN₂) and cryocooler (electric cooler) would be used to cool HPGe detectors. Detector assembly also contains lead shielding chamber to reduce the background radiation emission. The later part is Multichannel Analyzer (MCA) means a DAQ card along with acquisition and analysis software to measure the pulse height, type and activity of incoming radiation.

II. METHODOLOGY

Laboratory-based Environmental Gamma Spectrometry comprises of detector assembly, associated processing electronics and a PC with gamma acquisition and analysis software. The detector assembly contains High Purity Germanium (HPGe) detector, the cooling system and the shielding chamber.

2.1: Detector

The choice of the best HPGe detector in case of Gamma Spectrometry for one particular measurement situation is based on some basic concepts such as how the detection process works, how gamma rays penetrate materials and the principles of gamma-ray spectroscopy. On the basis of these concepts the following parameters would be taken into consideration while the best choice of a detector.

2.1.1: Minimum Detectable Activity (MDA)

One measure of the quality of a spectrum is the minimum detectable activity (MDA) of the detector system. The

resolution, background and efficiency of the detector are related to the MDA. This relationship may be simply stated as below

$$MDA(E) \sim \frac{\sqrt{R(E)B(E)}}{\epsilon(E)} \quad (1)$$

R(E) is the energy resolution of the detector as a function of energy; B(E) is the background counts per KeV (unit energy) as a function of energy and $\epsilon(E)$ is the absolute efficiency of the detector as a function of energy. The MDA varies with energy because the quantities on which it depends vary with energy. Here we have separated out all the factors in the MDA that only depend on the detector itself. The gamma rays per decay, the shield and count time affect the MDA, but will do so in the same way for all detectors.

2.1.2: Detector Resolution

Energy resolution is the dominant characteristic of a germanium detector. Gamma-ray spectrometry using high purity germanium detector is enhanced by the excellent energy resolution which can help to separate and resolve various close energy gamma-ray peaks in a complex energy spectrum. The full width at half maximum of the full energy peak known as FWHM and sometimes referred as a measure of energy resolution. The units of FWHM are expressed in KeV for Ge detector and are defined at specific, characteristic full energy peaks associated with standard sources such as 662 KeV for a ¹³⁷Cs source or 1332 KeV for a ⁶⁰Co source. The energy resolution of the germanium detector can be affected by the number of electron-hole pairs created in the detector, incomplete charge collection and electronic noise contributions. The effect of these three factors depends on the properties of the detector and the gamma-ray energy [4].

2.1.3: Detector Efficiency

The detector efficiency in Eq.2 will potentially have the most effect on MDA. In this Eq.2, $\epsilon(E)$ is the absolute efficiency at the specified energy. $\epsilon(E)$ will depend on the detector-to-sample geometry, and many other energy dependent factors, including gamma-ray absorption in matrix, detector dead layers and the intrinsic efficiency of the detector. The IEEE-325 relative efficiency is no longer a suitable indicator.

The absolute detector efficiency at that energy is calculated by dividing the net count rate in the full-energy peak by the decay corrected gamma-ray-emission rate of the standard source. Efficiency curves were constructed from these full-energy-peak efficiencies.

$$\epsilon_{abs} = \frac{\text{Total number of counts recorded under the photo peak}}{\text{Total number of photons emitted by the standard sources}}$$

$$\epsilon_{abs} = \frac{\text{cps experimental}}{\text{cps theoretical}}$$

$$\epsilon_{abs} = \frac{(\frac{C}{S})_{std} - (\frac{C}{S})_{sample} - (\frac{C}{S})_{BG}}{(\frac{C}{S})_{theo} \text{Exp}(-\ln(2) \cdot \frac{t}{t_{1/2}})} \quad (2)$$

$(\frac{C}{S})_{std}$ Count of soil sample with standard solution, $(\frac{C}{S})_{sample}$ Count of soil sample without standard solution, $(\frac{C}{S})_{BG}$ Count of background, $(\frac{C}{S})_{theo}$ Counting of gamma ray of used standard solution, t the time of decay, $t_{1/2}$ half-life of the radionuclide [5].

2.1.4: Compton Suppression System (CSS)

For a given HPGe detector, a Compton Suppression System (CSS) will always reduce Compton Background. It is also called an "active shield." It reduces the cosmic background because a cosmic ray produces events (counts) in detectors.

2.1.5: Dead Layers, Windows and Absorption

Any gamma rays stopped in the dead layer do not produce an output. Below 150 KeV, the GMX has higher efficiency and below 100 KeV, the difference increases rapidly as one goes down in energy. This is because the dead layer of the GEM (~600 microns) is much larger than that of the GMX (~0.3 microns).

Thin window PROFILE X series GEM-FX8530, compared to a GEM80 76 mm diameter x 87 mm depth. The much higher absolute efficiency of the FX85 at all energies below 160 KeV.

The absorption processes are a function of energy and described by the exponential attenuation equation below:

$$I = I_0 e^{-\mu(E)X} \quad (3)$$

Where I_0 is the unattenuated gamma-ray flux, I is the flux after passing through the material and μ is the linear attenuation coefficient of the absorber and x is the thickness.

2.1.6: Detector Cooling System

A High Purity Germanium (HPGe) detector is required a High Voltage for performing its proper operation and hence the detector should be cooled sufficiently in order to reduce the thermal generation of charge carriers to an acceptable level. Otherwise, the noise due to leakage current would destroy the energy resolution of the detector. Liquid Nitrogen (LN₂) which has temperature

77°K (-196° C) is the common cooling medium of the detector. The Liquid Nitrogen (LN₂) Dewar served as a reservoir of liquid nitrogen [4]. Electric Coolers offer compared to liquid nitrogen (LN₂) to cool HPGe detectors, the limited cooler life time, higher initial investment and need for periodic maintenance have always been major drawbacks. With the introduction of pulse tube coolers in CANBERRA's Cryo- Pulse 5 and Cryo-Pulse 5 plus, these issues are no longer present [6].

2.1.7: Detector Shielding Arrangement

The detector shielding arrangement is usually fabricated by using locally available lead. Because of high density (11.4gm/cc), large atomic number (Z=82) and comparatively low cost, lead is the most widely used material for construction of the shields. The shielding of the detector from the environment radiation is an absolute necessity for low level measurement of activity. The shielding not only reduces the background resulting from cosmic radiation, natural radioactive traces in the building material or in the surface of the earth but also from nearby nuclear facilities and other radiation sources like the ambient air, which presumably contains trace amounts of radioactive gases such as Radon.

2.1.7.1: Background Radiation

The counting system must have a background as low as is attainable with a minimum spectral lines originating from natural radionuclides which may be present in the system components and the surrounding environment, i.e., the walls, floors, furnitures etc of the counting facility. Construction materials such as concrete, plaster and paints which contains barites (barium sulphate) will tend to cause elevated backgrounds due to natural radionuclides [4].

2.1.8: Detector Interaction Mechanism

Four major interaction mechanisms play an important role in the measurement of photons. These mechanisms are: photoelectric effect, coherent scattering, incoherent scattering and pair production. The photon energy of major interest for environmental spectrometry studies ranges between a few KeV to 1500 KeV. The term "low energy" will be used here for the energy range 1 to 100 KeV, "medium energy" for energies between 100 and 600 KeV and "high energy" for energies between 600 and 1500 KeV.

2.1.8.1: Photoelectric Effect

In the photoelectric effect, there is a collision between a photon and an atom resulting in the ejection of a bound electron. The photon disappears completely, i.e. all its energy, E_p , is transferred to the electron. The amount of

energy, E_e , which is transferred to the electron, can be calculated if the binding energy, E_b , of the ejected electron is known:

$$E_e = E_p - E_b \quad (4)$$

2.1.8.2: Coherent Scattering

In the coherent scattering process no energy is transferred to the atom. The electromagnetic field of the photon sets atomic electrons into vibration. The electrons then re-emit radiation of the same magnitude as the interacting photon and mainly in the forward direction. The cross-section for coherent scattering decreases rapidly with increasing photon energy. This process can be neglected for photon energies above 100 KeV. The differential cross section per atom for this process as a function of scattering angle θ is written as follows:

$$\frac{\partial \sigma_{coh}}{\partial \theta} = \frac{Zr_0^2}{2} (1 + \cos^2(\theta)) [F(x, Z)]^2 \cdot 2\pi \cdot \sin(\theta) \quad (5)$$

with the parameter x defined as:

$$x = \frac{\sin(\theta/2)}{\lambda} \quad (6)$$

Where r_0 is the classical electron radius, $F(x, Z)$ is the atomic form factor and λ the photon wavelength.

2.1.8.3: Incoherent or Compton scattering

In the incoherent or Compton scattering process, only a portion of the photon energy is transferred to an atomic electron. The remaining energy appears as a secondary photon. The direction (scattering angle θ) and energy of the secondary photon, E_p' , are related by the following equation:

$$E_p' = \frac{E_p}{1 + \alpha(1 - \cos(\theta))} \quad (7)$$

With α defined as

$$\alpha = \frac{E_p}{m_0 c^2} \quad (8)$$

Where m_0 is the rest mass for an electron and c is the speed of light in vacuum.

2.1.8.4: Pair Production

The pair production mechanism only occurs for photon energies above 1022 KeV. Here photons are converted to electron-positron pairs under the effect of the field of a nucleus. Since one electron and one positron are formed, the photons must have energies equivalent to at least two

electronic masses (2 x 511 KeV) and the excess photon energy is shared between the created electron and positron pair. The annihilation of the positrons produces two photons in opposite directions, each with 511 KeV. The total cross-section for this process increases with energy above the threshold energy.

$$\sigma_{Total} = \sigma_{Photoelectric} + \sigma_{Pair Production} + \sigma_{Coherent Sc.} + \sigma_{Incoherent Sc.} \quad (9)$$

The total probability of interaction per unit path length for a photon is proportional to the sum of the total individual cross-sections [1].

2.2: Processing Electronics

The electrical charge output from the detector would be acquired and processed through an Electronic System consists of preamplifier and high-voltage filter, a main amplifier, a count-rate meter, a pulse height analyzer, a precision pulse generator, a detector bias supply and an oscilloscope[7].

2.2: Gamma Acquisition and Analysis

The Genie™ 2000 is Gamma Acquisition and Analysis (GAA) Software. The window in fig.2 is its user interface for acquiring and analyzing nuclear spectra. It consists of the Title Bar, the Menu Bar, the Toolbar and the Display Status Line at the top of the screen, the Control Panel, the Spectral Display, the Status Pages, and the Report Window in the main part of the window and at the bottom of the screen, the Analysis Status Line [8].

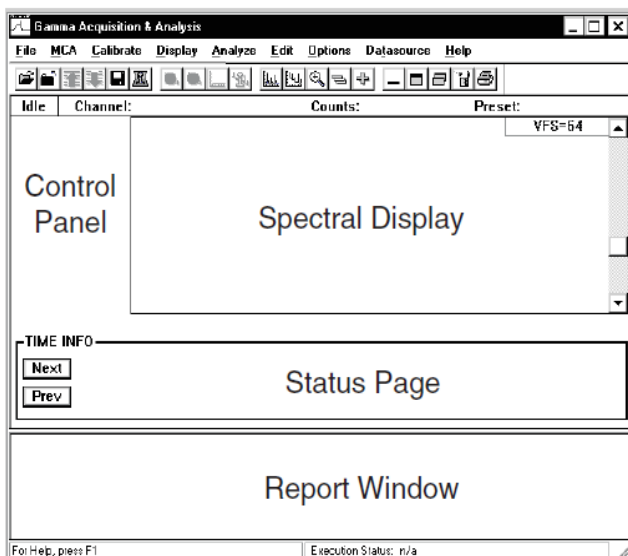


Fig.2: The Basic Gamma Acquisition and Analysis (GAA) Software Window.

2.3.1: Energy Calibration

Energy calibration establishes a linear relationship between the spectrum's channels and their energy levels.

By calibrating two peaks, one at each end of the spectrum, the energy of any other peak can be estimated fairly accurately [7]. For instance, the ⁴⁰K and ¹³⁷Cs radionuclides would be measured from their respective γ -ray energies 1460 and 661.66 KeV respectively [9, 10].

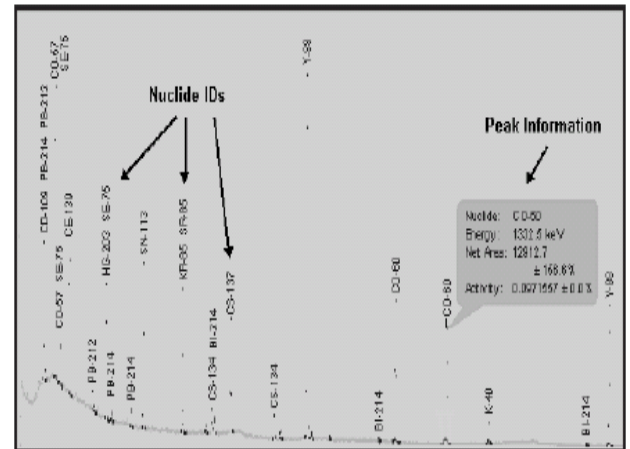


Fig.3: Nuclide IDs and Peak Information

2.3.2: Efficiency Calibration

For radioactivity measurement, the gamma-ray spectrometry with a high-purity germanium (HPGe) coaxial detector is widely used. In the method, a detection efficiency curve, that is, a set of photopeak efficiencies over the energy region of interest must be known in advance. The detection efficiency curve depends not only on a detection system but also on a sample shape and a sample matrix with different density and height of environmental samples.

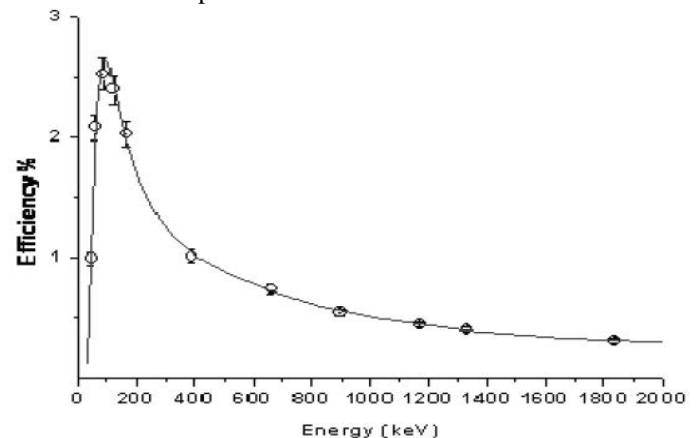


Fig.4: Efficiency calibration curve obtained from the reference geometry bottle 250 ml with different gamma-ray energies.

The efficiency curve in fig.4 shows the energy range 46.54-1836 KeV as well as two regions of different behavior because distinct attenuation and absorption processes dominate. At low energies, the efficiency rises rapidly because of abrupt reduction in the attenuation in

radioactive source, detector cap or inner dead layer. A maximum is reached for an energy value which depends on the detector and source characteristics. Above a few hundreds KeV the efficiency decreases monotonically.

2.3.3: Calculation Specific Activity

Absolute Efficiency, ϵ_{abs} would be used to calculate the specific activity in Bq.kg^{-1} . Therefore, $A_E \gamma, i$ of a radionuclide i and a peak at energy $E\gamma$, is given by

$$A_E (\gamma, i) = \frac{NP}{t_c \cdot I_\gamma(E_\gamma) \epsilon(E_\gamma) \cdot M} \quad (10)$$

Where NP is the number of counts in a given peak area corrected for background peaks of a peak at energy $E\gamma$, $\epsilon(E_\gamma)$ the detection efficiency at energy $E\gamma$, t_c is the counting lifetime in second, $I_\gamma(E_\gamma)$, the number of gammas per disintegration of this nuclide for a transition at energy $E\gamma$, and M is the weight of the measured food or environmental samples in kg [6].

2.4: Discussion and Analysis

The Laboratory-based Environmental Gamma Spectrometry is a multidisciplinary research tool for detection and measurement of activity and energy in different radionuclides. The state of the art Environmental Gamma Spectrometry is High Purity Germanium (HPGe) detector, Cooling System, Shielding, the associated processing electronics, Gamma acquisition and analysis software. Although there are many other components that constitute the system, the performance and ability of the system mainly depends on the right choice of the detector. Therefore, the characteristic parameters such as MDA, depends on detector resolution, background energy and detector efficiency, appropriate cooling and shielding arrangement should be taken in consideration while selecting a detector for a specific application. Moreover, detector types like coaxial, well-type or broad energy as well as dominant carriers n-type or p-type also essential. The system optimization can be done through CSS, thickness of windows, dead layers and absorption process. The efficiency of the detector depends not only on gamma abundance but also on geometric effects and coincidence summing. Monte Carlo simulation of the system for incomplete charge collection module may enhance the system performance. The sample metrics and sample geometry affect the performance of the Gamma Spectrometry in the same way. The associated processing electronics must be wide flexibility and good agreement with detector system. The standardization and accreditation of the acquisition and analysis software should be maintained.

III. CONCLUSION

An ample study of laboratory-based Gamma Spectrometry for food and environmental samples has

been presented in this paper. Syntheses of the system components, system evaluation and optimization have been provided. User interface regarding Gamma Acquisition and Analysis, efficiency calibration, energy calibration and factors affecting the efficiency calibration also have been described briefly. The system is suitable for identifying concentration of low to high energy environmental radiotracers.

ACKNOWLEDGEMENTS

The authors wish to express deep gratitude to Dr. Dilip Kumar Saha, Chairman, Engr. Jafar Sadique, Member (Engineering), Mr. Mahbubul Hoq, Member (Physical Science) and Dr. Imtiaz Kamal, Member (Planning and Development), Bangladesh Atomic Energy Commission for their support and cooperation in the research.

REFERENCES

- [1] F. J. Hernandez "Optimization of environmental gamma spectrometry using Monte Carlo methods" Ph.D. thesis, Uppsala University, Sweden. 2002.
- [2] Jeong Hee Han and Jeong-Heon Choi, Broad Energy HPGe Gamma Spectrometry for Dose Rate Estimation for Trapped Charge Dating, J. of Analytical Sci. & Technol., Vol. 1(2), pp.98 -108, 2010.
- [3] ORTEC, The Best Choice of High Purity Germanium (HPGe) Detector, www.ortec.com, Available on-line 2013.
- [4] Nurul Absar "Study of the Radioactivity in Soil and Tea Leaf and Transfer Factor of Radionuclides", M.Phil. thesis, Chittagong University, Bangladesh, 2012.
- [5] D. Willems, H. van der Weijden, Thales Cryogenics B.V.- J. Douwen, State-of-the art cryocooler solutions for HPGe detectors, www.canberra.com, Available on-line 2013.
- [6] S. Harb, K. Salahel Din and A. abbady, Study of Efficiency Calibrations of HPGe Detectors for Radioactivity Measurements of Environmental Samples, Proc. of the 3rd Envi. Phys. Conf., Aswan, Egypt-207, 19-23 Feb. 2008.
- [7] ORTEC Solid-State Photon Detector Operator's Manual, Revision B, USA, 2012.
- [8] Genie™ 2000 Tutorials, 3.1 Basic Spectroscopy Software and Documentation, Canberra Industries, Inc, USA, 2006.
- [9] IAEA, Measurement of Radionuclides in Food and the Environment, Technical Reports Series 295, 1989.
- [10] ICRP, Radionuclide Transformation, International Commission on Radiological Protection, Oxford: Pergamon Press, 1983.

Deterministic Stabilization of a Dynamical System using a Computational Approach

Isobeye George¹, Jeremiah U. Atsu², Enu-Obari N. Ekaka-a³

¹Department of Mathematics/Statistics, Ignatius Ajuru University of Education, PMB 5047, Port Harcourt, Nigeria,

²Department of Mathematics/Statistics, Cross River University of Technology, Calabar, Nigeria,

³Department of Mathematics, Rivers State University, Port Harcourt, Nigeria.

Abstract— The qualitative behavior of a multi-parameter dynamical system has been investigated. It is shown that changes in the initial data of a dynamical system will affect the stabilization of the steady-state solution which is originally unstable. It is further shown that the stabilization of a five-dimensional dynamical system can be used as an alternative method of verifying qualitatively the concept of the stability of a unique positive steady-state solution. These novel contributions have not been seen elsewhere; these are presented and discussed in this paper.

Keywords— Deterministic, stabilization, dynamical system, steady-state solution, changing initial data.

I. INTRODUCTION

Agarwal and Devi (2011) studied in detail the mathematical analysis of a resource-dependent competition model using the method of local stability analysis. Other relevant mathematical approaches to the concept of stability analysis have been done [Rescigno (1977);Hallam, Clark and Jordan (1983);Hallam, Clark and Lassiter (1983);Hallam and Luna (1984);Freedman and So (1985); Lancaster and Tismenetssky (1985);De Luna and Hallam (1987); Zhien and Hallam (1987);Freeman and Shukla (1991);Huaping and Zhien (1991);Garcia-Montiel and Scatena (1994); Chattopadhyay (1996);Hsu and Waltman (1998); Dubey and Hussain (2000);Hsu, Li and Waltman (2000);Thieme (2000); Shukla, Agarwal, Dubey and Sinha (2001); Ekaka-a (2009); Shukla, Sharma, Dubey and Sinha (2009); Yan and Ekaka-a (2011);Dhar, Chaudhary and Sahu (2013); Akpodee and Ekaka-a (2015)]. The method of this present study uses the technique of a numerical simulation to quantify the qualitative characteristics of a complex dynamical system with changing initial data.

II. MATHEMATICAL FORMULATION

We have considered the following continuous multi-parameter system of nonlinear first order ordinary differential equations indexed by the appropriate initial conditions according to Agarwal and Devi (2011):

$$\frac{dx_1}{dt} = a_1x_1 - a_2x_1^2 - \alpha x_1x_2 + \alpha_1x_1R - k_1\delta_1x_1T, \quad x_1(0) = x_{10} \geq 0, \quad (1a)$$

$$\frac{dx_2}{dt} = b_1x_2 - b_2x_2^2 - \beta x_1x_2 + \beta_1x_2R - k_2\delta_2x_2T, \quad x_2(0) = x_{20} \geq 0, \quad (1b)$$

$$\frac{dR}{dt} = c_1R - c_2R^2 - \alpha_1x_1R - \beta_1x_2R - k\gamma RT, \quad R(0) = R_0 \geq 0, \quad (1c)$$

$$\frac{dP}{dt} = \eta x_1 + \eta x_2 - (\lambda_0 + \theta)P, \quad P(0) = P_0 \geq 0, \quad (1d)$$

$$\frac{dT}{dt} = Q + \mu\theta P - \delta_0T - \delta_1x_1T - \delta_2x_2T - \gamma RT, \quad T(0) = T_0 \geq 0, \quad (1e)$$

where

x_1 and x_2 are the densities of the first and second competing species, respectively, R is the density of resource biomass, P is the cumulative concentration of precursors produced by species forming the toxicant, T is the concentration of the same toxicant in the environment under consideration, Q is the cumulative rate of emission of the same toxicant into the environment from various external sources, a_1 and b_1 are the intrinsic growth rates of the first and second species, respectively, a_2 and b_2 are intraspecific interference coefficients, α , β are the interspecific interference coefficients of first and second species, respectively, α_1 and β_1 are the growth rate coefficients of first and second species, respectively due to resource biomass. k_1 , k_2 and k are fractions of the assimilated amount directly affecting the growth rates of densities of competing species and resource biomass, η is the growth rate coefficient of the cumulative concentration of precursors. λ_0 is its depletion rate coefficient due to natural factors whereas θ is the depletion rate coefficient caused by its transformation into the same toxicant of concentration T . μ is the rate of the formation of the toxicant from precursors of competing species. δ_1 , δ_2 and γ are the rates of depletion of toxicant in the environment due to uptake of toxicant by species and their resource biomass, respectively.

It is assumed that the resource biomass grows logistically with the supply rate of the external resource input to the system by constant c_1 and its density reduces due to certain

degradation factors present in the environment at a rate c_2 . It is further assumed that the toxicant in the environment is washed out or broken down with rate δ_0 .

Research Question

For the purpose of this study, we have considered the following vital research question: How does a given dynamical multi-parameter system of continuous nonlinear first-order ordinary differential equations respond to a qualitative characteristic, that is, assuming a point $(x_{1e}, x_{2e}, R_e, P_e, T_e)$ is an arbitrary steady-state solution, as the independent variable t approaches infinity ($t \rightarrow \infty$), do $x_1 \rightarrow x_{1e}$, $x_2 \rightarrow x_{2e}$, $R \rightarrow R_e$, $P \rightarrow P_e$, $T \rightarrow T_e$ under some simplifying initial conditions? This mathematical idea is a necessary and sufficient condition that quantifies the concept of the stabilization of the steady-state solution $(x_{1e}, x_{2e}, R_e, P_e, T_e)$ (Yan and Ekaka-a, 2011). In other words, for a complex system of nonlinear first-order ordinary differential equations whose interacting functions are continuous and partially differentiable, what is the likely qualitative characteristic of such a system? The focus of this chapter will tackle the following proposed problem that is clearly defined next.

Research Hypothesis

It is a well-established ecological fact that the initial ecological data, which mathematicians called initial conditions, are not static characteristic values of a

dynamical system. The corresponding core research question is, when the initial data change, how does the dynamical system respond to this change over a longer period of time? This hypothesis if successfully tested and proved in this research, has the potential to provide an insight in the further study of ecosystem stability and ecosystem planning.

Method of Analysis

A well-defined MATLAB ODE45 function has been used to construct tables to determine the effect of changing values of initial data on the stability of the dynamical system for large values of the independent variable t . Following Agarwal and Devi (2011), the values of parameter values which are used in the numerical simulations for system (1) are:

$$a_1 = 5, \quad a_2 = 0.22, \quad \alpha = 0.007, \quad \alpha_1 = 0.2, \quad k_1 = 0.1, \\ \delta_1 = 0.05, \quad b_1 = 3, \quad b_2 = 0.26, \quad \beta = 0.008, \quad \beta_1 = 0.04, \\ k_2 = 0.2, \quad \delta_2 = 0.04, \quad \eta = 0.5, \quad \lambda_0 = 0.01, \\ \theta = 3, \quad \mu = 0.2, \quad \delta_0 = 7, \quad \gamma = 0.3, \quad c_1 = 10, \\ c_2 = 0.3, \quad k = 0.1, \quad Q = 30.$$

III. RESULTS AND DISCUSSIONS

Some twenty (20) numerical simulations are observed to determine the effect of changing values of initial data on the stability of the dynamical system for $t = 3650$ days as shown in Table 1 below:

Table.1: Numerical simulation of a dynamical system for changing initial data at $t = 3650$ days, using a MATLAB ODE45 numerical scheme.

Example	Initial Data (ID)	Independent Variable t days	x_{1e}	x_{2e}	R_e	P_e	T_e
1	1	3650	25.4443	15.2308	30.7270	6.7195	2.1454
2	2	3650	25.3091	15.2308	30.6851	6.7195	2.1086
3	3	3650	25.3551	15.2308	30.6872	6.7195	2.1054
4	4	3650	25.3783	15.2308	30.6901	6.7195	2.1042
5	5	3650	25.3923	15.2308	30.6931	6.7195	2.1041
6	6	3650	25.4018	15.2308	30.6958	6.7195	2.1046
7	7	3650	25.4085	15.2308	30.6983	6.7195	2.1055
8	8	3650	25.4129	15.2308	30.6979	6.7195	2.1066
9	9	3650	25.4169	15.2308	30.6997	6.7195	2.1080
10	10	3650	25.4202	15.2308	30.7014	6.7195	2.1094
11	11	3650	25.4229	15.2308	30.7030	6.7195	2.1108
12	12	3650	25.4252	15.2308	30.7045	6.7195	2.1123
13	13	3650	25.4272	15.2308	30.7058	6.7195	2.1138
14	14	3650	25.4288	15.2308	30.7071	6.7195	2.1153
15	15	3650	25.4303	15.2308	30.7083	6.7195	2.1168
16	16	3650	25.4316	15.2308	30.7094	6.7195	2.1183

Example	Initial Data (ID)	Independent Variable t days	x_{1e}	x_{2e}	R_e	P_e	T_e
17	17	3650	25.4328	15.2308	30.7105	6.7195	2.1197
18	18	3650	25.4338	15.2308	30.7115	6.7195	2.1211
19	19	3650	25.4347	15.2308	30.7125	6.7195	2.1225
20	20	3650	25.4356	15.2308	30.7134	6.7195	2.1239

where

- ID 1 = (2, 0.01, 0.01, 0.1, 0.1), ID 2 = (0.10, 0.01, 0.01, 0.1, 0.1),
- ID 3 = (0.15, 0.01, 0.01, 0.1, 0.1), ID 4 = (0.20, 0.01, 0.01, 0.1, 0.1),
- ID 5 = (0.25, 0.01, 0.01, 0.1, 0.1), ID 6 = (0.30, 0.01, 0.01, 0.1, 0.1),
- ID 7 = (0.35, 0.01, 0.01, 0.1, 0.1), ID 8 = (0.40, 0.01, 0.01, 0.1, 0.1),
- ID 9 = (0.45, 0.01, 0.01, 0.1, 0.1), ID 10 = (0.50, 0.01, 0.01, 0.1, 0.1),
- ID 11 = (0.55, 0.01, 0.01, 0.1, 0.1), ID 12 = (0.60, 0.01, 0.01, 0.1, 0.1),
- ID 13 = (0.65, 0.01, 0.01, 0.1, 0.1), ID 14 = (0.70, 0.01, 0.01, 0.1, 0.1),

- ID 15 = (0.75, 0.01, 0.01, 0.1, 0.1), ID 16 = (0.80, 0.01, 0.01, 0.1, 0.1),
- ID 17 = (0.85, 0.01, 0.01, 0.1, 0.1), ID 18 = (0.90, 0.01, 0.01, 0.1, 0.1),
- ID 19 = (0.95, 0.01, 0.01, 0.1, 0.1), ID 20 = (1, 0.01, 0.01, 0.1, 0.1).

Considering Table 1, we deduced mathematically that, as $t \rightarrow \infty$ for the given initial conditions, $x_1 \rightarrow x_{1e}$, $x_2 \rightarrow x_{2e}$, $R \rightarrow R_e$, $P \rightarrow P_e$, $T \rightarrow T_e$. We have shown that as the initial data are changing, the system is approaching its steady-state. This shows that changes in the initial data of a dynamical system will affect the stabilization of the steady-state solution which is originally unstable.

Table.2: Test of stability of steady-state solutions for changing values of initial data, using a MATLAB ODE45 numerical scheme.

Example	Initial Data (ID)	Steady-state solution (or point)	λ_1	λ_2	λ_3	λ_4	λ_5	TOS
1	1	1	-18.1705	-9.3804	-5.7543	-3.0150	-4.0180	Stable
2	2	2	-18.1498	-9.3527	-5.6958	-3.0150	-4.0180	Stable
3	3	3	-18.1527	-9.3547	-5.7159	-3.0150	-4.0185	Stable
4	4	4	-18.1547	-9.3568	-5.7260	-3.0150	-4.0186	Stable
5	5	5	-18.1563	-9.3589	-5.7321	-3.0150	-4.0187	Stable
6	6	6	-18.1576	-9.3607	-5.7362	-3.0150	-4.0187	Stable
7	7	7	-18.1587	-9.3623	-5.7391	-3.0150	-4.0186	Stable
8	8	8	-18.1588	-9.3621	-5.7411	-3.0150	-4.0187	Stable
9	9	9	-18.1596	-9.3633	-5.7428	-3.0150	-4.0187	Stable
10	10	10	-18.1604	-9.3644	-5.7442	-3.0150	-4.0187	Stable
11	11	11	-18.1610	-9.3654	-5.7453	-3.0150	-4.0186	Stable
12	12	12	-18.1616	-9.3664	-5.7463	-3.0150	-4.0186	Stable
13	13	13	-18.1622	-9.3672	-5.7472	-3.0150	-4.0186	Stable
14	14	14	-18.1627	-9.3680	-5.7478	-3.0150	-4.0185	Stable
15	15	15	-18.1632	-9.3688	-5.7485	-3.0150	-4.0185	Stable
16	16	16	-18.1637	-9.3695	-5.7490	-3.0150	-4.0185	Stable
17	17	17	-18.1641	-9.3701	-5.7495	-3.0150	-4.0185	Stable
18	18	18	-18.1645	-9.3708	-5.7500	-3.0150	-4.0184	Stable
19	19	19	-18.1649	-9.3714	-5.7505	-3.0150	-4.0184	Stable
20	20	20	-18.1653	-9.3720	-5.7507	-3.0150	-4.0184	Stable

where

Point 1 = (25.4443, 15.2308, 30.7270, 6.7195, 2.1454),
 Point 2 = (25.3091, 15.2308, 30.6851, 6.7195, 2.1086),
 Point 3 = (25.3551, 15.2308, 30.6872, 6.7195, 2.1054),
 Point 4 = (25.3783, 15.2308, 30.6901, 6.7195, 2.1042),
 Point 5 = (25.3923, 15.2308, 30.6931, 6.7195, 2.1041),
 Point 6 = (25.4018, 15.2308, 30.6958, 6.7195, 2.1046),
 Point 7 = (25.4085, 15.2308, 30.6983, 6.7195, 2.1055),
 Point 8 = (25.4129, 15.2308, 30.6979, 6.7195, 2.1066),
 Point 9 = (25.4169, 15.2308, 30.6997, 6.7195, 2.1080),
 Point 10 = (25.4202, 15.2308, 30.7014, 6.7195, 2.1094),
 Point 11 = (25.4229, 15.2308, 30.7030, 6.7195, 2.1101),
 Point 12 = (25.4252, 15.2308, 30.7045, 6.7195, 2.1123),
 Point 13 = (25.4272, 15.2308, 30.7058, 6.7195, 2.1138),
 Point 14 = (25.4288, 15.2308, 30.7071, 6.7195, 2.1153),
 Point 15 = (25.4303, 15.2308, 30.7083, 6.7195, 2.1168),
 Point 16 = (25.4316, 15.2308, 30.7094, 6.7195, 2.1183),
 Point 17 = (25.4328, 15.2308, 30.7105, 6.7195, 2.1197),
 Point 18 = (25.4338, 15.2308, 30.7115, 6.7195, 2.1211),
 Point 19 = (25.4347, 15.2308, 30.7125, 6.7195, 2.1225),
 Point 20 = (25.4356, 15.2308, 30.7134, 6.7195, 2.1239).

What do we learn from Table 2? On the basis of this sophisticated computational approach which we have not seen elsewhere, we hereby infer that the stabilization of a five-dimensional dynamical system can be used as an alternative method of verifying qualitatively the concept of the stability of a unique positive steady-state solution which could have been a daunting task to resolve analytically.

However, this key contribution is only valid as long as the intrinsic growth rate a_1 is bigger than the intra-competition coefficient a_2 of the first competing species; the intrinsic growth rate b_1 is bigger than the intra-competition coefficient b_2 of the second competing species and the intrinsic growth rate of the resource biomass c_1 is bigger than the intra-competition coefficient c_2 of the resource biomass. In the event that the intra-competition coefficients of these three populations outweigh their corresponding intrinsic growth rates, will the specified steady-state solutions still be stable? Without loss of generality, it is interesting to observe that each of the twenty (20) stable steady-state solutions is also qualitatively well-defined within the choice of the model dynamics in the absence of proper model parameter estimation. The idea is consistent with the earlier discovery of Ekaka-a (2009).

IV. CONCLUSION AND RECOMMENDATION

We have shown in this research that stabilization is an alternative way of testing for stability. Therefore, the application of a computational approach in the determination of the stability characteristic using the concept of stabilization is one of the contributions of this

work that can be used to move the frontier of knowledge in the field of numerical mathematics with respect to stability of a dynamical system. We recommend a further investigation of the effect of fixed initial data for changing values of the independent variable.

REFERENCES

- [1] Agarwal, M. and Devi, S. (2011). A resource-dependent competition model: Effects of toxicant emitted from external sources as well as formed by precursors of competing species. *Nonlinear Analysis: Real World Application*, 12, 751–766.
- [2] Akpodee, R. E. and Ekaka-a, E. N. (2015). Deterministic stability analysis using a numerical simulation approach, *Book of Proceedings – Academic Conference Publications and Research International on Sub-Sahara African Potentials in the new Millennium*, 3(1).
- [3] Chattopadhyay, J. (1996). Effects of toxic substances on a two-species competitive system, *Ecological Model*, 84, 287 – 289.
- [4] Dhar, J., Chaudhary, M. and Sahu, G. P. (2013). Mathematical model of depletion of forestry resource, effect of synthetic-based industries. *International Journal of Biological, Life Science and Engineering*, 7, 1 – 5.
- [5] De Luna, J. T. and Hallam, T. G. (1987). Effects of toxicants on populations: a qualitative approach IV. Resource-consumer-toxicant model, *Ecological Model*, 35, 249 – 273.
- [6] Dubey, B. and Hussain, J. (2000). A model for allelopathic effect on two competing species, *Ecological Model*, 129, 195 – 207.
- [7] Ekaka-a, E. N. (2009). *Computational and mathematical modeling of plant species interactions in a harsh climate*, Ph. D Thesis, University of Liverpool and University of Chester, United Kingdom.
- [8] Freedman, H. I. and Shukla, J. B. (1991). Models for the effect of toxicant in single species and predator–prey systems, *Journal of Mathematical Biology*, 30, 15–30.
- [9] Freedman, H. I. and So, J. W. H. (1985). Global stability and persistence of simple food chains, *Mathematical Bioscience*, 76, 69 – 86.
- [10] Garcia-Montiel, D. C. and Scantena, F. N. (1994). The effects of human activity on the structure composition of a tropical forest in Puerto Rico, *Forest Ecological Management*, 63, 57 – 58.
- [11] Hallam, T. G., Clark, C. E., and Jordan, G. S. (1983). Effects of toxicants on populations: a qualitative

- approach II. First order kinetics, *Journal of Mathematical Biology*, 18, 25 – 37.
- [12] Hallam, T. G., Clark, C. E., and Lassiter, R. R. (1983). Effects of toxicants on populations: a qualitative approach I. Equilibrium environmental exposure. *Ecological Model*, 18, 291–304.
- [13] Hallam T. G. and De Luna, J. T. (1984). Effects of toxicants on populations: a qualitative approach III. Environmental and food chain pathways, *Journal of Theoretical Biology*, 109, 411 – 429.
- [14] Hsu, S. B., Li, Y. S. and Waltman, P. (2000). Competition in the presence of a lethal external inhibitor, *Mathematical Bioscience*, 167, 177 – 199.
- [15] Hsu, S. B. and Waltman, P (1998). Competition in the chemostat when one competitor produces a toxin, *Japan Journal of Industrial and Applied Mathematics*, 15, 471–490.
- [16] Huaping, L, and Zhien, M. (1991). The threshold of survival for system of two species in a polluted environment, *Journal of Mathematical Biology*, 30, 49 – 61.
- [17] Lancaster, P. L. and Tismenetsky, M (1985). *The Theory of Matrices*, Second Edition, Academic Press, New York.
- [18] Rescigno, A. (1977). The struggle for life – V. One species living in a limited environment, *Bulleting of Mathematical Biology*, 39, 479 – 485.
- [19] Shukla, J. B., Agarwal, A., Dubey, B. and Sinha, P. (2001). Existence and survival of two competing species in a polluted environment: a mathematical model, *Journal of Biological Systems*, 9(2), 89 – 103.
- [20] Shukla, J. B., Sharma, S., Dubey, B. and Sinha, P. (2009). Modeling the survival of a resource-dependent population: Effects of toxicants (pollutants) emitted from external sources as well as formed by its precursors, *Nonlinear Analysis: Real World Application*, 54–70.
- [21] Thieme, H. R. (2000). Uniform persistence and permanence for non-autonomous semi-flows in population biology, *Mathematical Bioscience*, 166, 173 – 201.
- [22] Yan, Y. and Ekaka-a, E. N. (2011). Stabilizing a mathematical model of population system, *Journal of the Franklin Institute*, 348(10), 2744 – 2758.
- [23] Zhien, M. and Hallam, T. G. (1987). Effects of parameter fluctuations on community survival. *Mathematical Bioscience*, 86, 35 – 49.

Simulation modeling of the sensitivity analysis of differential effects of the intrinsic growth rate of a fish population: its implication for the selection of a local minimum

Nwachukwu Eucharia C.¹, Ekaka-a Enu-Obari N.², Atsu Jeremiah U.³

¹Department of Mathematics and Statistics, University of Port Harcourt, Port Harcourt, Nigeria

²Department of Mathematics, Rivers State University, Nkpolu, Port Harcourt, Nigeria

³Department of Mathematics/Statistics, Cross River University of Technology, Calabar, Nigeria.

Abstract— *The vulnerability of the differential effects of the intrinsic growth rates of the fish population on the uncertainty analysis can only be controlled by using the mathematical technique of a sensitivity analysis that is called a local minimum selection method based on a Matlab numerical scheme of ordinary differential equations of order 45 (ODE 45). The quantification of the p-norms sensitivity analysis depends on the application of the 1-norm, 2-norm, 3-norm, 4-norm, 5-norm, 6-norm and infinity-norm. In the context of this study, the best-fit intrinsic growth rate of fish population with a small error has occurred when its value is 0.303 which minimizes the bigger sensitivity values previously obtained irrespective of the p-norm sensitivity values. The novel results which we have obtained have not been seen elsewhere. These results are fully presented and discussed in this study.*

Keywords— *Uncertainty analysis, differential effects, p-norms sensitivity analysis, intrinsic growth rate, local minimum, ODE45.*

I. INTRODUCTION

Following Ekaka-a et al (2012), sensitivity analysis is a measure of the resultant effect due to a variation of a model parameter value on the model solution trajectories. It is a mathematical tool to enhance model validation and prediction. On the other hand, on-going debate among many researchers including Palumbi (1999), Sumali (2002), Pitchford (2007) and Bohnsack (1993) has shown that marine reserve is not only economically important but can also serve as a tool for equitable management of biodiversity especially in the context of fisheries. Kar and Charkraborty (2009), in their work titled marine reserves and its consequences as a fisheries management tool

described a prey-predator type fishing model with prey dispersed in a 2-patch environment, one of which is called a free fishing zone and another, a protected zone. Their main method of investigation uses the simulation process. One key contribution from their work states that prey-predator dichotomy do not matter when implementation of a reserve is considered. Their second result shows that reserves will be most effective when coupled with fishing effort controls in adjacent fisheries. Despite the fact that marine reserves and its consequences can be effectively utilized as a fisheries management tool, it is still an open research problem that these authors did not consider the technique of sensitivity analysis which is vital numerical incentive in a decision process that can lead to an effective fisheries management.

It remains an open problem to study the differential effects of varying the intrinsic growth rate of the fish population on the uncertainty analysis using a one-at-a-time sensitivity analysis Hamby 1995. It is against this background that we propose to use ODE45 RungeKutta numerical scheme with initial condition $2 \times 4 \times 2$ over a period of fifty (50) weeks to study the differential effects of the intrinsic growth rate of fish population on the sensitivity analysis that is indexed by seven classifications of the sensitivity analysis, namely: 1-norm error analysis, 2-norm error analysis, 3-norm error analysis, 4-norm error analysis, 5-norm error analysis, 6-norm error analysis and infinity-norm error analysis.

II. MATHEMATICAL FORMULATIONS

The mathematical model for this research work is based on the published article by Kar and Charkraborty (2009) given by the first order non-linear ordinary differential equations

which describes the prey-predator fisheries management model. Hence, we modify the model as follows:

$$\frac{d}{dt}x(t) = r_1x(t) - \beta_1x(t)^2 - \mu_1x(t)y(t) - \frac{\sigma}{\alpha}x(t) + \frac{\sigma}{\alpha-1}y(t) - mx(t)z(t) \quad (3.1)$$

$$\frac{d}{dt}y(t) = r_2y(t) - \beta_2x(t)y(t) - \mu_2y(t)^2 + \frac{\sigma}{\alpha}x(t) - \frac{\sigma}{\alpha-1}y(t) - ny(t)z(t) - qEy(t) \quad (3.2)$$

$$\frac{d}{dt}z(t) = r_3z(t) - \frac{r_3\gamma z(t)^2}{x(t)+y(t)} \quad (3.3)$$

$$x(0) = 2, y(0) = 4, z(0) = 2 \quad (3.4)$$

In this model, $x(t)$ represents the fish stock in the reserved area at time t , $y(t)$ is the fish stock in the unreserved area at time t , $z(t)$ is the biomass density of the predator species at time t . r_1 is the intrinsic growth rate of fish stock x , r_2 is the intrinsic growth rate of fish stock y , r_3 is the intrinsic growth rate of the predator species, γ is the equilibrium ratio between prey biomass and predator biomass, m is maximum relative increase in predation to the reserved area or simply put, the contribution of z to inhibit the growth of fish stock (x) in the reserved area, n is maximum relative increase in predation to the unreserved area or simply put, the contribution of z to inhibit the growth of fish stock (y) in the unreserved area. The predation terms are therefore defined as mxz and nyz with respect to fish stocks in the reserved and unreserved area respectively. In addition, σ is the mobility coefficient, α is the size of the reserved area, $1 - \alpha$ is the size of the unreserved area, q is catch ability coefficient, E is effort applied for harvesting fish population in the unreserved area.

Further mathematical interpretation can be invoked to describe the interaction of the three equations. In equation (3.1), $\frac{d}{dt}x(t) = r_1x(t)$ shows that without interaction with other y and z species, the x population grows unboundedly as time increases. The same observation is made for the y and z populations. This is mathematically correct but practically unrealistic, hence the need for the interaction between the species. We can deduce the following interpretations term by term:

$\beta_1x(t)^2$ is the contribution of fish stock in the reserved area to inhibits its original exponential growth.

$\mu_1x(t)y(t)$ is the contribution of fish stock in the unreserved area to inhibit the growth of fish population in the reserved area.

$\frac{\sigma}{\alpha}x(t)$ is the effect of the ratio of the migration rate/mobility coefficient to the size of the reserve area to inhibit the growth of fish stock in the reserved area

$\frac{\sigma}{\alpha-1}y(t)$ is the effect of the ratio of the migration rate/mobility coefficient to the size of the unreserved area to enhance the growth of fish stock in the reserved area

$mx(t)z(t)$ is the contribution of z to inhibit the growth of fish stock on the reserve area

$\beta_2x(t)y(t)$ is the contribution of fish stock in the reserved area to inhibit the growth of fish population in the unreserved area.

$\mu_2y(t)^2$ is the contribution of fish stock in the unreserved area to inhibits its original exponential growth.

$\frac{\sigma}{\alpha}x(t)$ is the effect of the ratio of the migration rate/mobility coefficient to the size of the reserve area to inhibit the growth of fish stock in the unreserved area

$\frac{\sigma}{\alpha-1}y(t)$ is the effect of the ratio of the migration rate/mobility coefficient to the size of the unreserved area to inhibit the growth of fish stock in the unreserved area

$ny(t)z(t)$ is the contribution of the predator biomass to inhibit the growth of fish stock on the unreserved area

$qEy(t)$ is the contributed effect of the fishing effort and Catchability coefficient to inhibit the growth of the fish stock in the unreserved area.

$\frac{r_3\gamma z(t)^2}{x(t)+y(t)}$ is equilibrium ratio on the fish stocks in the reserved and unreserved area due to activities of the predator biomass.

For the purpose of our mathematical analysis, the value for model parameter r is the same value for: $r_1, r_2, \beta_1, \beta_2, \mu_1, \mu_2$ and $s = r_3$. In addition, we shall adopt the model parameter values as proposed by Kar and Charkraborty (2009): $r = 0.3, \sigma = 0.2, m = 1, n = 1, q = 0.0025, s = 0.1, \gamma = 0.95, E = 95$.

III. METHOD OF ANALYSIS

The core part of the algorithm which we have utilized to calculate the sensitivity of a model parameter is hereby described by the following steps which has also been implemented in the work of Ekaka-a et al (2013):

Step I: identify and code the control system of given model equations of continuous non-linear first order ordinary differential equation in which the model parameter is not varied. For the purpose of this analysis, the three solution trajectories are denoted by $x, y,$ and z .

Step II: identify and code a sub-model of the control system of given model equations of continuous non-linear

first order ordinary differential equation in which the model parameter is varied one-at-a-time. In this case, the three solution trajectories are denoted by x_m , y_m , and z_m .

Step III : code an appropriate Matlab program using ODE Runge-Kutta scheme to execute the program in Step I and Step II. With the initial conditions and a time range, the execution program will produce the solution trajectories for the programs in step I and step II.

On the execution program, specify the difference between the solution trajectories of the codes in step I and step II as $F_1 = x - x_m$, $F_2 = y - y_m$ and $F_3 = z - z_m$

Step IV: Use the execution program to calculate the 1-norm, 2-norm, 3-norm, 4-norm, 5-norm, 6-norm and infinity-norm for the three solution trajectories of the control model equations and similarly for the solution trajectories for the difference between the solution trajectories. For example, for the x and x_m solution trajectories which assume precise data points such as x_j and x_{mj} , where the subscript j takes on the values of 1, 2, 3, 4, ..., n, the 1-norm for the x solution trajectory is defined as the sum of the absolute values of x_1, x_2, x_3 , up to the n th point x_n . In the same manner, the 2-norm of the x_j solution trajectory is defined by the positive square root of the sum of the squares of absolute values of x_1, x_2, x_3 , up to the n th point x_n . Similarly, the 3-norm for the x solution trajectory is defined as the sum of the absolute values (cubed) of x_1, x_2, x_3 , up to the n th point x_n . The 4-norm for the x solution trajectory is defined as the sum of the absolute values (to fourth power) of x_1, x_2, x_3 , up to the n th point x_n . The 5-norm for the x solution trajectory is defined as the sum of the absolute values (to fifth power) of x_1, x_2, x_3 , up to the n th point x_n . The 6-norm for the x solution trajectory is defined as the sum of the absolute values (to sixth power) of x_1, x_2, x_3 , up to the n th point x_n . The infinity norm for x_m is defined by the maximum value of the set of the absolute values of x_1, x_2, x_3 , up to the n th point x_n . The same procedure holds for the calculation of 1-norm, 2-norm, 3-norm, 4-norm, 5-norm, 6-norm and infinity norm for y and z solution trajectories.

Step V: In the execution program, calculate the difference between the solution trajectories of the control model equation and the varied model equation by $F_1 = x - x_m$, $F_2 = y - y_m$ and $F_3 = z - z_m$ for the given range of data points when $j = 1, 2, 3, 4, \dots, n$ such that the difference between the solution trajectories of the control model equations and the varied model equations would be $F_1 = x_j - x_{mj}$, $F_2 = y_j - y_{mj}$ and $F_3 = z_j - z_{mj}$.

For the purpose of this analysis, we will also calculate the 1-norm, 2-norm, 3-norm, 4-norm, 5-norm, 6-norm and

infinity norm of F_1, F_2 and F_3 . For example, 1-norm of F_1 will be the sum of the absolute values of the data points $(x_1 - x_{m1}), (x_2 - x_{m2}), (x_3 - x_{m3}), (x_4 - x_{m4}), \dots, (x_n - x_{mn})$ where x_1 and x_{m1} stand for the first data point of x solution trajectory and the first data point of the modified x_m solution trajectory respectively. x_2 and x_{m2} stand for the second data point of x solution trajectory and the second data point of the modified x_m solution trajectory respectively and so forth. The 1-norm of F_2 will be the sum of the absolute values of the data points $(y_1 - y_m), (y_2 - y_{m2}), (y_3 - y_{m3}), (y_4 - y_{m4}), \dots, (y_n - y_{mn})$ where y_1 and y_{m1} stand for the first data point of y solution trajectory and the first data point of the modified y_m solution trajectory respectively. y_2 and y_{m2} stand for the second data point of y solution trajectory and the second data point of the modified y_m solution trajectory respectively and so forth. Similarly, the 1-norm of F_3 will be the sum of the absolute values of the data points $(z_1 - z_{m1}), (z_2 - z_{m2}), (z_3 - z_m), (z_4 - z_{m4}), \dots, (z_n - z_{mn})$ where z_1 and z_{m1} stand for the first data point of z solution trajectory and the first data point of the modified z_m solution trajectory respectively. z_2 and z_{m2} stand for the second data point of z solution trajectory and the second data point of the modified z_m solution trajectory respectively and so forth. The 2-norm, 3-norm, 4-norm, 5-norm, 6-norm and infinity norm can similarly be calculated for the differences of three solution trajectories F_1, F_2 and F_3 .

Step VI: To calculate the cumulative percentage effect of variation of a chosen model parameter one-at-a-time when other parameters are fixed on each solution trajectory. For x solution trajectory, we will calculate the following values: (1-norm of F_1 divided by the 1-norm of x) multiplied by 100; (2-norm of F_1 divided by the 2-norm of x) multiplied by 100; (3-norm of F_1 divided by the 3-norm of x) multiplied by 100; (4-norm of F_1 divided by the 4-norm of x) multiplied by 100; (5-norm of F_1 divided by the 5-norm of x) multiplied by 100; (6-norm of F_1 divided by the 6-norm of x) multiplied by 100 and (infinity-norm of F_1 divided by the infinity-norm of x) multiplied by 100.

To calculate the percentage cumulative effect of variation of a model parameter one-at-a-time when other parameters are fixed on y solution trajectory, we will calculate the following values: (1-norm of F_2 divided by the 1-norm of y) multiplied by 100; (2-norm of F_2 divided by the 2-norm of y) multiplied by 100; (3-norm of F_2 divided by the 3-norm of y) multiplied by 100; (4-norm of F_2 divided by the 4-norm of y) multiplied by 100; (5-norm of F_2 divided by the 5-norm of y) multiplied by 100; (6-norm of F_2 divided by

the 6-norm of y) multiplied by 100 and (infinity-norm of F_2 divided by the infinity-norm of y) multiplied by 100.

To calculate the percentage cumulative effect of variation of a model parameter one-at-a-time when other parameters are fixed on z solution trajectory, we will calculate the following values: (1-norm of F_3 divided by the 1-norm of z) multiplied by 100; (2-norm of F_3 divided by the 2-norm of z) multiplied by 100; (3-norm of F_3 divided by the 3-norm of z) multiplied by 100; (4-norm of F_3 divided by the 4-norm of z) multiplied by 100; (5-norm of F_3 divided by the 5-norm of z) multiplied by 100; (6-norm of F_3 divided by the 6-norm of z) multiplied by 100 and (infinity-norm of F_3 divided by the infinity-norm of z) multiplied by 100.

Due to the unstable values of the 1-norm, 2-norm, 3-norm, 4-norm, 5-norm, 6-norm and infinity-norm specifications, we adopt to use a compact value for related percentage values of these norms. For example, the cumulative percentage value of 1-norm sensitivity in terms of the difference in solution trajectories involves the sum of the 1-norm values due to F_1 solution trajectory, 1-norm values due to F_2 solution trajectory and 1-norm values due to F_3 solution trajectory. The same procedure can be followed to calculate the cumulative percentage values for 3-norm, 3-norm, 4-norm, 5-norm, 6-norm and infinity-norm

sensitivities in terms of F_1 solution trajectory, F_2 solution trajectory and F_3 solution trajectory.

The cardinal points of sensitivity analysis results interpretation are:

- ✓ the parameter which when varied a little and produces the biggest cumulative effect on the solution trajectories is called a most sensitive parameter. And it is highly uncertain. This by implication will attract error in prediction and thus require further validation.
- ✓ the parameter which when varied a little and produces lower or least sensitivity values is called a less or least sensitive parameter and requires lesser validation.

Method for Best-fit parameter value selection

In order to select the best-fit parameter value for each model parameter, we recommend that

- ✓ At 100% variation, the coordinates of the solution trajectories have same values, sums, squares and square roots = 0. Therefore, the norm values at 100% are zero.

The Local minimum value is selected at a point where the smallest norm value occurs before or after the 100% variation.

IV. RESULTS AND DISCUSSION

On the application of the define method of analysis, we hereby present and discuss the following results:

Table.1: sensitivity analysis results for model parameter r

r	1-norm	2-norm	3-norm	4-norm	5-norm	6-norm	∞ -norm
0.0030	143.9520	78.8284	82.0093	66.2747	56.624	50.6594	29.8099
0.0060	143.1933	78.4409	81.6042	65.9501	56.348	50.4130	29.6754
0.0090	142.3997	78.0321	81.1766	65.6070	56.056	50.1521	29.5334
0.0120	141.5698	77.6010	80.7256	65.2447	55.747	49.8763	29.3837
0.0150	140.7023	77.1468	80.2503	64.8624	55.421	49.5850	29.2259
0.0180	139.7958	76.6685	79.7499	64.4593	55.077	49.2776	29.0605
0.0210	138.8491	76.1654	79.2236	64.0350	54.715	48.9538	28.8879
0.0240	137.8610	75.6368	78.6706	63.5887	54.334	48.6131	28.7078
0.0270	136.8304	75.0818	78.0903	63.1201	53.934	48.2553	28.5200
0.0300	135.7565	74.4999	77.4821	62.6287	53.514	47.8800	28.3243

What do we learn from Table 1?

We have observed from table 1 that as the value of the model parameter r increases monotonically from 0.003 (approx) to 0.03 (approx), the 1-norm error data decreases monotonically from the value of 143.95 (approx.) to 135.76 (approx.), the 2-norm error data decreases monotonically from the value of 78.83 (approx.) to 75.50 (approx.), the 3-norm error data decreases monotonically from the value of 82.01 (approx.) to 77.48 (approx.), the 4-norm error data

decreases monotonically from the value of 66.27 (approx.) to 62.63 (approx.), the 5-norm error data decreases monotonically from the value of 56.62 (approx.) to 53.51 (approx.), the 6-norm error data decreases monotonically from the value of 50.66 (approx.) to 47.88 (approx.) and the infinity-norm error data decreases monotonically from the value of 29.81 (approx.) to 28.32 (approx.).

On the basis of this present analysis we have observed that $r = 0.003$ is associated with relatively higher uncertainty when compared to the value of $r = 0.03$ irrespective of the type of p -norm we have used to calculate the sensitivity analysis. Despite the observed uncertainty analysis results due to a one percent to ten percent variation of the intrinsic growth rate of the fish population, it is clear that the statistical range of the p -norm sensitivity values are listed as follows: the range of 1-norm statistical range is 8.19, the

range of 2-norm statistical range is 3.33, the range of 3-norm statistical range is 4.53, the range of 4-norm statistical range is 3.64, the range of 5-norm statistical range is 3.11, the range of 6-norm statistical range is 2.78, the range of infinity-norm statistical range is 1.49.

These bigger sensitivity values which indicate high uncertainty of the intrinsic growth rate of the fish population can be further minimized.

Table.2: local minimum results for parameter r

r	1-norm	2-norm	3-norm	4-norm	5-norm	6-norm	∞ -norm
0.2880	4.3024	2.2917	2.4375	2.0011	1.739	1.5812	1.0897
0.2910	3.2128	1.7106	1.8194	1.4936	1.298	1.1803	0.8137
0.2940	2.1326	1.1350	1.2072	0.9910	0.861	0.7831	0.5401
0.2970	1.0617	0.5648	0.6007	0.4931	0.429	0.3897	0.2688
0.3000	0.0000	0.0000	0.0000	0.0000	0.000	0.0000	0.0000
0.3030	1.0527	0.5595	0.5951	0.4885	0.425	0.3860	0.2663
0.3060	2.0964	1.1138	1.1847	0.9724	0.845	0.7685	0.5304
0.3090	3.1314	1.6630	1.7688	1.4517	1.262	1.1473	0.7926
0.3120	4.1577	2.2071	2.3475	1.9265	1.674	1.5225	1.0527
0.3150	5.1755	2.7463	2.9209	2.3969	2.083	1.8943	1.3106

What do we learn from Table 2?

Table 2 shows a result of the cumulative effect of 96 to 105 percent variation of model parameter r . At 100percent variation, there are no changes in the original and the varied solution trajectories, hence the zero values.

Observe that as the model parameter value increase monotonically from a low value of 0.2880 to 0.0000 corresponding to 100 percent variation and then increases monotonically to 0.3150 approximately in column I, the 1-norm sensitivity value decreased monotonically from a value of 4.30 to 0.0000 corresponding 100 percent variation and then increases monotonically to 5.18 approximately in column II, the 2-norm sensitivity value decreased monotonically from a value of 2.29 to 0.0000 corresponding 100percent variation and then increases monotonically to 2.75 approximately in column III, the 3-norm sensitivity value decreased monotonically from a value of 2.44 to 0.0000 corresponding 100percent variation and then increases monotonically to 2.92 approximately in column IV, the 4-norm sensitivity value decreased monotonically from a value of 2.00 to 0.0000 corresponding 100percent variation and then increases monotonically to 2.40 approximately in column V, the 5-norm sensitivity value decreased monotonically from a value of 1.74 to 0.0000 corresponding 100percent variation and then increases monotonically to 2.08 approximately in column VI, the 6-

norm sensitivity value decreased monotonically from a value of 1.58 to 0.0000 corresponding 100percent variation and then increases monotonically to 1.90 approximately in column VII, the infinity-norm sensitivity value decreased monotonically from a value of 1.09 to 0.0000 corresponding 100percent variation and then increases monotonically to 1.31 approximately in column VIII.

The local minimum is selected at the greatest lower bound of the data points for each p -norm results. For instance, the local minimum value for model parameter r is 0.303 where 1-norm local minimum value = 1.0527, 2-norm local minimum value = 0.5595, 3-norm local minimum value = 0.5951, 4-norm local minimum value = 0.4885, 5-norm local minimum value = 0.4250, 6-norm local minimum value = 0.3860 and infinity-norm local minimum value = 0.2663.

V. CONCLUSION

This present study has been able to reduce the uncertainty in the intrinsic growth rate of a fish population due to its variations using a combination of a numerical scheme and the mathematical p -norms. The present results compliment the earlier contribution of Ekaka-a et al (2012) that only considered the sensitivity analysis in the context of a shorter experimental time. This present proposed numerical scheme can be extended to study the sensitivity analysis of other

model parameter values which we did not consider in this study in our future investigation.

REFERENCES

- [1] E. N. Ekaka-a, N. M. Nafu, A. I. Agwu, (2012), Examination of extent of sensitivity of a mathematical model parameter of survival of species dependent on a resource in a polluted environment, International Journal of Information Science and Computer Mathematics, vol. 8, no 1-2, pp 1-8.
- [2] EnuEkaka-a, Olowu, B. U., Eze F. B., Abubakar R. B., Agwu I. A., Nwachukwu E. C., (2013), Journal of Nigerian Association of Mathematical Physics, Vol 23, pp 177-182.
- [3] Palumbi S. (1999). The ecology of marine protected areas: Working paper from the Department of Organismic and Evolutionary Biology, Harvard University.
- [4] Rodwell L. D, Edward B. Barbier, Callum M. Roberts, Tim R. Mcclanahan (2002), A model of tropical marine reserve-fishery linkages. Natural Resource Modeling, 15(4).
- [5] Sumalia U. (2002) Marine protected area performance in a model of the fishery. Natural Resource Modeling, 15(4).
- [6] J. Pitchford, E.Codling, D. Psarra. Uncertainty and sustainability in fisheries. Ecological Modelling, 2007, 207: 286–292.
- [7] Kar, T. and Chakraborty, K. (2009): Marine reserves and its consequences as a fisheries management tool, World Journal of Modelling and Simulation, (2009) 5(2), pp. 83-95.
- [8] J. Bohnsack. Marine reserves: They enhance fisheries, reduce conflicts, and protect resources. Oceanus, 1993,63–71.
- [9] Hamby, D.M. (1994). A review of techniques for parameter sensitivity analysis of environmental models, *Environmental Monitoring and Assessment* 32: 135-154.

Rates of Soft Ground Tunneling in Vicinity of Existing Structures

Ayman S. Shehata¹, Adel M. El-Kelesh², Al-Sayed E. El-kasaby¹, Mustafa Mansour¹

¹Department of Civil Engineering, Benha Faculty of Engineering, Benha University, Egypt

²Construction Engineering and Utilities Department, Faculty of Engineering, and Geo-Construction Research and Development Center (GRDC-ZU), Zagazig University, Egypt

Abstract— *Soft ground tunneling in the vicinity of existing structures is a major challenge to tunneling engineers. Tunneling works cause inevitable ground movements that may lead to unrecoverable damages to adjacent structures. Tunneling rates significantly affect such risks. However, a guideline that determines appropriate tunneling rates and accounts for the effects of tunneling on the structures existing in the vicinity is not available. Tunneling records in terms of TBM advance speed (AS), utilization factor (U), and advance rate (AR) for tunnels constructed without causing significant risks on the existing structures are presented in the paper. These records are discussed for different types of existing structures. Ranges of these records for tunneling without causing detrimental effects on different types existing structures are recommended. Useful observations are also made on the variation of these records with the ground type and composition and the precautions to be adopted to mitigate the tunneling risks on existing structures.*

Keywords— *Soft ground, mechanized tunneling, utilization factor, ground conditions, tunnel boring machine (TBM), productivity, advance speed, advance rate.*

I. INTRODUCTION

The term ‘Hard Point’ is used to describe the structures that exist in the vicinity of tunneling works. The hard points include for instance buildings, footings of bridges and underground utilities such as shafts, sewer tunnels and electrical cables. Excavation by tunnel boring machines (TBMs) inevitably results in ground movements that may cause adjacent structures to deform, distort, and possibly sustain unrecoverable damages. A determination of the appropriate tunneling method that mitigates the tunneling risks on adjacent structures is a major challenge in soft ground tunneling. The difficulty stems from the many and critical factors involved in the process, such as the potential for ground loss because of tunneling, variable ground conditions under a hard point, and effect of tunneling on the integrity of existing structures. Tunneling advance rate, as a tunneling parameter, has

been reported as a factor that affects the ground movements caused by TBM excavation (e.g., Toan and Hung 2007).

Tunnel construction duration is a critical factor in tunneling projects and is estimated on the basis of the tunneling advance rate as follows:

$$D = \frac{L}{AR} \quad (1)$$

where D (days) = construction duration, L (m) = length of tunnel, and AR (m/day) = advance rate of TBM and is defined as the distance of boring and ring erection divided by the total time (shift or day). AR is determined using the following expression

$$AR = \frac{AS \times U \times 60 \times 24}{100000} \quad (2)$$

where AS (mm/min) = advance speed of TBM and is defined as the stroke length of TBM into the ground divided by the operating time of excavation (i.e. the instantaneous penetration rate of TBM), and U (%) = utilization factor of TBM and is defined as the time of excavation by TBM divided by the total time. Therefore, accurate determination of AR or AS and U is necessary for the development of reliable tunnel construction time plans and cost estimate and control.

Management of tunneling works in the vicinity of hard points and the relevant risks necessitates determination of appropriate AR at the hard points. A guideline that determines AR in soft ground in the vicinity of hard points is not available. AR is usually determined on the basis of empiricism and experiences of practitioners. Little effort however has been made to establish a guideline that determines AR and accounts for the different types and conditions of hard points. Moreover, the literature lacks reported data on AR and the corresponding effects on hard points. The current paper presents field records of AR , AS , and U for tunnels actually constructed in Egypt in the vicinity of existing hard points. It also discusses these records for different types of hard points. The paper starts with an elaboration of the effects of tunneling works and rates on the conditions of existing structures in the vicinity of tunneling works. This is followed by a brief description of the project from which the records were obtained. Then, the records are presented and discussed.

II. EFFECT OF TUNNELING RATES ON CONDITION OF EXISTING STRUCTURES

Volumes of excavation larger than the volume of ground occupied by a tunnel are not uncommon in tunneling. Such differences in volumes, known as volume losses, inevitably result in ground movements. Toan and Hung (2007) reported that the net volume of surface settlement trough in most ground conditions is approximately equal to the volume loss because of tunneling. Such ground movements may cause adjacent structures to deform, rotate, distort, and possibly sustain unrecoverable damages (Zhang et al. 2012). Toan and Hung (2007) also indicated that the magnitude of volume loss depends on many different factors such as the tunneling method, tunneling advance rate, tunnel size, and ground type. The existence of structures in the vicinity of a constructed tunnel is therefore rated among the highrisk factors in tunneling in urban areas (Kovari 2004).

It has been reported that the tunneling induced ground movements and thus the risks on adjacent structures can be mitigated by adopting the following measures (e.g., Toan and Hung 2007; Goh et al. 2016; Sheng et al. 2016):

- Adopting appropriate tunneling advance rates to minimize the ground movements caused by the machine ground interaction.
- Adopting larger thrust forces to increase the depth of cutting and maintain the desired advance speed.
- Monitoring the lateral movement of tunnels to ensure that the generated drag forces have insignificant impact on the existing structures.
- The minimum pressure applied at the face should be slightly higher than the hydrostatic pressure, particularly when going below existing structures. This is done mainly by controlling the rotational speed of the screw and the amount of muck discharge at the outlet of the screw conveyor.
- Setting the cutterhead rotation to low revolutions so that any torque spikes that are indicative of obstructions encountered during the course of crossing sensitive structures are easily detected.
- Erecting the lining immediately after excavation and providing tight control of the tunneling process.
- Pre-planning for cutterhead interventions just before the TBMs go below existing structures for checking the cutterhead condition and making any necessary replacements of the cutting tools.

Sheng et al. 2016 reported a significant case history on the tunneling of the Downtown Line Stage 3 (DTL3) of Mass Rapid Transit (MRT) system across Singapore Island. The DTL3 alignment is overcrossing the existing

North East Line (NEL) rail tunnel and undercrossing the existing North South Line (NSL) and Circle Line (CCL) with clear distance of less than one bored tunnel diameter, and overburden ranges from 20.0 to 45.0 m; the diameter of DTL3 is 6.35 m. DTL3 is located approximately 1.3 m above NEL tunnel, 8.7 m below NSL tunnel and 3.3 m below CCL tunnel. The ground consists mainly of siltstone with layers of mudstones and sandstone. They observed that the advance speed of the TBM was reduced to less than 5, 10 – 13, and 8 – 15 mm/min when overcrossing NEL, undercrossing NSL, and undercrossing CCL, respectively.

The aforementioned reveals that TBM tunneling in soft ground may cause significantly detrimental effects on existing structures in the vicinity. In addition, tunneling rate is an important factor that significantly affects the conditions of existing structures in the vicinity of tunneling. Therefore, appropriate tunneling rates should be determined to mitigate tunneling risks on adjacent structures.

III. PROJECT DESCRIPTION AND GROUND CONDITIONS

The network of the Greater Cairo metro consists of three lines (Lines 1 to 3) as shown in Fig. 1. Line 3 is approximately 47.87 km long and consists of 39 stations. The construction of the line has been divided into four main phases as indicated in Figs. 1 and 2 and summarized in Table 1. At the time of publishing this paper, the construction of Phases 1 and 2 has been completed, Phase 3 has been under study, and Phase 4 has been constructed. The types of TBMs used in the line are indicated in Fig. 2 and Table 1. Phases 1 and 4A were fully excavated using slurry TBMs (TBM 1 and 2 for Phase 1 and TBM 4 for Phase 4A) and constructed in 24 and 14 months, respectively. However, Phase 2 was fully excavated in 26 months using two different types of TBMs: Slurry and EPB TBMs. The tunnel segment extending from Abbasia station to Cairo Fair station (Lot 11-c) was fully excavated using TBM 2, while that extending from Cairo Fair station to Haroun station was fully excavated using EPB TBM (TBM 3).

Field records of the construction of Lot 11-c (Phase 2A), approximately 1,950 m in length, are used in the current paper. The records indicate that the construction of this phase progressed at a rate of 11.0 m per working day. A photo of the used TBM (TBM2) is shown in Fig. 3 and its general specifications are summarized in Table 2. In the construction of Lot 11-c, TBM 2 was excavating under many hard points which include different types of existing structure such as buildings, footings of Bridges, sewer tunnels, annexed structure and tunnel shafts. A general description of the hard points at the location of

Lot 11-c and their ground strata and distances from the tunnel are shown in Tables 3 to 6. Figure 4 shows several existing structures and the vertical alignment of the tunnel at the location of Lot 11-c.

The general strata of ground as indicated by site investigations at the location of Lot 11-c consist of the following:

- Unit (1): It stands for recent man-made fill material.
- Unit (2): It includes all the sand formations in variable depths and are composed of following sub-layers:
 - Unit (2-a): for upper sand formation.
 - Unit (2-b): for middle sand formation.
 - Unit (2-b. G): for middle gravelly sand formation.
 - Unit (2-c): for lower cemented sand formation.
- Unit (3): It includes all the clay formations in different depths and are composed of the following sub-layers:
 - Unit (3-a): for upper clay formation.
 - Unit (3-b): for lower laminated clay formation.
- Unit (4): It is available only at the area of the Cairo Fair station and includes very weathered rock formation.

The estimated parameters of these strata are summarized in Table 7.

IV. FIELD RECORDS AND DISCUSSION

Figure 5-a shows a longitudinal section of ground through the tunnel alignment at the location of Lot 11-c. The figure also shows that the ground layers excavated by TBM 2 are the lower clay, middle sand, lower sand, and middle gravelly sand layers, which are designated in Table 7 as Units (3-b), (2-b), (2-c), and (2-b. G), respectively. Figures 5-b and 5-c show the variations of *AS* and cutterhead speed (*CHS*), respectively, with the number of rings erected during construction of Lot 11-c. The colored circles in Figs. 5-b and 5-c indicate the types and locations of the hard points at the location of Lot 11-c; the locations of hard points are shown at the corresponding rings of the tunnel. The TBM *AS*, *CHS*, penetration rate (*PR*), *U*, and *AR* at the locations of the hard points in Lot 11-c are summarized in Tables 8 to 11. The records of *AS*, *CHS*, and *PR* are obtained from the ring erection reports while those of *U* and *AR* are obtained from the machine daily reports. These records are shown in Tables 8 to 11 for the existing buildings, pile foundations of bridges, utility lines, and annexed structures, respectively. The general formations of ground excavated by TBM 2 below the hard points are indicated

in Tables 3 to 6 and designated as Units (2-b), (2-c), (2-b. G), and (3-b).

Figure 5-a shows that TBM 2 experienced a clear mixed face ground at the location between rings 4,050 and 4,550 where it was excavating in the sand, gravel, and clay/silt-clay layers. At the location between rings 4,050 and 4,250, it is seen in Fig. 5-a that the thickness of the clay/silt-clay layer increases in the direction of tunnel advancement. Figure 5-b shows at the same location that *AS* decreases with the tunnel advancement. It is interesting to note at the location between rings 4,250 and 4,550 that a decrease in the thickness of the clay/silt-clay layer (Fig. 5-a) with tunnel advancement is corresponding to an increase in *AS* (Fig. 5-b). This implies that *AS* increases with the decrease of clay content or increase of sand content in the excavated ground. At the locations between rings 4,600 and 4,650 and at ring 5,016 where TBM 2 was cutting in the middle sand and gravelly sand layers, respectively, the highest values of *AS* (58 mm/min in Fig. 5-b) and cutter head speed (2.4 rpm in Fig. 5-c) were recorded. This is generally consistent with the above observation on the variation of *AS* with the type and composition of excavated ground. Figure 5 shows that these highest values were recorded at locations before and after the locations of the hard points.

At the locations of the hard points in Lot 11-c, the ground is dominated by layers of sands and gravelly sands. However, Fig. 5 shows that the values of *AS* and *CHS* at the locations of the hard points are less than the highest values of 58 mm/min and 2.4 rpm, respectively. In this regard, it should be mentioned that when tunneling in the vicinity of hard points, *AS* is usually decreased to minimize the induced movements of ground. *CHS* is also decreased to minimize the wearing rate of the cutting tools of the cutterhead.

Though excavated in different ground layers and in the vicinity of different existing structures, the tunnel in Lot 11-c was constructed successfully without significant signs of distresses in the structures existing in the vicinity. Therefore, a documentation of the adopted tunneling records of *AS*, *CHS*, *PR*, *U* and *AR* will essentially represent a useful contribution to the practical database of tunneling works. The adopted records can be summarized as follows:

- The records in Table 8 for TBM 2 boring in the vicinity of existing buildings show that *AS*, *CHS*, *PR*, *U* and *AR* are in the ranges 42.55 – 50.55 mm/min, 1.91 – 2.06 rev/min, 22.27 – 24.50 mm/rev, 28.00 – 45.00%, and 20.00 – 29.00 m/day with average values of 48.43 mm/min, 2.03 rev/min, 23.82 mm/rev, 34.00%, and 24.88 m/day, respectively.
- The records in Table 9 for TBM 2 boring in the vicinity of existing pile foundations of bridges show

that *AS*, *CHS*, *PR*, *U* and *AR* are in the ranges 29.44 – 48.09 mm/min, 1.72 – 1.89 rev/min, 17.19 – 25.39 mm/rev, 33.00 – 42.00%, and 21.00 – 22.00 m/day with average values of 38.76 mm/min, 1.81 rev/min, 21.29 mm/rev, 38.00%, and 21.50 m/day, respectively. At the location between rings 5,180 and 5,295 TBM 2 was boring between two groups of the pile foundations of the existing 6th October Bridge western ramp and under sewer tunnels. The distance between the tunnel and one of the pile groups is approximately 1.68 m (see Fig. 6). This is the smallest distance between the tunnel and the hard points throughout the tunnel alignment. At this location, *AS* and *CHS* were significantly decreased to 29.44 mm/min and 1.72 rpm, respectively, and the corresponding *U* was 42.00%.

- The records in Table 10 for TBM 2 boring under existing utility tunnels of 1.00 – 2.25 m in diameter show that *AS*, *CHS*, *PR*, *U* and *AR* are in the ranges 30.26 – 40.32 mm/min, 1.69 – 1.93 rev/min, 16.96 – 20.86 mm/rev, 42.00 – 43.00%, and 21.00 – 23.00 m/day with average values of 34.29 mm/min, 1.77 rev/min, 19.31 mm/rev, 34.00%, and 22.50 m/day, respectively.
- The records in Table 11 for TBM 2 boring in diaphragm walls of existing annexed structures show that *AS*, *CHS*, *PR*, *U* and *AR* are in the ranges 9.80 – 12.70 mm/min, 2.03 – 2.31 rev/min, 5.00 – 6.00 mm/rev, 28.00 – 46.00%, and 5.00 – 6.00 m/day with average values of 11.25 mm/min, 2.17 rev/min, 5.50 mm/rev, 37.00%, and 5.50 m/day, respectively (see Fig. 7).

Figure 8 shows a representation of the average tunneling records of *AS*, *CHS* and *U* for the types of hard points existing in Lot 11-c.

It is worth mentioning that the relatively high values of *U* recorded during tunneling in the vicinity of the hard points in Lot 11-c are attributed to the following additional precautionary measures:

1. The rings were erected immediately after excavation. This contributed to the reduction of the delay times.
2. Hyperbaric interventions were routinely made before starting excavation in the vicinity of the hard points. This increases the cutting efficiency of the cutterhead in the ground and mitigates any residual risks.
3. Larger thrust forces were applied to increase the depth of cutting of the cutter tools and to maintain the advance speed.

A reduction in the delay and maintenance times contributes to the increase of *U*.

V. SUMMARY AND CONCLUSIONS

TBM tunneling in soft grounds inevitably results in ground movements that may cause unrecoverable damages to adjacent structures. The effects of TBM tunneling on adjacent structures are briefly reviewed in the paper. Management of tunneling works in the vicinity of existing structures (hard points) and the relevant risks necessitates determination of appropriate tunneling rates at the hard points. A guideline that determines appropriate rates of tunneling in the vicinity of hard points is not available. Moreover, the literature lacks reported data on tunneling rates and the corresponding effects on hard points. As a contribution to the database of tunneling works, the current paper presents field records of TBM tunneling advance speed (*AS*), utilization factor (*U*), and advance rate (*AR*) that are obtained from tunnels actually constructed in Egypt in the vicinity of hard points. It also discusses these records for different types of hard points: buildings, pile foundations, utility tunnels, and annexed structures. Ranges of *AS*, *U*, and *AR* for TBM tunneling without significant risks on the structures existing in the vicinity of tunneling works are also presented. In addition, observations and discussions on the variation of *AS*, *U*, and *AR* with the ground type and composition and precautions to be adopted to mitigate risks of tunneling on structures in the vicinity are presented in the paper.

REFERENCES

- [1] Arshad, and Abdullah, R.A. (2016). "A review on selection of tunneling method and parameters affecting ground settlements," *Electronic Journal of Geotechnical Engineering*, Vol. 21, 4459–4475.
- [2] Goh, K.H., Ng, S.S.G., and Wong, K.C. (2016). "Case histories of bored tunneling below buildings in Singapore downtown line," *International Journal of Geoengineering Case histories*, Vol. 3, 149–161.
- [3] ITA (International Tunneling Association) (2000). "Mechanized tunneling, recommendations and guidelines for tunnel boring machines (TBMs)," *Working Group 14*, 1 – 118.
- [4] Kovari, K., and Ramoni, M. (2004). "Key note lecture at international congress on mechanized tunneling: challenging case histories," *Urban tunneling in soft ground using TBM's*, Politecnico di Torino, Italy, 16–19.
- [5] Multi-Mode TBM. (2017). "TBM information," <<https://www.herrenknecht.com/en/innovation/research-development/machinescomponents/multi-mode-tbm.html>>(Aug. 20, 2017).
- [6] NAT (National Authority for Tunnels) (2017). "Information of greater Cairo metro line-3," *Line-3*, <<http://www.nat.org.eg/english/Line3.html>> (Aug. 20, 2017).

- [7] Ozfirat, M.K. (2015). "Selection of tunneling machines in soft ground by fuzzy analytic hierarchy process," Dokuz Eylul University, *Acta MontanisticaSlovaca*, Vol. 20, No. 2, 98–109.
- [8] Sheng, E. S. Y., Chuan, J. Y. T., Ikhung, H. K., Osborne, N. H., Boon, C. K., and Siew, R. (2016). "Tunneling undercrossing existing live MRT tunnels," *Tunneling and Underground Space Technology*, Vol. 57, 241–256.
- [9] Shield Tunneling (2017). <<http://helpiks.org/2-30162.html>> (Aug. 20, 2017).
- [10] Thomas, W.P. (2011). "Tunneling beneath open water, a practical guide for risk management and site investigations," *Professional Associate Finalist*, William Barclay Parsons Fellowship Program, Parsons Brinckerhoff, New York.
- [11] Toan, D. N., Hung, L. X. (2007). "Some aspects of risk management and subsidence," Hanoi Metro Pilot Line Project, Report at the Meeting between ITA and ITST on Tunneling, Hanoi.
- [12] Zhang, D., Fang, Q., Hou, Y. Li, P., and Yuen, W. L. (2012). "Protection of buildings against damages as a result of adjacent large-span tunneling in shallowly buried soft ground," *Journal of Geotechnical and Geo-Environmental Engineering*, Vol. 139, 903–13.

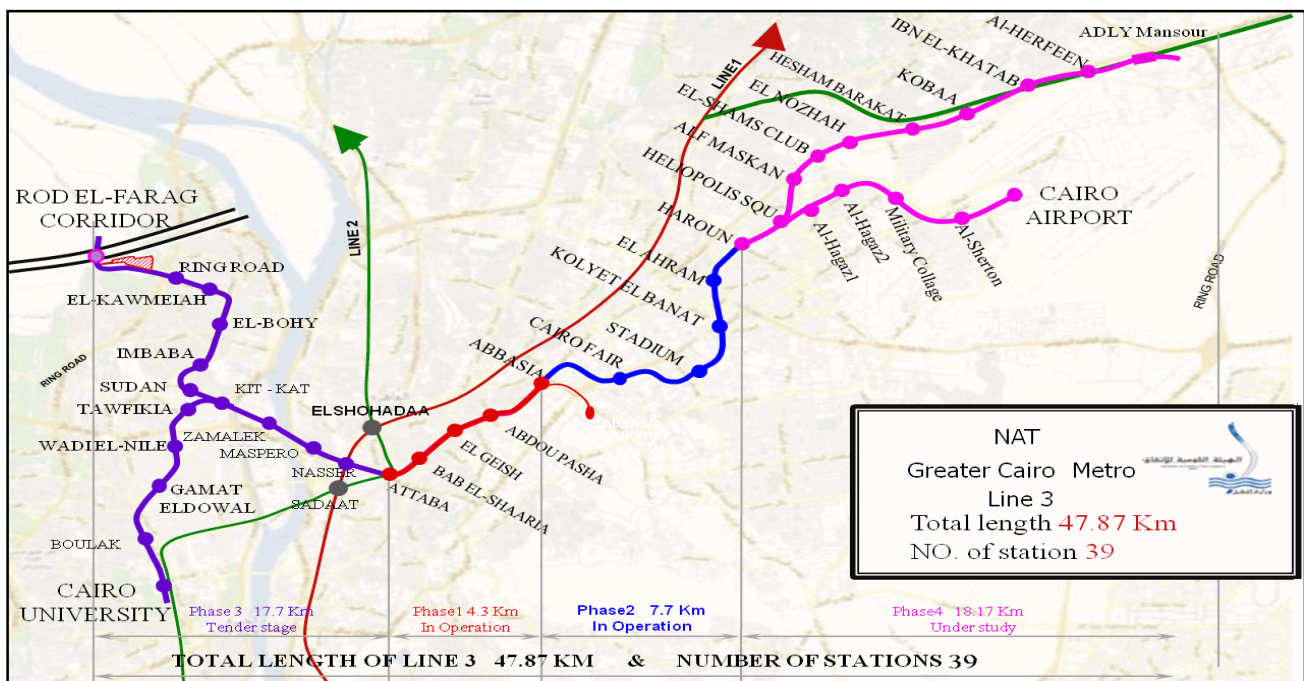


Fig. 1: Network of the Greater Cairo metro and route of Line 3 (NAT 2017).



Fig. 2: Construction phases of Line 3 and the used TBMs.



Fig. 3: The slurry TBM used in Line 3, Lot 11-c (Phase 2A), of the Greater Cairo metro (NAT 2017).

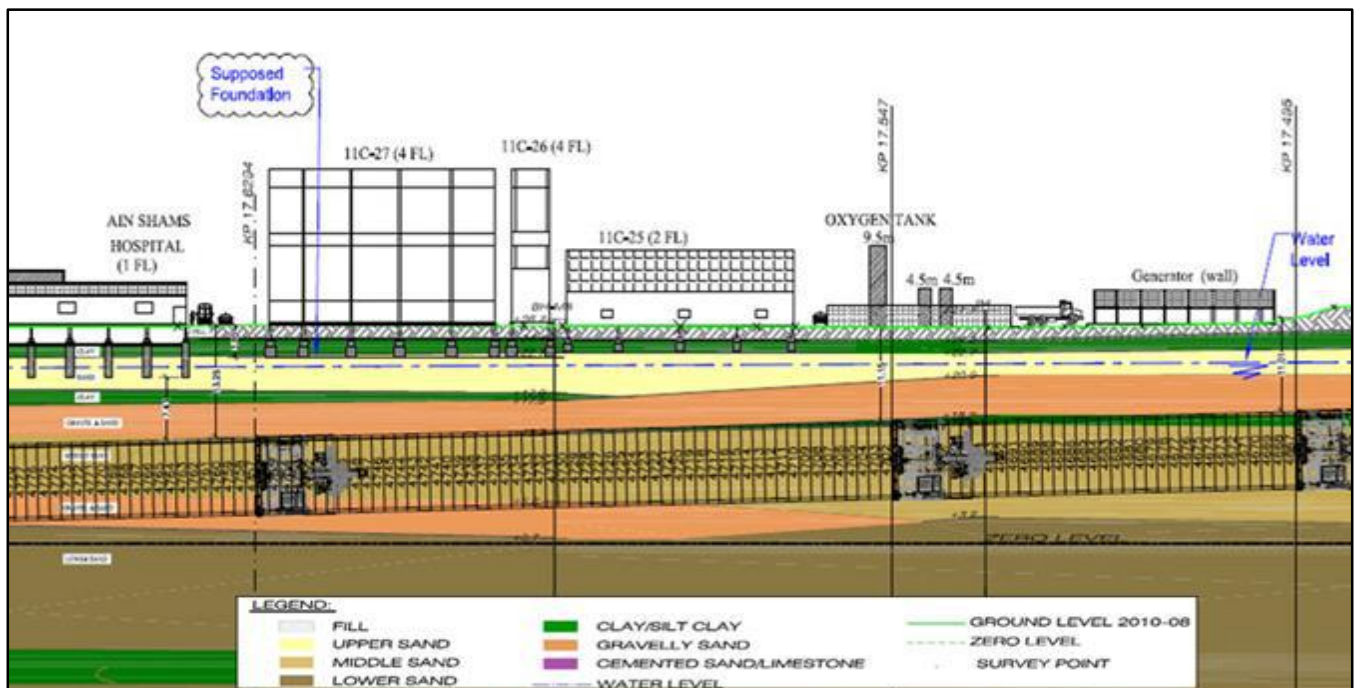
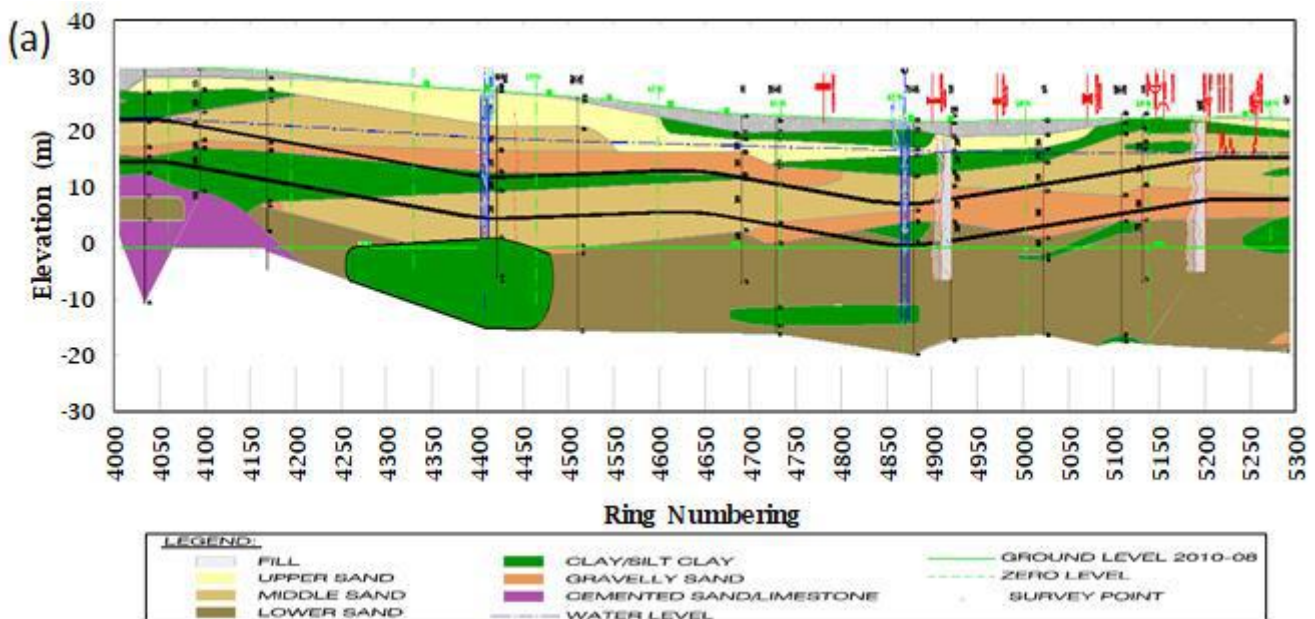


Fig. 4: Tunnel alignment under existing structures at location of Lot 11-c (Phase 2A); TBMs are shown for illustration.



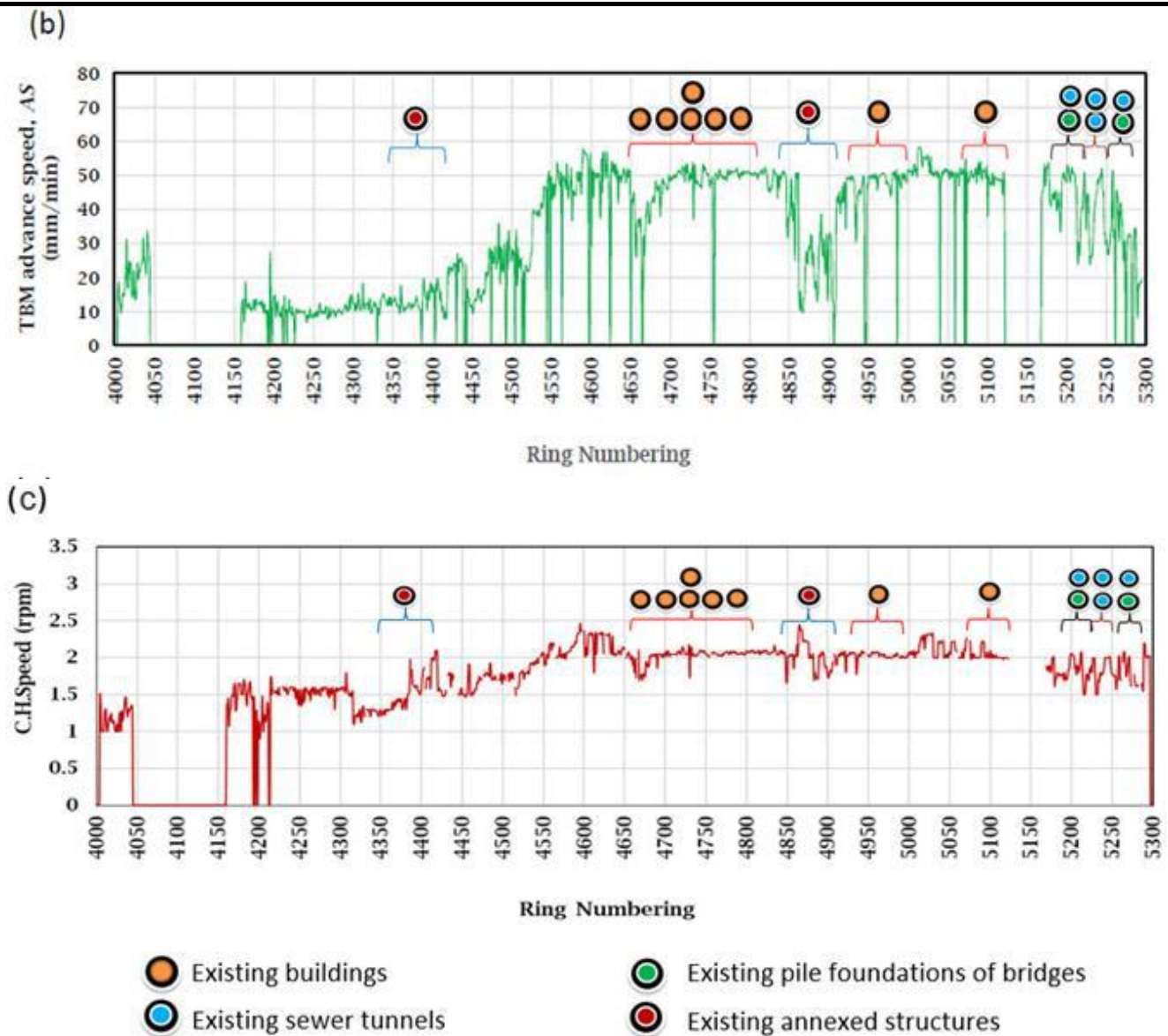


Fig. 5: Ground profile and TBM records at the location of Lot 11-c: (a) ground profile; (b) AS; (c) CH

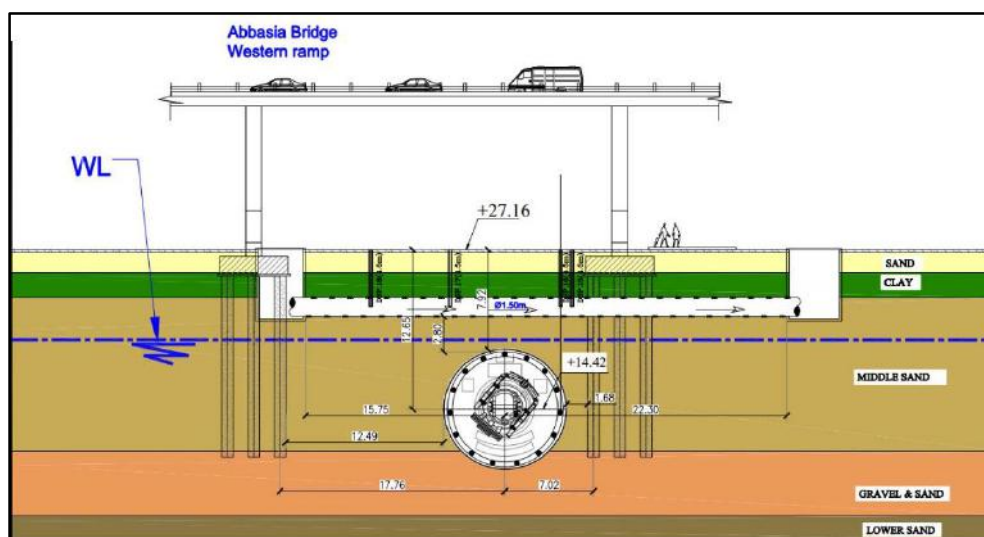


Fig. 6: TBM 2 boring between pile foundations of 6th October bridge western ramp, Lot 11-c.

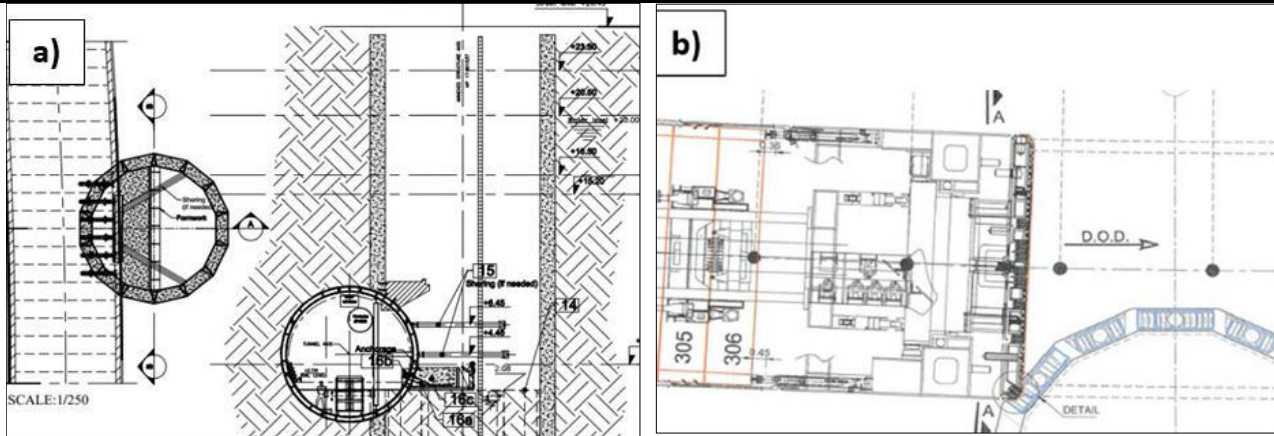


Fig.7: TBM 2 crossing annexed structure 11-B, Lot 11-c: (a) vertical section; (b) plan view.

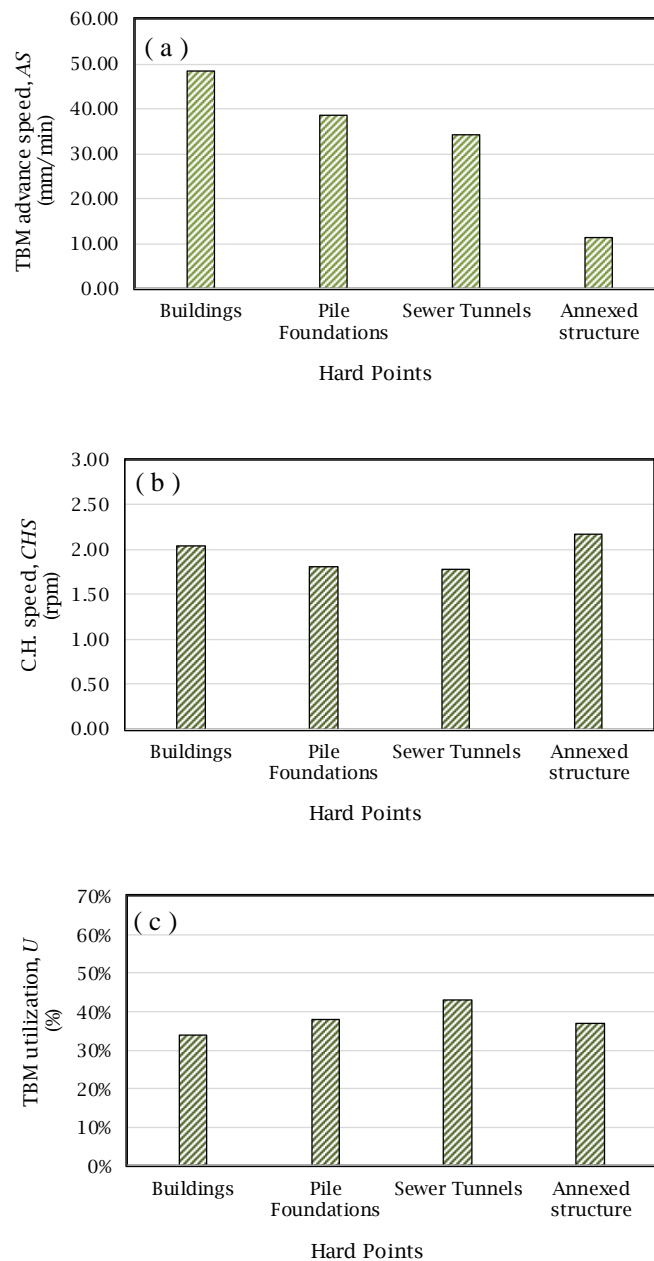


Fig.8: Average production records of TBM 2 for different types of hard points in the vicinity of tunneling works: (a) AS; (b) CHS; (c) U.

Table.1: Construction phases and types of TBMs used in Line 3 of the Greater Cairo metro.

Phase #	Stage #	Tunnel Path	Stage Length (km)	TBM Type	TBM No.
1	-	From Attaba station to Abbasia station	4.3	Slurry TBM	TBMs 1 & 2
2	A	From Abbasia station to Cairo Fair station	1.95	Slurry TBM	TBM 2
	B	From Cairo Fair station to Haroun station	5.75	EPBM	TBM 3
3	A	From Attaba station to Kit Kat station	4.00	---	Under study
	B	From Kit Kat station to Rod EL-Farag station	6.60	---	Under study
	C	From Kit Kat station to Cairo University station	7.20	---	Under study
4	A	From Haroun station to El-Shams Club station	5.15	Slurry	TBM 4
	B	From El-Shams Clubstation to Adly Mansour station	6.37	-----	Surface path
	C	From Helipolis station to Cairo Airport station	6.65	---	Under study

Table.2: General specifications of slurry TBM (TBM 2) used in Lot 11-c (Phase 2A) of Line 3.

Specification	TBM 2
Shield diameter (m)	9.46
Shield length (m)	11.3
Max. advance speed (mm/min)	80
Max. rotational speed (rpm)	3
Max. thrust force (ton)	5500
Stroke length (m)	2
Max. torque of cutter head (ton.m)	2000
Cutting tools type: disc cutter, rippers, scrapers (no.)	22, 8, 168

Table.3: Existing buildings and their ground strata and distances from the tunnel at the location of Lot 11-c.

Building	No. of Floors	Ground Formation	Vertical Distance to Tunnel Crown (m)	Horizontal Distance to Tunnel Axis (m)
11-c-31	1	Middle sand and clay	11.01	9.25
Oxygen Station	1	Middle sand	11.15	0
11-c-25	2	Middle sand	9.44	0
11-c-26	4	Middle sand	9.44	11
11-c-27	4	Middle sand	9.44	0
Ain Shams Hospital	1	Middle sand and gravelly sand	9.45	0
Faculty of Arts	7	Gravelly sand	12.6	0
Ain Shams Information Center-11-c-06	3	Gravelly sand and middle sand	8.61	8.35

Table.4: Existing pile foundations of bridges and their ground strata and distances from the tunnel at the location of Lot 11-c.

Pile Foundation	Status	Ground Formation	Vertical Distance to Tunnel Crown (m)	Horizontal Distance to Tunnel Axis (m)
Foundation of 6th October Bridge Western Ramp	Crossing between two groups of pile foundations	Middle sand and gravelly Sand	8.50	6.18
Foundation of 6th October Bridge Eastern Ramp	Crossing between two groups of pile foundations	Middle sand and gravelly sand	8.70	7.00

Table.5: Existing utility tunnels and their ground strata and distances from the tunnel at the location of Lot 11-c.

Sewer (Utility) Tunnel	Status	Ground Formation	Vertical Distance to Tunnel Crown (m)	Horizontal Distance to Tunnel Axis (m)
Sewer tunnel, Diameter (1.00 m)	TBM crossing between 2-pile group and sewer tunnel	Middle sand and gravelly sand	4.90	0.00
Sewer tunnel, Diameter (2.25 m)	Normal case "TBM crossing Sewer tunnel only"	Middle sand and gravelly sand	2.90	0.00
Sewer tunnel, Diameter (1.80 m)	Normal case "TBM crossing Sewer tunnel only"	Middle sand and gravelly sand	2.10	0.00
Sewer tunnel, Diameter (1.50 m)	TBM crossing between 2-pile group and sewer tunnel	Middle sand and gravelly sand	2.80	0.00

Table.6: Existing annexed structures and their ground strata and distances from the tunnel at the location of Lot 11-c.

Annexed Structure	Status	Ground Formation	Vertical Distance to Tunnel Crown (m)	Horizontal Distance to Tunnel Axis (m)
Structure 11-A	TBM crossing and cutting in diaphragm wall of annexed structure	Middle sand, gravelly sand and clay	0.00	0.00
Structure 11-B	TBM crossing and cutting in diaphragm wall of annexed structure	Middle sand and clay	0.00	0.00

Table.7: General ground strata at location of Lot 11-c and estimated ground parameters.

Stratum	Material Code	Depth (m)	SPT N	Dr (%)	K_0	γ_b (Mg/m ³)	C_u (KPa)	ϕ_u (°)	E_u (MPa)
Recent Man-Made Fill	Unit (1)	0.0 – 3.0	12	38	0.50	1.80	0.0	30	12
Upper Sand Formation	Unit (2-a)	3.0 – 6.0	34	69	0.43	1.95	0.0	35	45
Upper Clay Formation	Unit (3-a)	6.0 – 10.0	18	--	0.53	1.85	120	0.0	25
Middle Sand Formation	Unit (2-b)	10.0 – 11.3	74	92	0.37	2.00	0.0	39	95
Middle Gravelly Sand Formation	Unit (2-b. G)	11.3 – 22.7	85	96	0.36	2.10	0.0	40	145
Lower Laminated Clay Formation	Unit (3-b)	15.6 – 26.0	26	--	0.52	1.88	160	0.0	40
Lower Cemented Sand Formation	Unit (2-c)	22.7 – 35.0	90	100	0.36	2.10	0.0	40	150
Weathered Rock Formation	Unit (4)	24.6 – 28.7	---	---	---	---	---	---	---

SPT N= N-value of Standard Penetration Test, Dr = Relative density of soils, γ_b = Bulk density, C_u = Undrained cohesion, ϕ_u = Undrained angle of internal friction, E_u =Young's modulus (undrained).

Table.8: Daily field records of TBM 2 under existing buildings at the location of Lot 11-c.

Building	Average TBM Advance Speed, AS (mm/min)	Average TBM Cutterhead Speed (rev/min)	Average TBM Penetration Rate (mm/rev)	Machine Utilization, U (%)	AR (m/day)
11-c-31	42.55	1.91	22.27	45%	29
Oxygen Station	48.80	2.05	23.83	32%	26
11-c-25	50.29	2.06	24.36	28%	20
11-c-26	47.76	2.04	23.44	35%	26
11-c-27	49.51	2.06	24.02	35%	26
Ain Shams Hospital	50.55	2.06	24.50	37%	27
Faculty of Arts	48.42	2.04	23.78	33%	25
Ain Shams Information Center-11-c-06	49.55	2.03	24.38	28%	20
Average	48.43	2.03	23.82	34%	24.88

Table.9: Daily field records of TBM 2 under existing bridge footings at the location of Lot 11-c.

Pile Foundation	Average TBM Advance Speed, AS (mm/min)	Average TBM Cutterhead Speed (rev/min)	Average TBM Penetration Rate (mm/rev)	Machine Utilization, U (%)	AR (m/day)
Foundation of 6th October Bridge Western Ramp	29.44	1.72	17.19	42%	21.00
Foundation of 6th October Bridge Eastern Ramp	48.09	1.89	25.39	33%	22.00
Average	38.76	1.81	21.29	38%	21.50

Table.10: Daily field records of TBM 2 under existing utility tunnels at the location of Lot 11-c.

Sewer Tunnels (Utility Tunnels)	Average TBM Advance Speed, AS (mm/min)	Average TBM Cutterhead Speed (rev/min)	Average TBM Penetration Rate (mm/rev)	Machine Utilization, U (%)	AR (m/day)
Sewer Tunnel, Diameter = 1.00 m	32.97	1.69	19.47	43%	23.00
Sewer Tunnel, Diameter = 2.25 m	33.62	1.69	19.93	43%	23.00
Sewer Tunnel, Diameter = 1.80 m	40.32	1.93	20.86	43%	23.00
Sewer Tunnel, Diameter = 1.50 m	30.26	1.78	16.96	42%	21.00
Average	34.29	1.77	19.31	43%	22.50

Table.11: Daily field records of TBM 2 under existing annexed structures at the location of Lot 11-c.

Annexed structure	Average TBM Advance Speed, AS (mm/min)	Average TBM Cutterhead Speed (rev/min)	Average TBM Penetration Rate (mm/rev)	Machine Utilization, U (%)	AR (m/day)
Annexed structure 11-A	12.70	2.31	6.00	28%	5.00
Annexed structure 11-B	9.80	2.03	5.00	46%	6.00
Average	11.25	2.17	5.50	37%	5.50

Packing Improvement by using of Quality Function Deployment Method: A Case Study in Spare Part Automotive Industry in Indonesia

Humiras Hardi Purba, Adi Fitra , Gidionton Saritua Siagian, Widodo Dumadi

Master of Industrial Engineering Program, Mercu Buana University, Jln. Menteng Raya No 29, Jakarta Pusat, DKI Jakarta, 10340, Indonesia

Abstract—Sales for automotive in Indonesia especially for 4-wheels vehicles and 2-wheels production is increase every year. Increase sales in Indonesia will be related to the needs of Spare Parts of the vehicle. Based on that, sector spare part need improvement to increase the sales and quality of spare part to gain trust of customer for buy spare part original and not buy spare part not original. Improvement will focus for packing this is because packing is one of element which can be increased sales and the difficulty to make improvements in a short time and with low investment in the field of production. QFD will be used to find best improvements for packing. Planning improvement for packing such as change material carton box (flute), redesigning, adding barcodes and hologram stickers. Results Use QFD for packaging repair. Customers are more focused on unboxing easy packing with a value of 249.5 points from 40% and substitute solid material packaging with 135 points with 22% of QFD Technical priorities. With the following results customers prefer secure packing compared with interesting packing.

Keywords— Spare Parts, Sales, Packing, Indonesia, Improvement, QFD.

I. INTRODUCTION

Spare Parts are used to replace damaged parts in a machine. Automotive spare part sector in Indonesia there are two types. Part made by sole agent and made by the factory which specially made spare part modification. Spare part modification there are several types where the usage can be long life time or short life time.

Spare parts can be considered as an important business area [1]. Manufacturing and automotive industries are also important in many countries, with their respective share of the business in the spare-parts area [2]. Relationship of total car sales to the needs of automobile spare parts. Indonesia has achieved sales of 1.06 million per year and an estimated 4.5% increase in 2017 [3]. With the higher market share of spare parts, it is necessary to make improvements in order to increase sales and trust

from customers. Increasing trust from customers, Customer will prefer to buy original spare part compared to the spare part is not the original from sole agent.

Making improvements for Packing is a very important issue in local and international business due to the tight competitive environment in which manufacturers are trying to improve the quality and design of product packages. Success of Product can be seen, from Packing contributes to a well-designed Product sale. No good Packing with bad products or quality products with bad Packing can increase sales. However, when the same product compares, packaging plays a distinctive role by creating distinctions among other products. With the role of packing relationship in the increase of sales. QFD will be used to determine the items to be repaired. This item improvement is expected after the improvement can improve customer confidence that impact on loyalty and sales. Focus for packing improvement will be packing using QFD method.

II. LITERATUR REVIEW

Packing is materials protect the product against external factors from the place of production to the end-consumer while promoting the product [6]. In designing the packing repairs should keep the part safe when shipping. Protective packing and planned transportation plan can decrease the loss and 1 damage up to 75%.

Packing should provide protection, presentation and promotion product economically and environmentally-sensitive throughout the life cycle of it. The packing of a product should comply with its characteristics. Products with various characteristics require various packing and handling conditions. For instance, food materials, chemicals, fluid and hazardous materials and etc. require different practices [7].

The technical characteristics of packing vary in accordance with the products they contain. Materials with various characteristics are used in packing [8]: (a) Paper and Cardboard : Cardboard boxes , Fiber Boxes , Fiber barrels , bags and cases, (b) Metal : Aluminum foils and

labels , Metal boxes , Barrels , kegs , Covers, Press tubes , Cage, Metal stripes, columns and bands, (c) Glass : Bottles , Jars , Syringes , Glass Containers , Bulbs, (d) Plastic (Including cellulose and rubbers) : Bags and sacks , Boxes and Kegs , Buffers and Filling material , Films, layers and plates , molded bottles , Heat-treated trays , containers and bubble wraps, (e) Wood (including plywood) ; Boxes , Cages , Baskets , Pallet and Containers , Wood Wool, (f) Textiles: Bailing Materials Bags and Sacks.

There are several reasons for preferring packages with different kinds and materials. These can be listed as below [8]: (i) Paper and Cardboard: It is among the ones among the first rank because, it is cheap and easy to process paper, (ii) Metal: Tin and aluminum are used for manufacturing metal packages. The most common field where tin is used is canning. Use of aluminum boxes have been gradually increasing because they are easy to use, weigh light, do not need any paint, suitable for heating and disposable, (iii) Wood: Wood packages are preferred because they can be used more than once and they are cheap. Wood packages as environmental friendly packages have been drawing quite attention recently, since environmental problems have been considered important, (iv) Glass bottles and jars: Usually, delicate food products are put in glass jars. It is not possible to change them with other packing materials. Glass bottles and jars are preferred because it is possible to use them for storing other products by washing them, (v) Plastic Packages: They are used extensively in packing because they are light, suitable for coloring and labeling and they are cheap. Packing is the last point of manufacturers for convincing consumers before consumers make the purchasing decision. An efficient packing should have some particular characteristics. It is possible to list them as in the following [7]: (a) Physical Characteristics, (b) Protecting product quality, (c) Product improvement characteristics, (d) Product information, (e) Usage efficiency, (f) Mechanical characteristics, (g) Storing characteristics, (h) Transportation specifications, (i) Compatibility for trading, and (j) Recycling specifications. Spare part using packaging with carton box type. Built to facilitate some of the Spare part using packaging. Facilitate price, storage location and safety when delivery from factory to customer.

Carton box or better known by the term cardboard in the community is needed. One of the main functions of course to pack or pack the goods / materials before shipped or marketed. Because of its light weight, low cost, ease of assembly and disassembly, good sealing performance, certain cushioning and anti-vibration ability

and easy recovery and waste treatment, corrugated box is widely applied in various fields [20].

Types of materials used in cardboard boxes have a variety of types. Knowledge of the type of carton box is important to determine the type of carton to be ordered with the need and budget to order the carton box. Adjustment of carton box type material with the need will be very important to determine how strong the cardboard box we need. If you need carton box to carry goods with heavy weight, it is advisable to order carton box made with high quality materials and have a good level of strength so it is not easily broken. As for those of you who only need carton box to pack a light item, you can order carton box made with cheap material to save the cost of ordering.



Fig.1. Type of carton box

- a) Single wall (3 layers of paper) / 3 ply: Such a carton material has a shape composed of a top layer, a bottom layer and a corrugated layer in the center. Thin material features make this type of cardboard box is usually only used for the distribution of goods delivery within the local area. Such materials are commonly used for the packaging of goods such as toys, electronic goods, beverages, food or as a barrier coating.
 - b) Double wall (7 layers of paper) / 5 ply : This type of cardboard box has a seven-layer arrangement of four flat layers interspersed with a wavy layer with one wavy layer on the middle that has the thickest thickness among the others. The total thickness of the double wall layer is 7 mm. This type of carton is widely used in the packaging of goods shipped to the local area and abroad because the material is thicker and stronger.
 - c) The carton box type triple wall has ten layers consisting of flat and wavy layers with a total thickness of 10 mm. This material is strongest among the two carton boxes materials so it is used as a packing tool of export goods sent overseas
- Flute is the thickness of the cardboard itself. Flute has various models as shown below.

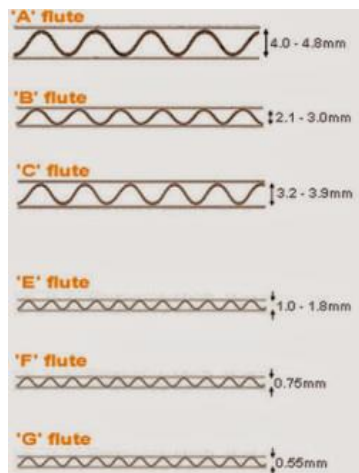


Fig.2. Type of Thickness Carton Box (Flute)

Kraft type paper is commonly used as the outer part of the box. Kraft type cardboard material has better strength than paper with medium material. This is because Kraft type of paper material made from wood base material with pine type which has long fiber then processed into pulp / pulp. At least this Kraft paper has at least 80% virgin fiber fibers and the rest improves recycled paper. The strength of Kraft paper can be used to measure the rate of possible breakage of the box or also called bursting strength. This type of paper has small moisture and moisture content compared to medium type paper. The paper weight itself is used as the power count parameter of the stacking power as well as the weight of the item to be packed inside the cardboard box. The weight of this paper is measured by cutting paper with the size of 1 meter x 1 meter and then weighed in units of gram / m².

The Kraft paper is distinguished by the following types of gram: 469 gram, 127 gram, 125 gram, 120 gram, 112 gram, 110 gram. In Indonesia, Kraft liner paper available only ranges from 110 gram - 300 gram.



Fig.3. Kraft type Paper

Packing now have some communication function for sales. Packing reflects positive or negative ideas to consumers. Packing promotes the brand and product to consumers. Relation between the product and consumer is based on instruction characteristic of its package.

Sales for Spare part now already increase 19.5 in 2017 for Honda only in Indonesia and will be increase in Lebaran

Holiday up to 20% from January sales [4]. Packing will greatly affect the price of goods, here are some examples. Firms can adjust the price through a certain number of changes to be made on packing. It is possible to list these changes as below [5]:

- Decreasing the product amount without changing its package
- Increasing the price by enlarging the package
- Increasing the price by making the package smaller
- Decreasing the price by enlarging the package
- Decreasing the product amount by enlarging its package
- Lowering the package, amount and the price
- Changing only the package without making any changes on the product.

Sales Function Packing has an important effect on purchasing decision of consumer. Especially, packing has great impact on unplanned purchases. The consumers are firstly attracted to packages and therefore packing is one of the most important issues of sales. That's why, packing is called as "the silent dealer [8]. Consumers can decide to buy a product which they do not consider buying or do not know anything about only by considering information provided by its package.

New packing technologies provide competitive advantages in the markets. Packing technology has begun creating competitive advantage also in the logistic process. Packing costs, technological developments and environmental effects show that packing decisions are an extremely strategic issue for firms [8].

Packing has four basic characteristics to customer, [9]:

- Visibility:** It is a characteristic of packing which attracts the attention of consumers at the sales point. For instance; packages with creative and eccentric design and shiny colors.
- Information:** This is the information on the packages. For instance; benefits of the product, its contents, directions and etc.
- Emotional Appeal:** It is the effort of package for creating appeal on consumers. For instance, creating happiness, elegancy and etc. emotions on consumers.
- Workability:** Packing covers very different workability issues. For instance; protection, storing, keeping, convenience and etc.

The QFD process begins with the determination of customer requirements and ends with the realization of the processes necessary for production. The QFD methodology is generally understood as a work style and work philosophy with the aim of truly satisfying the customer. Focus on two major issues: What does the

customer want and how can it be achieved? For this purpose, all employee knowledge and skills are involved in strategies and actions to achieve this goal, hereby avoiding irregularities [10].

QFD has the ultimate goal: success for customers, employees, and employers. Which are described with the following objectives [11]: (a) customer enthusiasm, (b) intensification of teamwork, (c) clear, coordinated and measurable objectives, (d) reduce losses in the value chain, (e) fewer and shorter development steps, (f) systematic documentation, (g) integration of expert knowledge, and (h) development and quality improvement.

III. METHODOLOGY

The concept for the improvement packing process to meet the needs of the customers indirectly. What makes a customer can choose goods based on from packing. To get the data we collect data, either by direct observation to the field and also collecting data from libraries, and analyzing competing products for the same market. The methodology used in this journal is:

- a) Survey literature to know the desires of the customer
- b) Gemba study (interview and questionnaire) to understand the type of packing that is on the market today
- c) Analyze VOC Voice of customer for packing design needs
- d) Analyze competitor products to benchmark to know the weaknesses and advantages of competitors' products.
- e) Create QFD house with the calculation and determination of factor weights involving voice, technical requirements and competition and interconnection
- f) Perform analysis based on QFD and create new design concepts based on the results of the value obtained

Using QFD can result in the development of better products at a price that the customer is willing to pay, based on its application in different companies [12]. The following advantages and benefits from QFD, there is customer satisfaction [13]. Reduction in product lead times [14], improved communications through teamwork [15] and better designs (Mehta, 1994). In addition, Bicknell and Bicknell (In Chan and Wu (2002a)) reported that tangible benefits when QFD is properly used are: a 30-50% reduction in engineering changes, 30-50% shorter design cycles, 20-60% lower startup costs, and 20-50% fewer warranty claims [16].

Surveys will be conducted to determine the effect of packing on customers to choose or buy a spare part. This survey was conducted to determine the voice of customer "Voice of Customer "(VOC) to the goods desired by the customer. The data collected will be the basis in determining the improvement and basic data from QFD. Based on the needs of the customers will be arranged according to the interests of the subjects that will be allocated to the range. The rating is based on customer feedback obtained from customer surveys. To proceed to the next stage of product development, information obtained from a survey on customer requirements, technical description, and relative importance is used to build the House of Quality (HOQ) [17]. Next step to create customer need use range 1 -5. 5 show very need and the smallest scale is 1. This date we will use survey and as customer voice. To proceed to the next stage of product development, information obtained from a survey on customer requirements, technical description, and relative importance is used to build a Quality House [19]. Here are some examples of questionnaires submitted to buyers and sellers of spare parts. Questions addressed to the customer:

- a) Are You Motorist?
- b) Are you Biker?
- c) What is your consideration to buy spare parts?
- d) What is your favorite packing spare part?
- e) Why you like it?
- f) What is the most important factor for your packing spare parts?
- g) What Your Opinion About Fake Spare Part for Packing?
- h) What is your opinion about Original Spare Part for packing?
- i) Have you ever bought a non-original Spare part?
- j) Where do you usually buy Spare Part?
- k) Does Packing be one of your parameters in determining the purchase of Spare Part?
- l) Do you see first Part and Packing before being paired in a vehicle?
- m) Do you bring home a broken Spare Part that has been replaced at the Workshop?
- n) What is important is the guarantee of Original spare part in the original spare part?
- o) Do you know how to distinguish between genuine and fake spare parts?

Next is to make a survey question to the spare part seller. Spare part seller who conducted the survey is a seller outside the sole agent:

- a) Do you sell non-Original Spare parts?
- b) Which is more in search by the customer for spare part (Original / Non-Original)?

- c) Which is more purchased by customer for spare part (Original / Non-Original)?
- d) Which is more to buy by customer for spare part (Original / Non-Original)?
- e) What is customer complaints against packing the original spare parts?
- f) What is customer complaints against packing non-original spare parts?
- g) Whether the customer is interested in packing spare parts?
- h) Whether the customer is interested in the installation instructions part?
- i) Is the customer concerned with packing material?
- j) Is Customer concerned with Color packing?

IV. RESULT AND ANALYSIS

Packing process is very important which a plus in the eyes of customer. The priority for improvement is very important by knowing which priority so that the improvement process can be done and produce better value for the customer. The unimportant part in the customer's eyes can be changed by pressing the cost of replacing part of the packing itself with cheaper material or eliminating the part

Basically, there are have 7 steps that must be done in QFD, there is affinity diagram, tree diagram, the weighting of customer need, competitive benchmark, technical requirement (how's), interrelationship what's and how's, and design target and the house of quality [13]. Step 1 is preparing affinity diagram for grouping customer need based on data VOC (Voice of Customer). This data use to focus what is the value in customer for packing spare part in Indonesia.

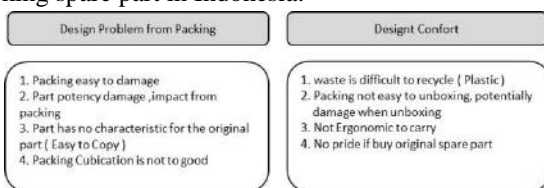


Fig.4: Affinity Diagram for Packing Improvement

Step 2: tree Diagram is used for plotting the issue from group in step 1 to determine the satisfaction aspect of customer need in the improvement effort packing design



Fig.5: Weight of Customer Need (Voice of Customer)

Step 3: Weighting of Customer Need is used for conducting customer need priority to the product (motorcycle helmet), to know the level of customer interest to the product [19].

Packing not Easy to Damage	5	4. INTERRELATIONSHIP MATRIX	2. PLANNING MATRIX
Packing for more safety	5		
Uniq Packing for Hard to Copy	3		
Cubication of Packing	3		
Easy Recycling Packing	4		
Packing to Easy Unboxing	4		
Packing for more Ergonomic	3		
Car Brand and Hologram Decal	5		

Customer Needs Customer Important

Fig.6: Weight of customer Needs (Voice of Customer)

By using range 1-5 and brainstorming results in Product Development that customer needs are most important with scale 5: Packing not easy to damage, Improve packing for more safety and add car brand and hologram decal. This option is based on to guarantee the part delivered and to the customer must be in good condition. Usually the customer only sees the packing first compared to the goods inside. They assume if the packing is damaged means the goods inside are also damaged.

Step 4: Competitive Benchmark is used for conducting benchmarks with competitors' products competitor A & competitor B based on survey results and brainstorming product development team to see the position of the product to competitors.

Customer Needs	Interrelationship	Planning Matrix							
Packing not Easy to Damage	5	3	5	5	5	1.4	1.1	7.7	35
Packing for more safety	5	3	4	4	5	1.4	1.4	9.8	39
Uniq Packing for Hard to Copy	3	3	4	4	3	1.0	3.3	3.9	8
Cubication of Packing	3	4	4	4	4	1.0	2.5	4.5	9
Easy Recycling Packing	4	3	4	3	4	1.3	1.3	6.2	12
Packing to Easy Unboxing	4	3	3	3	3	1.0	1.3	5.2	10
Packing for more Ergonomic	3	4	3	3	3	1.2	2.2	4.3	9
Car Brand and Hologram Decal	5	3	5	5	5	1.4	1.3	9.1	38

Our Current Rating
 Competitor Rating (A)
 Competitor Rating (B)
 Our Planned CS Rating
 Improvement Factor
 Sales Point
 Overall Weighting
 % of total weight

Fig.7: Competitive Benchmark

By using scale 1-5, and based on brainstorming results in Product Development, that the top three percentages in total benchmarking are: Packing not easy to damage (15%), improve packing to more safety (19%), Add car branch and Hologram Decal (18%). This shows that from the competitor side these three factors are very dominant in making the product design plan.

Example for calculation (*Packing not Easy to Damage*)
 Improvement Factor :
 ((Our Planned CS Rating - CS Rating our textbooks) *0.2) + 1

$$: ((5 - 3) * 0.2) + 1 = 1.4$$

With using same case

Overall Weighting :

Weigh Customer Voice * Improvement Factor * Sales Point

$$: (5 * 1.4 * 1.1) = 7.7$$

% of total weight : (Overall Weighting Customer needs / Total Overall Weighting Total) * 100

:

$$(7.7) / (7.7 + 9.8 + 3.9 + 4.5 + 6.2 + 5.2 + 4.3 + 9.1) * 100 = 15$$

CS Rating our textbooks, CS rating competitor A, CS rating competitor B, Our Planned CS Rating, and Sales Point there is input related with product development brainstorming and data collection.

Step 5: Technical Requirements (HOWs), to determine from technical aspect for product development plans to meet customer needs.

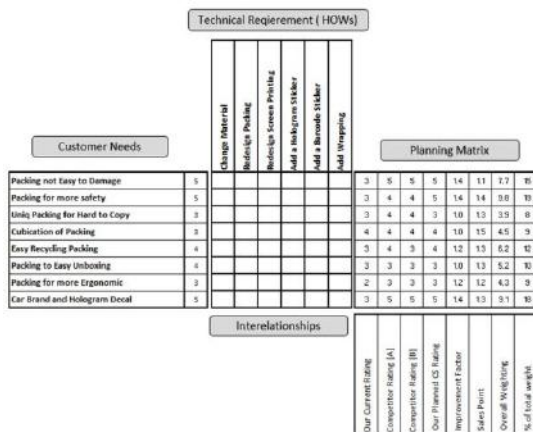


Fig.8. Technical Requirement (HOWs) Applied to the HOQC

Step 6: Interrelationship WHATs and HOWs, to determining the level of relationship (relation) between customers' needs and needs in terms of technical aspects

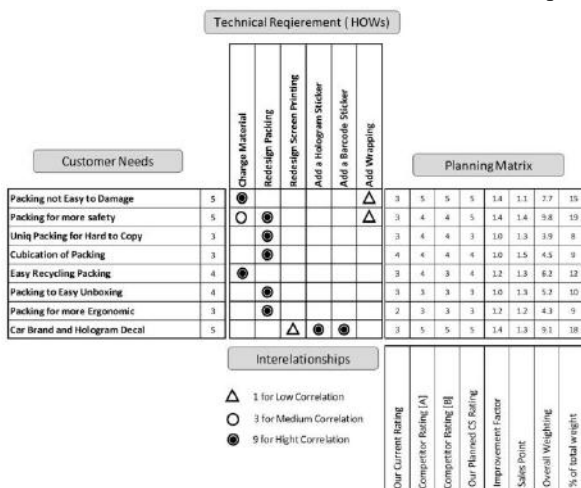


Fig.9: Interrelationship between WHATs and HOWs

By using score: 1 (week), 3 (Medium), and 9 (high), based on brainstorming results in sections Product Development obtained a high correlation is in several things, there are some of point for focus from interrelationship diagram:

- Packing not easy to Damage vs Change Material (9 Point)
- Packing for More Safety vs redesign packing (9 Point)
- Unique packing for hard to copy vs redesign packing (9 Point)
- Cubic of packing vs redesign packing (9 Point)
- Easy recycling packing vs change material (9 point)
- Packing easy to unboxing vs Change material (9 Point)
- Packing for more ergonomic redesign packing
- Adding Car brand and Hologram vs add barcode vs Hologram Sticker.

Step 7: Design Target and House of Quality, calculation, and weighting of design targets to determine priorities in conducting product development related to customer need (WHATs), technical requirement (HOWs) and benchmarking result to competitors so that the products produced in accordance with customer needs and able to compete with competitor products.

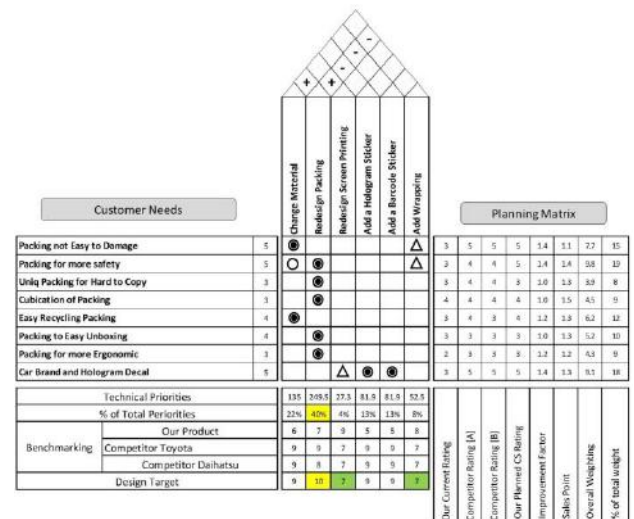


Fig.10: Completed HOQ

From the comparison result data in QFD House, Product Design for packing improvement spare part will be done with the following criteria:

- The first point for improvement is redesign (10) customer needs packing that can guarantee the quality of the part. Secure packing until received by the customer. Packing a unique so as to facilitate the customer to disguise whether this part of the original or fake. With a compact design makes it easy for storage and also makes it easier when unboxing so it does not make parts to be damaged.
- The second point, replacing the material (9). By replacing better and stronger material so that parts become safe and the replacement or addition of this packing material is sought which

makes it easier to recycle by avoiding the use of Styrofoam.

- c) The Third point for improvement is add Barcode (9) and Hologram (9). This improvement uses for increase trust customer because they already buy original part. And this barcode can connect to internet to check authenticity spare part
- d) The Four point to improvement Redesign print screen (7) and wrapping (7). After we ask to customer and seller about these two issues we find that customer and seller is doesn't care about this issue. The most important is quality of part. Customer and supplier almost remove the packing of spare parts and spare parts that are damaged so the economic value is lost here. With this data we can do by not using the use of color print out carton and coated by plastic. This is done by doing a comparison with competitor spare parts where they also do the same thing.



Fig.11. Sample before Improvement



Fig.12. Sample Target Improvement

V. CONCLUSION

1. Based on a review of VOC's voice of customer. The color of the packing is not very influential on packing. Customers only want a more solid packing. The easiest thing is to replace the thicker carton box material called Flute. The process of replacing this material will certainly increase the cost of packing spare parts. But because the customer is not too influential with the color packing, this can be done budget transfer from print to a better material. By

replacing the packing material will look more solid and more exclusive and this one of reasons customer chose the product

2. Another improvement has to be done to change the design from packing for easier unboxing process. This seems often unthinkable. Impact from difficult to unpacking the customer using sharp objects and potential of spare part material to be damaged.
3. Other improvements by removing the installation instructions (which in screen printing in packing). The installation instructions are rarely used by the customer because the spare part is usually installed in the workshop. One of the improvements that can be used by connecting the barcode code with website online, if the customer wants to see the installation process just by doing scan spare part and we can see instruction on website.

VI. REFERENCES

- [1] Wagner SM, Lindemann E. A case study-based analysis of spare parts management in the engineering industry. *Production Planning & Control: The Management of Operations*. 2008; 19:397-407. DOI: <https://doi.org/10.1080/09537280802034554>
- [2] Vargas C.A, Cortes ME. Automobile spare-parts forecasting: a Comparative study of time series method. *International Journal of Automotive and Mechanical Engineering*. 2017 Volume 14, issue 1pp. 3898-3912. DOI: <https://doi.org/10.15282/ijame.14.1.2017.7.0317>
- [3] <https://www.gaikindo.or.id/pasar-domestik-mobil-indonesia-baik-45-persen-pada-2016>
- [4] <http://jatim.tribunnews.com/2017/06/13/penjualan-spare-part-honda-lebihi-target-tahun-2017-diprediksi-akan-meningkat-saat-h-7-lebaran>
- [5] Kocamanlar, E. (2008) "A Model Proposal about the Effect of Packing in Fast Moving Consumer Goods on the Purchasing Behavior" Postgraduate Thesis, İstanbul, the Institute of Science of the Technical University of İstanbul.
- [6] Gökalp, F. (2007) "The Role of Packing in Purchasing Behavior of Food Products" *Ege Academic Review*, 7(1):79-97.
- [7] Rundh, B. (2009) "Packaging Design: Creating Competitive Advantage with Product Packaging" *British Food Journal*, 111(9):988-1002.

DOI:

<https://doi.org/10.1108/00070700910992880>

- [8] İnce, M. (2010) “Analyzing the Effects of Packing as a Communication Instrument on Customer Choice” Postgraduate Thesis, İstanbul, The University of Marmara, The Institute of Science.
- [9] Yıldız, O.E. (2010) “The Effect of Packing in Creating Brand Awareness” Communication Theories and Researches Magazine, 31:181-194.
- [10] Deutsche Gesellschaft für Qualität e.V., Frankfurt. (2001) QFD – Quality Function Deployment, Berlin, Wien, Zürich: Beuth Verlag GmbH.
- [11] Klein B. (2012) QFD – Quality Function Deployment-Konzept, Renningen: Expert Verlag
- [12] Hales, R. and Staley, D. (1995) Mix target costing, QFD for successful new products, Marketing News, 29(1),
- [13] Kauffmann, P., Unal, R., Fernandez, A. and Keating C. (2000) A model for allocating resources to research programs by evaluating the technical importance and research productivity, Engineering Management Journal, Vol.12, No.1, 5-8.
- [14] Hauser, J. R. and D. P. Clausing, the House of Quality, Harvard Business Review, May/June 1988.
- [15] A Griffin and JR Hauser (1992) Patterns of Communication among Marketing, Engineering and Manufacturing, A Comparison between Two New Product Teams, Management Science 38 (3), 360-373.
- [16] Jaiswal (2012) Case Study on Quality Function Deployment (QFD), ISSN: 2278-1684 Volume 3, Issue 6: 31
- [17] Hamidullah, R. Akbar, S. Noor, W. Shah & Inayatullah (2010) QFD as a Tool for Improvement of Car Dashboard, University of Engineering and Technology Peshawar, Pakistan, Journal of Quality and Technology Management Volume VI, Issue 1, June.: 1 - 3
- [18] Goetsch, D.L. and Davis, S.B. (2010) Quality Management for Organization Excellence, 6th ed. Upper Saddle River, NJ: Pearson Education Inc., pp. 296-311.
- [19] Sun Cheng etc. Paper Packaging Structure Design. Beijing: Light Industry Press; 2006. DOI:10.1016/j.proenv.2011.09.

Gravitational Model to Predict the Megalopolis Mobility of the Center of Mexico

Juan Bacilio Guerrero Escamilla, Sócrates López Pérez, Yamile Rangel Martínez, Silvia
Mendoza Mendoza*

*Academic Area of Sociology and Demography, Institute of Social Sciences and Humanities, Autonomous University of the State of Hidalgo. Pachuca City, Hidalgo State, México. Kilometer 4.5, Pachuca / Actopan Road, San Cayetano Neighborhood, P.C. 42084, Phone(51) 771-7172000 ext. 5200 to 5234.

Abstract— Since 1950, Mexico has presented an accelerated migration process to the country's capital, Mexico City. Here is where new settlements emerged increasing its population, and as a positive consequence, employment improved together with provisions. This growth occurred until the 1980s, when a conurbation happened with some municipalities of the State of Mexico, creating the Metropolitan Area of the Valley of Mexico. In the beginning of the 21st century, new challenges arose with the integration of more metropolitan areas in the states of Mexico (Valley of Toluca), Hidalgo, Morelos, Puebla, Tlaxcala and Queretaro.

This document is the result of two extensive research projects that took place from 2008 to 2016, along with the population institutions of the states that were integrated. The objective was to demonstrate the existence of the Megalopolis and its operation, based on a socio-demographic model to understand its composition and characteristics. However, when limited to demographic variables, it was difficult to analyze its operation. Therefore, the Gravitational Model was designed to establish the great diversity of mobility relationships to account for the functional composition. Thus, the population mobility that commutes daily to the interior of the Megalopolis will be the fundamental factor to explain its operation.

Keywords— Mexico Megalopolis, Gravitational model, Population mobility, Commuters model, Metropolitan Areas of Mexico, Urbanization of cities of Mexico.

I. INTRODUCTION

In the last fifty years, Mexico has gone through a number of demographic phenomena, including migration processes. These have varied in intensity according to the time period and great diversity in its forms, whether internal inter-municipal, rural-urban, interstate and international. Internal migration is highlighted, since it has been the main way to

define the setup of the current territory, the geographical distribution of its population, the definition and composition of its regions, the growth and consolidation of cities, and the current relationship between urban-rural populations.

At the same time, these internal population movements have been determinant factors for demographic dynamics, changes in the country's geographical distribution, economic diversification, integration of employment markets, and the population of big cities that have become attraction centers of population migration [1]. This demographic phenomenon is no longer the movement of the population from the countryside to the city. Now, migration is taking place among various urban centers, reaching high levels in the medium cities, generating mass displacements from the center of the Megalopolis towards a new network of intermediate cities and metropolitan areas of the states surrounding Mexico City as well as the Municipalities of the State of Mexico [3].

1.1 Integration of Metropolitan Areas in Mexico

In Mexico, the form of settlement defined as Metropolitan Areas (ZM as per its Spanish acronym for "Zona Metropolitana"), is a phenomenon that has been very dynamic, enabling to define population nuclei throughout the country and exceeding the municipal and state limits. These (ZM's) are characterized by being an urban region that includes a central nucleus linked to other smaller conglomerates (cities or municipalities); these are intertwined by sharing specific functions, such as industry, services, commerce and culture. This implies the formation of a system in which a central city establishes a network of relations with other cities or municipalities, as well as maintaining a high population density, where the size is related to the group of municipal administrations that are integrated [1]. The ZM's were starting points for the emergence of large spaces of differentiated trading, its own dynamics and resources, the application, design and development of large investment projects in various sectors,

and its own dominant center. ZM's are linked to peripheries and suburban spaces, with social groups and culture that gives them their own identity. This leads us to conceptualize the megalopolis of Mexico, beyond the simple integration or absorption of small cities, with urban agglomerates, emergence of suburbs, and dormitory cities or satellites.

The ZM with the largest population, major dynamism, economy, mobility and integration of states and municipalities, is the one that has been formed around Mexico City [7]. This ZM, under various demographic processes, has been growing at an accelerated rate in the last decades of the last century. This leads to new population dynamics and changes in its various indicators, rates, growth, displacement and migration [2]. This urban region is the sum of numerous cities that have been integrated. According to their growth, an increasingly bigger area is being formed, through nuclei that integrate millions of inhabitants, grouped in different cities and with clear relationships of functionality and trade. All of this is forming a megacity, megalopolis or megapolis [4].

1.2. The Megalopolis

The term megalopolis is understood as those urban regions that reach or surpass 10 million inhabitants, within the space or territory occupied by several cities [5]. In some cases, it is also defined when they have a population density of at least 2,000 inhabitants per km². However, the concept does not stop there, the studies carried out during the 1960s on large cities in North America defined Megalopolis in broader terms, since it wasn't limited to population volumes, which led to an integration and functioning of a wider body of cities and urban areas. The term megalopolis was defined as the formation of a set of Metropolitan Areas, whose accelerated urban growth leads to the contact of the area of influence of one another. Thus, the megalopolis usually consists of conurbations of large cities. This concept also includes a Global City that according to its author Saskia Sassen, applies to the cities that have a series of characteristics. These characteristics are the result of globalization and the constant growth of urbanization, including its broader and more comprehensive forms as political, economic and cultural categories.

The most common trend in the formation of a Megalopolis is the urbanization of large territories that have different ZM's that are linked to a single urban system, characterized by maintaining a dynamic interaction between two or more ZM's. The study mentioned previously, points out that these areas are wealthy and productive, forming a new urban

system which houses the most prosperous and well-educated groups with access to social services [5].

1.3 Central Mexico area Megalopolis

One of the first proposals of the central Mexico area megalopolis was in 1976. It established the existence of 12 metropolitan areas [15] within the context described by the UN in 1966, by considering them as the territorial extension that includes the political-administrative unit that contains the central city, and the contiguous political-administrative units that have urban characteristics such as workplaces or residences of non-agricultural workers. Also, they maintain a direct, constant and intense socio-economic interrelationship with the central city and vice versa [3]. Later, in an analysis from the 1980s, the Megalopolis was defined as the integration of 26 Metropolitan Areas, which included the 12 ZM's of the previous period [11], and defined the formation of the city in a first stage, in which the population, as well as the economic activity, housing and urban services tend to concentrate in the center of the city. This is followed by a second phase of physical expansion of the city and expansion of its influence radius; suburbanization is generated and new work centers and concentration of services appear within the urban area. If, in this process, the city absorbs one or more political-administrative units, close and external, they will grow around it and with that, a Metropolitan Area will appear [10].

In 1993, new areas were aggregated to the territory. Jaime Sobrino identified 37 metropolitan areas by pointing to the metropolitan areas with contiguity and integration graphs. At the same time, he integrated a statistic and applied the main components method with the variables of demographic growth rates, urbanization rate, GDP of the municipal manufacturing industry and coverage of drinking water services [14].

Recently, new proposals have been presented under a delimitation, considering the urban character of the municipality and the intermunicipality trips due to commuting. In addition, the demographic dynamics and the economic importance of the municipality are identified in 48 Metropolitan Areas which population represented almost half of the national population in the year 2000 [13].

The National Institute of Statistics Geography and Informatics (INEGI, as per its Spanish acronym), marked 32 Metropolitan Areas integrated by 205 municipalities, considering the size of the city and its relation of physical contiguity, and also based on the cartography of the national geostatistic framework and urban AGEB [6].

In more recent studies, and following the international urbanization trends, a metropolitan area is considered a central place that remains as a political-administrative unit, containing an urban area with 50 thousand or more inhabitants. However, for any unit to be part of a metropolitan area, it must be in territorial contiguity and maintain certain physical-geographical, socioeconomic and functional integration variables.

In 1995, the National Population Council (CONAPO, as per its Spanish acronym) identified 31 Metropolitan Areas and defined it as a set of two or more municipalities that contained, within its boundaries, a city of 100 thousand or more inhabitants, and whose population and productive activities had urban characteristics.

In 2003, CONAPO identified 42 Metropolitan Areas, integrated by 243 municipalities, pointing to its definition, the size and conurbation (physical union), the functional integration related to the displacement of the employed population between the municipalities of residence and work, as well as criteria on the urban character of the municipalities.

The Secretariat of Social Development (SEDESOL, as per its Spanish acronym), based on the National Urban Development Program 1990-1994, 1995-2000, 2001-2006; specified that a Metropolitan Area was defined as "Those city networks, where the metropolization processes that involve cities of Mexico and the United States of America or cities that have more than a million inhabitants".

II. THEORETICAL FRAMEWORK AND DEVELOPMENT OF THE GRAVITATIONAL MODEL

In the report on Urban Poverty and Metropolitan Areas in Mexico presented by the National Council for the Evaluation of the Social Development Policy (CONEVAL, as per its Spanish acronym) in 2013, a metropolitan area was defined as a group of municipalities in a single unit sharing a central city and that are functionally interrelated. This concept was developed in the United States in the early 1920s and refers to a large city where its limits exceed the political-administrative unit of a municipality. This process of metropolization is understood as "the special dynamics generated by the changes made in the production mode that involves the trend association of city networks or urban agglomerations constituting an urban conglomerate with common characteristics: economic, social, functional and productive, which define the flow of goods, people and financial resources".

Within the center of the country's metropolitan areas, continuous displacements of the population are generated, which are known as *commuting*. That is to say, it is the travel done by the inhabitants of a metropolitan area from their place of residence to their destination, where the intensities of displacements provide elements to determine the strength that drives the city's growth.

A City is defined as an agglomeration that includes considerable extensions that surpass its limits and that were historically marked by a past political decision. At present, cities in metropolitan areas at the center of the country expand beyond their original administrative area, reaching spaces of other cities, forming a large metropolitan area that exceeds its administration.

In this context, metropolitan areas reach a depletion limit in the proper use of their resources, which causes major problems, such as an inefficient infrastructure with low maintenance, low tax collection, increased insecurity and excess pollution. These problems result in continuous population displacements among the different metropolitan areas, resulting in an economic and social dynamic where mobility is related with a cost-benefit analysis.

Based on the above, the population mobility experienced in the metropolitan areas of the center of the country is the result of the economic and social growth that these regions have developed over time. This element gives rise to the need to measure the magnitude of mobility among the different areas. Therefore, this document has a theoretical basis in the gravitational law, because by its application it will be possible to predict the dynamics of the inhabitants commuting, and with this, measure the degree of speciality, by identifying the benefits and difficulties that each one of them currently present.

The gravitational law (2nd law of Issac Newton, 1642-1727) is part of mechanical physics and aims to describe the gravitational interaction between different bodies with mass. Newton demonstrated that the force of gravity has the direction of the line that connects the centers of the stars and the direction corresponds to an attraction [9].

Newton discovered that the force of attraction of two bodies is expressed as follows:

$$\vec{F} = |G| \frac{M * m}{R^2} \quad (1)$$

Where:
 \vec{F} is the force exerted between both bodies.
M is the mass of attraction of object one.
m is the mass of attraction of object two.
R is the distance that exists

between both objects.
 G is the universal gravitation constant.

Equation (1) means the following:
 “The force of gravity between two bodies is proportional to the product of their masses and inversely proportional to their square distance”

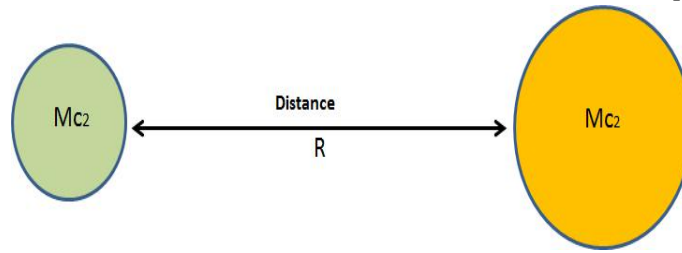


Fig.1: Graph of force of attraction between two bodies.

Source. Own elaboration, México, 2017.

That is, the greater the weight of the masses of both bodies, the greater their attraction, but this will depend on the distance between them, therefore we assume the following [8]:

- The greater weight of the mass between the bodies, the greater force of attraction.

- The smaller the distance between the bodies, the greater force of attraction.

Based on the above, the attraction force of one Metropolitan Area with respect to another will depend on the weight of their masses and inversely proportional to the distances and the time needed to cover those distances (Figure2).

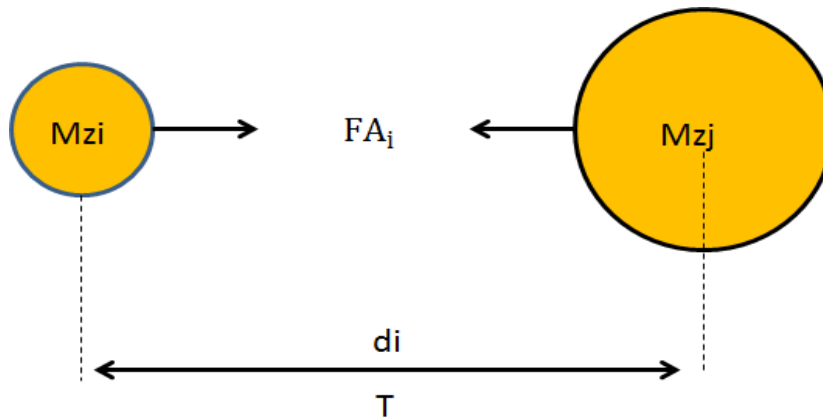


Fig.2: Graph of the force of attraction of two metropolitan areas.

Source. Own elaboration, México, 2017.

That is:

“The force of attraction between two metropolitan areas is proportional to their masses, and inversely proportional to the square of their distance”

Therefore, from the theory of gravitational law, the force of attraction of two Metropolitan Areas is expressed as follows:

$$FA_i = \left[\frac{(M_i)(M_j)}{(d_i)^2} \right] * 100; FA_i \in \mathcal{R}^+; i \neq j \quad (2)$$

Where:

- FA_i is the rate of the force of attraction between the i-th metropolitan area and the j-th metropolitan area.

- M_i is the attraction mass of the i-th metropolitan area.
- M_j is the attraction mass of the j-th metropolitan area.
- d_i is the distance between the i-th metropolitan area and the j-th metropolitan area (Km).

The dynamic mobility rate (commuting) of the i-th Metropolitan Area in relation to the others is expressed as follows:

$$FA_{Ti} = \int_b^a \frac{FA_i}{10} dPA \sim \sqrt[10]{\prod_{i=1}^{10} FA_i}; FA_i \in \mathcal{R}^+ \quad (3)$$

Its interpretation is as follows:

- The mobility rate between the metropolitan areas is identified as the degree of population displacement, which will depend on their confidence intervals.

$$\text{Lower limit (LI)} \left\{ \bar{X} - (1.96) \left(\frac{\sigma}{\sqrt{n}} \right) < \mu < \right.$$

Where:

- If $FA_{Ti} : FA_i \sim \mu$, there is moderate mobility.
- If $FA_{Ti} : FA_i < \mu$, there is low mobility.
- If $FA_{Ti} : FA_i > \mu$, there is high mobility.

Just as the force, the attraction mass of a metropolitan area is illustrated through its confidence intervals.

- If $M_i : M_j \sim \mu$, there is a moderate attraction mass.
- If $M_i : M_j < \mu$, there is a low attraction mass.
- If $M_i : M_j > \mu$, there is a high attraction mass.

- The force of attraction between metropolitan areas is interpreted as population mobility.
- The mass of attraction is interpreted as the social-economic benefit that a metropolitan area produces when living there.

Through the building of this model, it will be possible to know the dynamics of population mobility, which will be determined by the people's needs required to sustain their livelihood within their economic and social environment.

Predicting and identifying the dynamics of mobility as well as the specialization of metropolitan areas involves the development of a deterministic model (mathematical model). Therefore, building an abstract and simplified reality of the analyzed phenomenon, results in an empirical study where the results obtained can help to make decisions [12].

The development of the deterministic model of this research paper is presented in four phases[11]:

- 1- Mathematical formulation: this first phase consists of transcribing into mathematical language the mobility dynamic of the Metropolitan Areas.
- 2- Resolution: in this second stage, all the proper mathematical operations are executed, with the purpose of obtaining logical and adequate results regarding the mobility dynamic of the metropolitan areas.
- 3- Interpretation: in this stage, the results obtained in the model must be interpreted through the use of graphs of the mobility phenomenon in the metropolitan areas.

- 4- Predictions: in this last stage and through the interpretation of the model's results, the benefits and limitations of each one of the metropolitan areas must be identified, and with that, the specialization degree.

Based on the above, the study's target population is the commuters of the eleven metropolitan areas of the center of the country. This is because in 2008 they concentrated more than 40 percent of the economic activity of the country. In addition, they grouped more than 34.5 percent of the total population.

Predicting and identifying the mobility dynamics of commuters in the metropolitan areas involves the following assumptions:

- The population of the metropolitan areas is in constant mobility.
- This mobility is derived from a cost-benefit analysis.

III. METHODOLOGY OF THE GRAVITATIONAL MODEL

Based on the above, the mathematical formulation of the attraction force between two Metropolitan Areas is determined by the following algebraic expression:

$$FA_i = \left[\frac{(M_i)(M_j)}{(d_i)^2} \right] * 100; FA_i \in \mathcal{R}^+; i \neq j \quad (4)$$

So that:

$$FA_{Ti} = \int_b^a \frac{FA_i}{11} dPA \sim \sqrt[11]{\prod_{i=1}^{11} FA_i}; FA_i \in \mathcal{R}^+ \quad (5)$$

In order to evaluate the mobility or commuting rate among Metropolitan Areas, its mathematical resolution is to calculate the expected value of the attraction mass of the metropolitan area, which is obtained as follows:

$$E[M_i] = \sqrt[10]{(\bar{X}_1)(\bar{X}_2)(\bar{X}_3)(\bar{X}_4)(\bar{X}_5)(\bar{X}_6)(\bar{X}_7)(\bar{X}_8)(\bar{X}_9)(\bar{X}_{10})} \quad (6)$$

So that:

$$E[M_i] \in \mathcal{R}^+ \rightarrow 0 < E[M_i] \leq 100$$

Where:

- \bar{X}_1 is the attraction mass related to education
- \bar{X}_2 is the attraction mass related to health
- \bar{X}_3 is the attraction mass related to energy
- \bar{X}_4 is the attraction mass related to housing
- \bar{X}_5 is the attraction mass related to non-poverty
- \bar{X}_6 is the attraction mass related to water
- \bar{X}_7 is the attraction mass related to public security

- \bar{X}_8 is the attraction mass related to transportation and infrastructure
- \bar{X}_9 is the attraction mass related to non-contamination
- \bar{X}_{10} is the attraction mass related to employment

The expected value of any \bar{X}_i is obtained by standardizing the information through logarithms.

The estimation and interpretation of the results of the present model are structured from two aspects:

- 1- The prediction of the mobility dynamics of commuters of metropolitan areas, taking each one of their attraction masses as a reference.

- 2- The measurement and identification of the speciality of each one of the metropolitan areas, derived from the mobility dynamics of commuters.

By reading these results, it will be possible to make projections on the socio-economic trend that each one of the metropolitan areas must follow, which will provide the necessary elements to propose a megalopolitan management, with the purpose of obtaining a better distribution of the economic resources that each one of them generates.

The mobility dynamics of the metropolitan areas will be interpreted as the commuting degree that the inhabitants of each area are willing to experience.

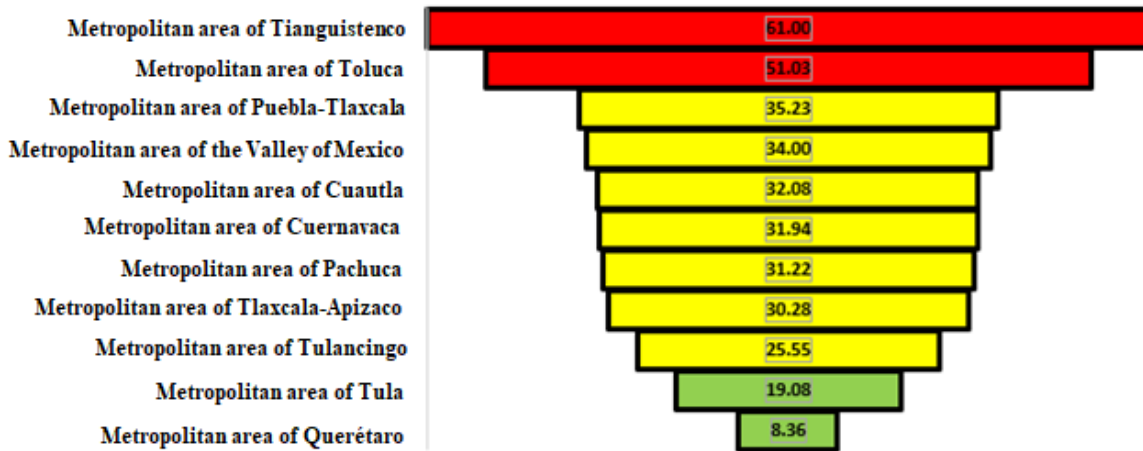


Fig.3: Mobility degree per Metropolitan Area.
 Source. Own elaboration, México, 2017.

Based on figure 4, it can be seen that the Tianguistenco and Toluca areas experience a high degree of mobility (61 and 51 units), when compared to the others. On the other hand, Tula and Queretaro are the ones with less mobility, while the other areas have a homogeneous behavior.

Example: the mobility rate of all the Metropolitan Areas is 29.50 units:

$$FA_{Ti} = \sqrt[11]{\prod_{i=1}^{11} FA_i}$$

$$= \sqrt[11]{(61)(51.03)(35.23)(34)(32.08)(31.94)(31.22)(30.28)(25.55)(19.08)(8.36)}$$

Therefore:

$$FA_{Ti} = \sqrt[11]{\prod_{i=1}^{11} FA_i} = 29.50 \text{ units}$$

Where:

- FA_i is the expected value of the attraction in the i -th attraction mass, which is obtained from the following algebraic expression:

$$FA_i = \left[\frac{(M_i)(M_j)}{(d_i)^2} \right] * 100; FA_i \in \mathcal{R}^+; i \neq j$$

The masses driving the mobility of all the metropolitan areas are the following (figure 5):

- Housing. As a social entity, it is the place where the family settles, lives, grows and thrives. Therefore, it is the economic and social development of the individual [3].

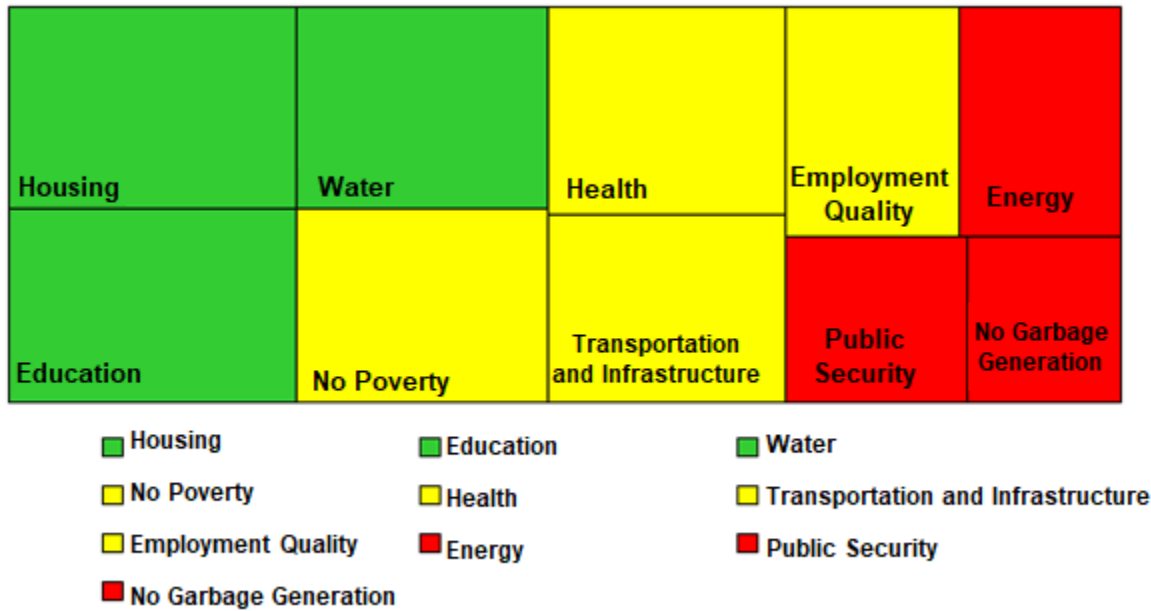


Fig.4: Rank of major influence masses in the commuting among the metropolitan areas in the center of the country. Source. Own elaboration, México, 2017.

- Education: The tool must transmit knowledge, values, customs, behaviors, attitudes and course of actions that the human being must acquire and use throughout their life.
- Water: it is the most important non-renewable resource for the survival of any living being. This resource gave rise to life and it sustains it; it is a factor that regulates the planet's weather. It creates and allows the existence of ecosystems and mankind.

Meanwhile, health, transportation, infrastructure, employment quality, and the fight against poverty generate a moderate mobility, probably due to the following factor: the gap between these attraction masses of each metropolitan area is not very wide. This is presumably

because of the living costs in each one of them. Most likely, the Valley of Mexico offers better quality jobs than any other Metropolitan Area, however the costs of living there is more expensive than the others. Therefore, a person would have to make a cost-benefit analysis on employment.

On the other hand, in spite of the increase of the environmental and insecurity issues throughout the country, they are not still elements that strongly detonate population mobility among the metropolitan areas.

Based on the above and according to figure 6, the metropolitan area that generates more attraction force is Queretaro, due to four factors (figure 6): highly qualified jobs, low poverty rates, efficiency in energy supply, transportation and infrastructure.

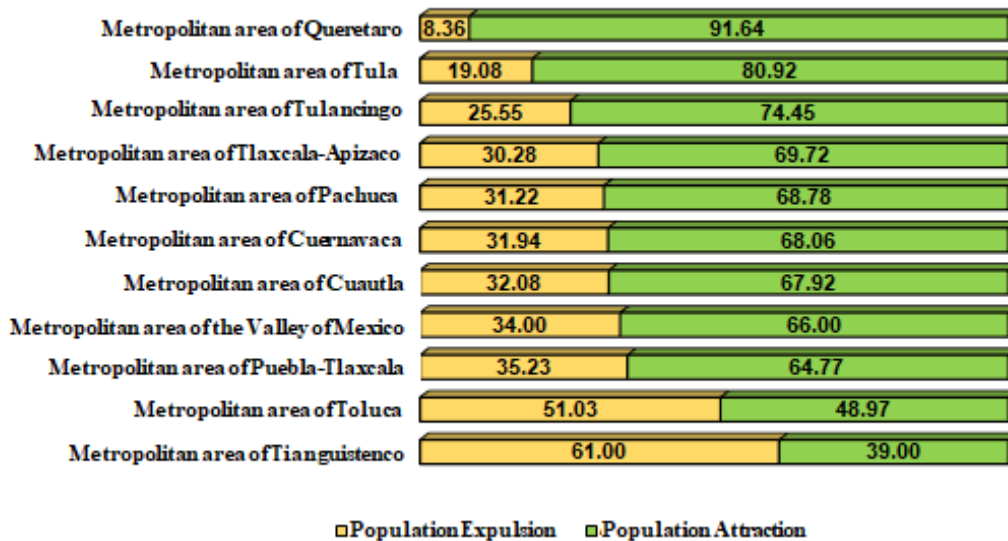


Fig.5: Expulsion and attraction per Metropolitan area.

Source. Own elaboration, México, 2017.

In the example, the mobility rate of all the Metropolitan Areas was 29.50 units, therefore, the attraction force between them would be 70.50 units

Therefore:

$$\begin{aligned}
 FA_{Ti} &= \sqrt[11]{\prod_{i=1}^{11} FA_i} = 29.50 \text{ units} \rightarrow FA_{Tj} = 100 - FA_{Ti} \\
 &= 100 - 29.50 = 70.50 \text{ units}
 \end{aligned}$$

In addition, education, health, water, public security and garbage collection behave similarly to the other metropolitan areas (except for Puebla-Tlaxcala and the Valley of Mexico, because in education and health they are above Queretaro). Their main limitation is house acquisition due to rising home prices as a result of the cost of living increment in the area.

The second metropolitan area with greater attraction is Tula due to two factors:

- It ranks 3rd in offering the best jobs because the *Miguel Hidalgo* refinery and the *Fortaleza* cement factory are located within its territory. Also, it has one of the most important archeological areas in the state of Hidalgo.
- Tula presents a moderate attraction force in education, health, energy, housing, water supply, public security, transportation, infrastructure, and fight against poverty. However, currently it has major issues with garbage collection which contributes to the high pollution rates. Most of the pollution comes from the *Miguel Hidalgo* refinery and the *Fortaleza* cement factory.

- Transportation and infrastructure have better quality in the Valley of Mexico, Toluca and Queretaro.
- Its garbage collection system is less efficient than Tianguistenco and Tulancingo.
- Their employment quality is inferior to Queretaro, Valley of Mexico and Tula.

For the metropolitan area of Cuautla, its force of attraction is 67.92 units and this behavior is due to the fact that its attraction masses exhibit a moderate behavior. However, the mobility of its population (32.08 units) is due to the following factors:

- In education, health and energy it is surpassed by the Valley of Mexico, Puebla-Toluca and Queretaro.
- The cost of housing is above Pachuca and Tulancingo, however, it is inferior to Queretaro and the Valley of Mexico.
- In the fight against poverty, it is more efficient than Toluca, but inferior to Queretaro.
- Its water supply is more efficient than that of Toluca, but less efficient than that of Puebla-Tlaxcala and Cuernavaca.
- In public security it is above Cuernavaca and the Valley of Mexico, and below Tianguistenco.
- Public transportation and infrastructure is more efficient than that of Tulancingo, however, it is below Queretaro, the Valley of Mexico and Toluca.
- Its garbage collection system is better than the Valley of Mexico and Tula, but inferior to Tianguistenco and Tulancingo.
- The employment quality does not compare to the Valley of Mexico, Queretaro and Tula, however, it is comparable with the other metropolitan areas, except for Tianguistenco.

The metropolitan area of the Valley of Mexico has an attraction force of 66 units due to the high indicators in education, health, energy, transportation and infrastructure, and employment quality but inferior to Queretaro's. Its main weaknesses are the high cost of housing, the public security system and the way garbage is collected. These indicators are also supported by data provided by INEGI in 2015. This showed that the activity with the highest prevalence in the Valley of Mexico is the tertiary sector (education, health and finance, among others), concentrating 66.27 percent of all activities.

For the metropolitan area of Puebla-Tlaxcala its attraction force is 64.77 units as a consequence of the great benefits it

offers in education, health and water supply (the Valley of Mexico is the only Area that surpasses it in education and health). Its other attraction masses present a moderate behavior, however, there are some areas that surpass it:

- In energy and housing by the Valley of Mexico, Pachuca and Tulancingo.
- In the fight against poverty by Queretaro.
- In public security by Tianguistenco but it is widely superior than Cuernavaca and the Valley of Mexico.
- In transportation and infrastructure, the Valley of Mexico, Toluca and Queretaro are superior.
- In garbage collection by Tianguistenco and Tulancingo.
- Employment quality by the Valley of Mexico, Queretaro and Tula.

The metropolitan areas with lower attraction force are Toluca and Tianguistenco (48.97 and 39.00 units):

- Toluca's attraction force is determined by the following:
 - Its strength in public transportation and infrastructure.
 - Its limitations in education, health, water supply, energy, and employment quality.
 - In public security and garbage collection it is moderate, however, it is inferior to Tianguistenco and Tulancingo.
- The force of attraction of Tianguistenco is determined by:
 - Its strength in public security and garbage collection.
 - Its weaknesses in education, health and quality of employment.
 - It shows a moderate behavior in public transportation, infrastructure, water, energy and housing

Based on the analysis of the results of all metropolitan areas, the prediction of this model focuses on the specialization of each area (Table 1):

- The Valley of Mexico specializes in education, health, transportation, infrastructure and quality employment. However, it presents major problems in house acquisition and public security.
- Queretaro specializes in the highest paid jobs among all the Metropolitan Areas. Also, a high specialization in efficiency of transportation and

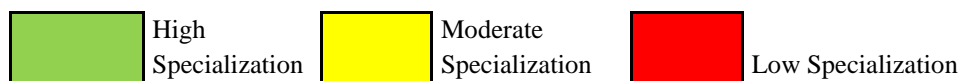
- infrastructure, energy supply, and the fight against poverty.
- Tula specializes in creating well-paid jobs, as a result of the electric and cement industries, as well as the tourism in its archaeological area.
- Pachuca specializes mainly in housing due to its low acquisition cost. Just like Pachuca and Tulancingo specialize in housing.
- Tlaxcala-Apizaco has a moderate specialization, since the majority of its attraction masses have an impartial behavior, except for energy supply.
- Puebla-Tlaxcala specializes in education, health and water.
- Cuautla has a moderate specialization in all its attraction masses.

- Cuernavaca specializes in water supply, however, it faces major insecurity problems.
- Toluca specializes in public transportation and infrastructure, however, its weakness is the fight against poverty and water supply.
- Tianguistenco specializes in garbage collection and public safety, however, it has too many limitations in education, health and employment quality.

As it can be seen, building and developing a gravitational model based on the mobility of metropolitan areas gives us the necessary elements to affirm where each one of them is economically heading, and with that, making decisions on how to manage and guide the central area of the country.

Table.1: Specialization of each Metropolitan Area.

METROPOLITAN AREA	Education	Health	Energy	Housing	Well-being	Water	Public Security	Transportation Infrastructure	Garbage management	Employment quality
Valley of Mexico	High	High	High	Low	Moderate	Moderate	Low	High	Low	High
Queretaro	Moderate	Moderate	High	Low	High	Moderate	Moderate	High	Moderate	High
Tula	Moderate	Moderate	Moderate	Moderate	Moderate	Moderate	Moderate	Moderate	Low	High
Pachuca	Moderate	Moderate	Moderate	High	Moderate	Moderate	Moderate	Moderate	Moderate	Moderate
Tulancingo	Moderate	Moderate	Moderate	High	Moderate	Moderate	Moderate	Low	Moderate	Moderate
Tlaxcala - Apizaco	Moderate	Moderate	Moderate	Moderate	Moderate	Moderate	Moderate	Moderate	Moderate	Moderate
Puebla - Tlaxcala	High	High	Low	Moderate	Moderate	High	Moderate	Moderate	Moderate	Moderate
Cuautla	Moderate	Moderate	Moderate	Moderate	Moderate	Moderate	Moderate	Moderate	Moderate	Moderate
Cuernavaca	Moderate	Moderate	Moderate	Moderate	Moderate	High	Low	Moderate	Moderate	Moderate
Toluca	Moderate	Moderate	Moderate	Moderate	Low	Low	Moderate	High	Moderate	Moderate
Tianguistenco	Low	Low	Moderate	Moderate	Moderate	Moderate	High	Moderate	High	Moderate



Source. Own elaboration, México, 2017.

IV. CONCLUSION

Through the application of the gravitational model, it was observed that the mobility of all the metropolitan areas in the center of the country is 29.50 units, that is to say, 30 of every 100 inhabitants commute. Specifically, the main drivers are housing, education and water. In addition, its

attraction force is 70.50 (71 of every 100 inhabitants have the intention of moving within the center of the country).

The metropolitan area of Queretaro is the one that experiences less population mobility. Moreover, it is the one that generates the greatest attraction force compared to the others, since it offers the best paying jobs in the center of the country. This causes a reduction on their poverty

indicators. In addition, they have built a solid infrastructure resulting in a wider distribution of their wealth. Regarding the population mobility, the metropolitan area of Tianguistenco presents the greatest population mobility and the lowest attraction force, because it has limitations in education, health and employment quality. Its main virtues are public security and garbage collection.

Based on the most influential masses in commuting (housing, education and water), the following could be identified: the metropolitan areas of the Valley of Mexico and of Puebla-Tlaxcala are the ones that offer better education centers, since both have higher education institutions (UNAM, IPN, CIDE, COLMEX, UDLA, BUAP, and UPAEP, among others). In health, just as in education, both areas are the most prominent in the center of the country, since they have important medical centers (Hospital Angeles, Hospital la Raza, Asociación Nacional de Hospitales Privados, Hospital Universitario BUAP, Hospital Puebla, and Sociedad de Beneficencia Española, among others). In water, the model predicted that the metropolitan areas of Puebla – Tlaxcala and Cuernavaca present better efficiency in the water supply. This stresses the importance of optimizing the water consumption and reducing the contamination throughout the socio-economic activities.

Other relevant results from the present model are the security problems that are collectively presented in the metropolitan areas, and to a greater extent in the Valley of Mexico and Cuernavaca. This phenomenon most likely stems from the lack of institutional, political and social agreements related to the functions of the different public powers, because in their absence, there is no link between the public security system and citizens. Therefore, a system is formed where corruption and impunity prevail.

In addition, the employment quality in most of the metropolitan areas is low except for the Valley of Mexico and Queretaro. This behavior is due to the low economic activity, as the result of the low labor productivity. In other words, there is not enough skilled labor, therefore, wages are low. As a consequence, there is little private investment.

REFERENCES

[1] CONAPO; SEDESOL; INEGI. (2012), Delimitation of Metropolitan Areas of Mexico 2010. National Population Council (CONAPO), Ministry of Social Development (SEDESOL), National Institute of Statistics and Geography (INEGI), Mexico.

[2] CORONA, Reina, & Luque, Rodolfo. (1992), "Recent Changes in Migration Patterns to the Metropolitan

Area of Mexico City (ZMCM)", Demographic and Urban Studies, vol. 7, no. 2-3, Mexico.

- [3] FLORES, Sergio. (2002), "Urban planning and sustainable regional development in the metropolitan area of Puebla-Tlaxcala" in Delgadillo, Javier, Iracheta, Alfonso, Current regional research in Central Mexico, CRIM, UNAM, Mexico, pp. 195-220.
- [4] FORSTALL, Richard. (2004), Which Are The Largest? Why Published Populations For Major World Urban Areas Vary So Greatly, Consultant, Richard P. Greene, Northern Illinois University, James B. Pick, University of Redlands, United Kingdom.
- [5] GOTTMANN, Jean. (1961), Megalopolis: The Urbanized Northeastern Seaboard of the United States. Editor Literary Licensing ISBN 1258423251, 9781258423254
- [6] INEGI. (2002), Statistical Notebooks of the Metropolitan Area of Mexico City. Edition 2002. National Institute of Statistics and Geography (INEGI), Mexico.
- [7] LOPEZ, Socrates. (2009), Sociodemographic diagnosis of the megalopolis of the center of the country. Autonomous University of the State of Hidalgo, Mexico, pp. 200.
- [8] MARTÍN, I. (2004). General Physics. Spain: University of Valladolid.
- [9] MEDINA, A. and Ovejero, J. (2011). Newton's laws and their applications. Spain: University of Salamanca.
- [10] NEGRETE, María, & Salazar, Héctor. (1986). "Metropolitan areas in Mexico, 1980", in Estudios Demográficos y Urbanos, vol. 1, no. 1, The College of Mexico, Mexico.
- [11] RÍOS, S. (1995). Modeling Spain: Editorial alliance.
- [12] RODRÍGUEZ, J. (2010). Mathematical models. Spain: Open University of Catalonia.
- [13] SOBRINO Jaime, (1993), "Government and metropolitan and regional administration", National Institute of Public Administration, A. C., Mexico.
- [14] SOBRINO Jaime, (2003), "Delimitation of the metropolitan areas of Mexico in 2000", in the National Population Council (coord.), The delimitation of zones, metropolitan, Mexico, CONAPO, SEDESOL, INEGI, Institute of Geography-UNAM, Mexico, pp. 121-151.
- [15] UNIKEL, Luis. (1976), Urban development in Mexico, diagnosis and future implications. The College of Mexico, Mexico, pp. 116

Artificial Neural Network Controller for Reducing the Total Harmonic Distortion (THD) in HVDC

Dr. Ali Nathem Hamoodi, Rasha Abdul-nafaa Mohammed

¹Lect., Dept. of Technical Power Eng., Technical College-Mosul
²Asist. Lect., Dept. of Technical Power Eng, Technical College-Mosul

Abstract— A neural network based space vector modulation (SVM) of voltage source inverter is proposed. The voltage source converter (VSC) is highly used in high voltage direct current (HVDC) transmission so that a detailed analysis and transmission of this system is carried out. In addition, a non-linear neural network controller is proposed to control the space vector pulse width modulation (SVPWM) to reduce the total harmonic distortion (THD) of the converter (inverter) output voltage. The inverter output current is analyzed with two switching frequency 1050Hz and 1450Hz with and without proposed ANN controller. The results show a THD enhancement about 0.74 % for 1050Hz and 0.68 % for 1450Hz.

Keywords— HVDC, VSC, THD , SVPWM, ANN.

I. INTRODUCTION

An electronic converter is required to convert DC to AC energy . VSC is used to interconnect generation system with AC network. Now VSC is one of the best converter because it has modern power semiconductor advantages as Turn-off (GTO) and (IGBT) [1-2].

The flow control of active and reactive power flow is become more flexible today because of VSC-HVDC technology [3-6].

The basic VSC model is shown in figure.(1).

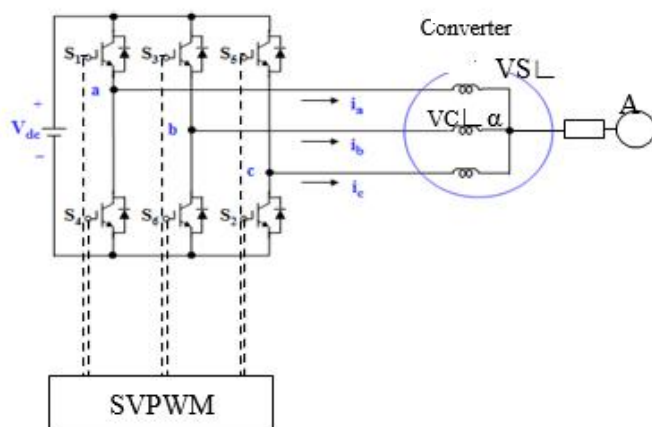


Fig.1: Model of six-pulse VSC-HVDC system.

This paper describes neural network controller based on SVPWM implementation of a 12-pulse voltage-fed inverter. In the beginning, (SVPWM) for a 12-pulse inverter is reviewed briefly. The general expressions of time segments of inverter voltage vector for all the regions have been derived.

A basic 12-pulse VSC-HVDC system is comprised of two 6-pulse IGBT converter station built with VSC topologies as shown in figure.(2)

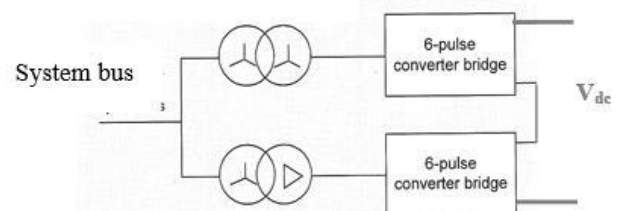


Fig.2: Series connection on DC sides

(SVPWM) has modern technology for voltage fed converter. It consider more improved as compared with PWM [7].

II. SVPWM TECHNIQUE.

SVPWM considered as best method for digital implementations where, switching frequency(2/3) [9,10]. The 6-switch three-phase voltage source inverter is shown in figure.3

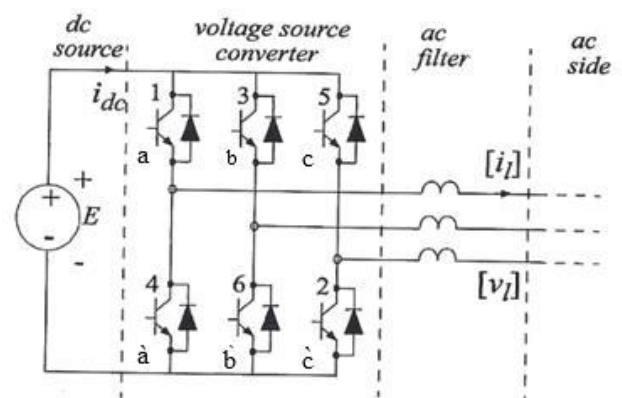


Fig.3: Six-switch three-phase voltage source inverter.

III. SWITCHING SEQUENCES.

In 3Φ inverter, the outputted voltage vectors with six sectors as illustrated in figure.4. [11].

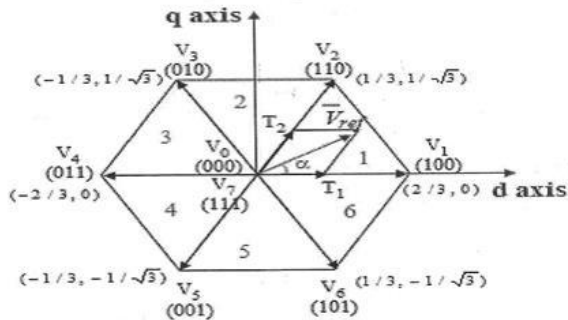


Fig.4: Basic switching vectors and sectors.

Where,
 (2T_Z): sampling time.
 V*:command vector.
 A: angle in each sector.

The eight switching sequences is shown in figure.5.

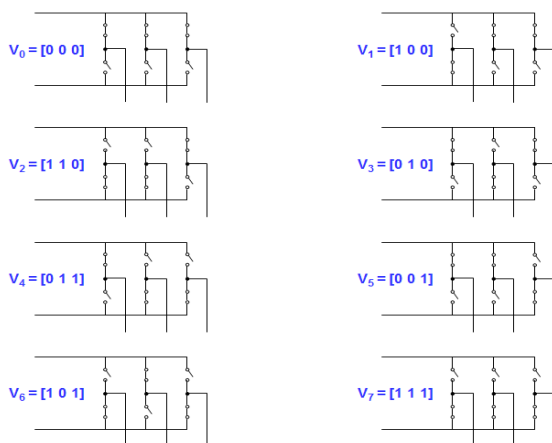


Fig.5: Switching sequences.

The eight combination, voltage vectors, switching sequences, phase voltages and output line to line voltages is shown in Table.1.

Table.1: Voltage vectors, switching sequences, phase voltages and line-to-line voltages.

Voltage Vectors	Switching Vectors			Line to neutral voltage			Line to line voltage		
	a	b	c	V _{an}	V _{bn}	V _{cn}	V _{ab}	V _{bc}	V _{ca}
V ₀	0	0	0	0	0	0	0	0	0
V ₁	1	0	0	2/3	-1/3	-1/3	1	0	-1
V ₂	1	1	0	1/3	1/3	-2/3	0	1	-1
V ₃	0	1	0	-1/3	2/3	-1/3	-1	1	0
V ₄	0	1	1	-2/3	1/3	1/3	-1	0	1
V ₅	0	0	1	-1/3	-1/3	2/3	0	-1	1
V ₆	1	0	1	1/3	-2/3	1/3	1	-1	0
V ₇	1	1	1	0	0	0	0	0	0

(Note that the respective voltage should be multiplied by V_{dc})

IV. REALIZATION OF SVPWM.

In order to realize the SVPWM , three steps must be investigated .

- a-Determining the voltages.
- b-Determining time durations.
- c-Determining the switching time.

The voltages in a, b, c, frame is transformed to space vector voltage in d-q frame shown in figure.6

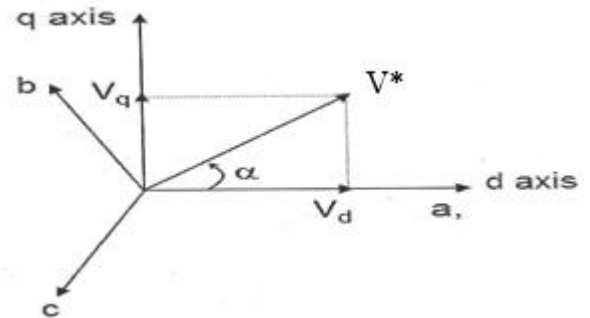


Fig. 6: Space vector in (d,q) frame.

V_d and V_q can be represented as:

$$\therefore \begin{bmatrix} V_d \\ V_q \end{bmatrix} = \frac{2}{3} \begin{bmatrix} 1 & -\frac{1}{2} & -\frac{1}{2} \\ 0 & \frac{\sqrt{3}}{2} & -\frac{\sqrt{3}}{2} \end{bmatrix} \begin{bmatrix} V_{an} \\ V_{bn} \\ V_{cn} \end{bmatrix} \dots\dots\dots(1)$$

$$|\bar{V}^*| = \sqrt{V_d^2 + V_q^2} \dots\dots\dots(2)$$

$$\alpha = \tan^{-1}\left(\frac{V_q}{V_d}\right) \dots\dots\dots(3)$$

$$\omega_s t = 2\pi f_s t$$

where,

f_s = switching frequency

α = Vector angle

V_d = horizontal component.

V_q = vertical component.

\bar{V}^* = the vector of V_{ref}.

- b- Determining time duration.

The terns router combination is depicted in figure.7.

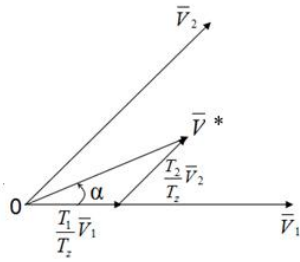


Fig.7: Reference vector combination.

The switching time duration at any sector is determined by the following equations:[12].

$$\begin{aligned} \therefore T_1 &= \frac{\sqrt{3} \cdot T_z \cdot |\bar{V}^*|}{V_{dc}} \left(\sin\left(\frac{\pi}{3} - \alpha + \frac{n-1}{3}\pi\right) \right) \\ &= \frac{\sqrt{3} \cdot T_z \cdot |\bar{V}^*|}{V_{dc}} \left(\sin\frac{n}{3}\pi - \alpha \right) \\ &= \frac{\sqrt{3} \cdot T_z \cdot |\bar{V}^*|}{V_{dc}} \left(\sin\frac{n}{3}\pi \cos\alpha - \cos\frac{n}{3}\pi \sin\alpha \right) \dots\dots\dots(4) \end{aligned}$$

$$\begin{aligned} \therefore T_2 &= \frac{\sqrt{3} \cdot T_z \cdot |\bar{V}^*|}{V_{dc}} \left(\sin\left(\alpha - \frac{n-1}{3}\pi\right) \right) \\ &= \frac{\sqrt{3} \cdot T_z \cdot |\bar{V}^*|}{V_{dc}} \left(-\cos\alpha \cdot \sin\frac{n-1}{3}\pi + \sin\alpha \cdot \cos\frac{n-1}{3}\pi \right) \end{aligned} \dots\dots\dots(5)$$

$$\therefore T_0 = T_z - (T_1 + T_2), \begin{cases} \text{(where, } n=1 \text{ through } 6) \\ \text{(that is, Sector 1 to 6)} \\ 0 \leq \theta \leq 60^\circ \end{cases} \dots\dots\dots(6)$$

Where,

T_1, T_2 and T_0 : is the time duration for each sector.

T_z : is the sampling time (inverse of the switching frequency (f_s)).

c-Determining the switching time of each transistor (S_1 to S_6). The switching times of the upper and lower transistors for each sector is shown in figure.8

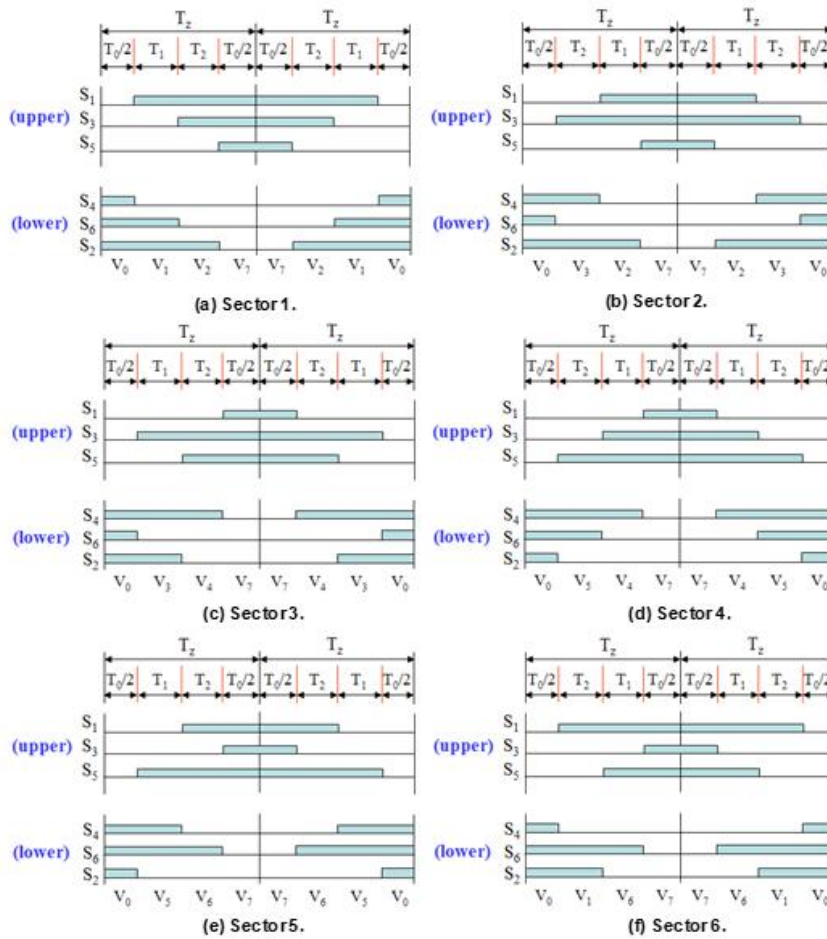


Fig. 8: PWM patterns at each sector.

V. SIMULATION WITHOUT ANN IMPLICATION VSI-HVDC BASED SVPWM.

Figure.9 presents Matlab/Simulinkmodel of a 12-pluse VSI-HVDC based on SVPWM.

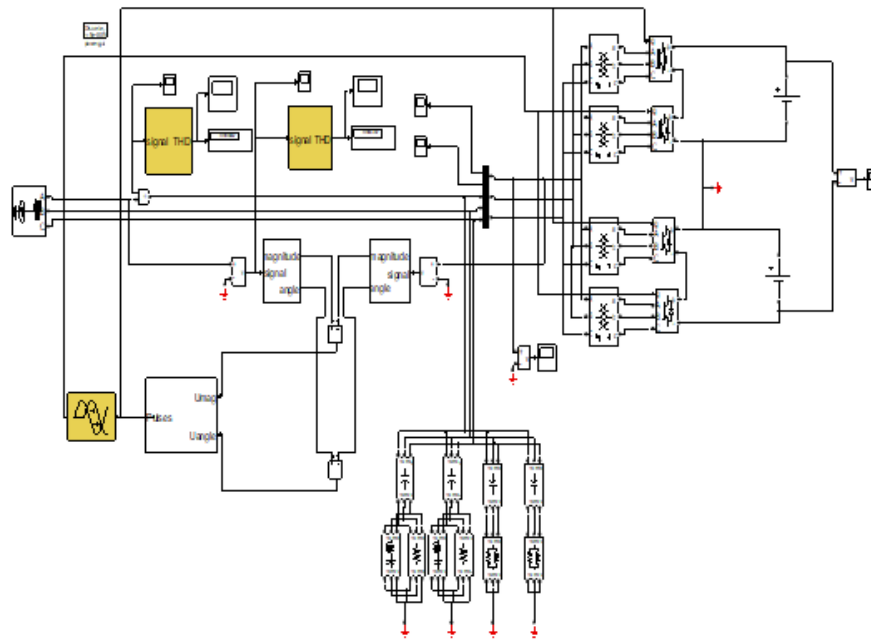


Fig.9: MATLAB/SIMULINK model of a VSI-HVDC on SVPWM.

The THD ratio of the line current for switching frequencies 1050Hz and 1450Hz is shown in figure. 10.

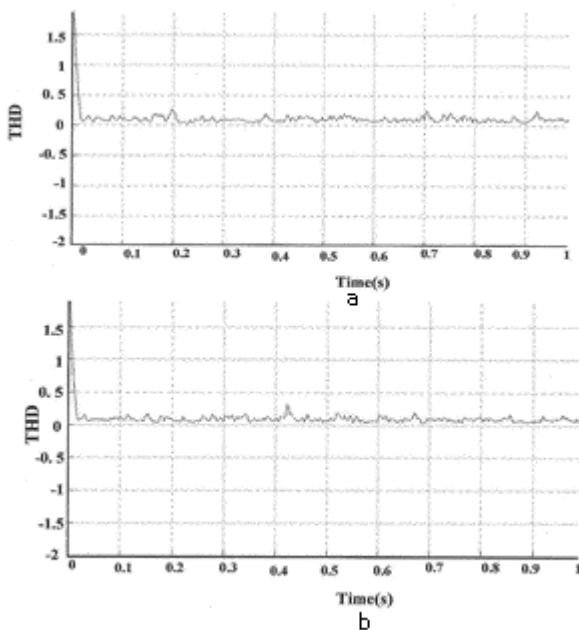


Fig.10: THD ratio of line current in time domain.
 (a) at switching frequency (1050Hz).
 (b) at switching frequency (1450Hz).

The THD ratio of the line to line voltage at 1050Hz and 1450Hz switching frequency is shown in figure.11.

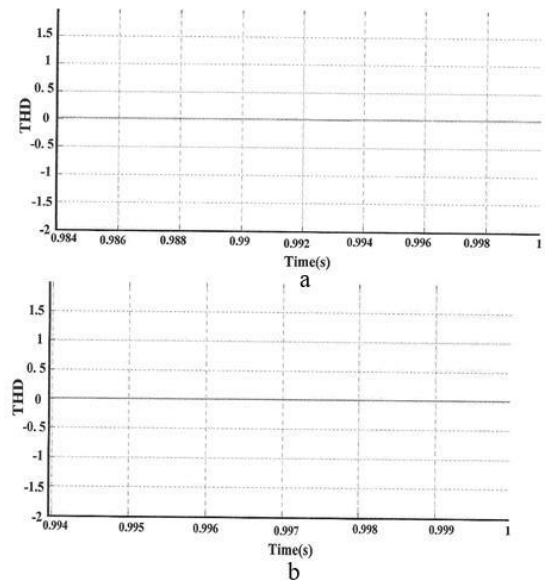


Fig.11: THD ratio of line to line voltage in time domain.
 (a) at switching frequency (1050Hz).
 (b) at switching frequency (1450Hz).

The THD ratio of the line current and line-line voltage shown in Table.2 are obtained directly by computer from figures 10 & 11.

Table.2: THD values for line current and line to line voltage

Switching frequency(Hz)	Line current THD value(%)	Line-line Voltage THD value(%)
1050	17%	2.088%
1450	8.625%	1.323%

VI. TRAINING METHOD

In this paper, back propagation Levenberg- marquard (LM) algorithm is used for training converter because this method has many advantages and gives high response .Leverberg-marquard (LM) algorithm is used.

VII. ANN-BASED SVPW IMPLICATION.

A feed forward ANN mapping and its timing calculation, the turn-on time T_{-ON} given as:[13].

$$T_{-ON} = \begin{cases} \frac{T_z}{2} + D |V^*| \begin{bmatrix} -\left(\sin \frac{n}{3}\pi \cos \theta - \cos \frac{n}{3}\sin \alpha\right) \\ -\left(-\cos \theta \sin \frac{n-1}{3}\pi + \sin \theta \cos \frac{n-1}{3}\pi\right) \end{bmatrix} \text{Sector} \\ \frac{T_z}{2} + D |V^*| \begin{bmatrix} -\left(\sin \frac{n}{3}\pi \cos \theta - \cos \frac{n}{3}\sin \theta\right) \\ +\left(-\cos \theta \sin \frac{n-1}{3}\pi + \sin \theta \cos \frac{n-1}{3}\pi\right) \end{bmatrix} \text{Sector} \\ \frac{T_z}{2} + D |V^*| \begin{bmatrix} +\left(\sin \frac{n}{3}\pi \cos \theta - \cos \frac{n}{3}\sin \theta\right) \\ +\left(-\cos \theta \sin \frac{n-1}{3}\pi + \sin \theta \cos \frac{n-1}{3}\pi\right) \end{bmatrix} \text{Sector} \\ \frac{T_z}{2} - D |V^*| \begin{bmatrix} +\left(\sin \frac{n}{3}\pi \cos \theta - \cos \frac{n}{3}\sin \theta\right) \\ -\left(-\cos \theta \sin \frac{n-1}{3}\pi + \sin \theta \cos \frac{n-1}{3}\pi\right) \end{bmatrix} \text{Sector} \end{cases}$$

where,

$$D = \sqrt{3} \times V_{ref} / V_{dc}$$

Turn-off time is depicted as:

$$T_{-OFF} = 2T_z - T_{A-on} \dots \dots \dots (8)$$

In general, from equation (12) can be written as:

$$T_{-ON} = \frac{T_z}{2} + f(V^*) \cdot g(\alpha) \dots \dots \dots (9)$$

where ,

$f(V^*)$ is the voltage amplitude scale factor.

And

$$g(\alpha) = \begin{cases} D \begin{bmatrix} -\left(\sin \frac{n}{3}\pi \cos \alpha - \cos \frac{n}{3}\sin \alpha\right) \\ -\left(-\cos \alpha \sin \frac{n-1}{3}\pi + \sin \alpha \cos \frac{n-1}{3}\pi\right) \end{bmatrix} \text{Sector} = 1,6 \\ D \begin{bmatrix} -\left(\sin \frac{n}{3}\pi \cos \alpha - \cos \frac{n}{3}\sin \alpha\right) \\ +\left(-\cos \alpha \sin \frac{n-1}{3}\pi + \sin \alpha \cos \frac{n-1}{3}\pi\right) \end{bmatrix} \text{Sector} = 2 \\ D \begin{bmatrix} +\left(\sin \frac{n}{3}\pi \cos \alpha - \cos \frac{n}{3}\sin \alpha\right) \\ +\left(-\cos \alpha \sin \frac{n-1}{3}\pi + \sin \alpha \cos \frac{n-1}{3}\pi\right) \end{bmatrix} \text{Sector} = 3,4 \\ D \begin{bmatrix} +\left(\sin \frac{n}{3}\pi \cos \alpha - \cos \frac{n}{3}\sin \alpha\right) \\ -\left(-\cos \alpha \sin \frac{n-1}{3}\pi + \sin \alpha \cos \frac{n-1}{3}\pi\right) \end{bmatrix} \text{Sector} = 5 \end{cases} \dots \dots \dots (10)$$

$g(\alpha)$: T-on pulse width.

In the under modulation region, $f(V^*) = V^*$ as depicted in figure. 12.

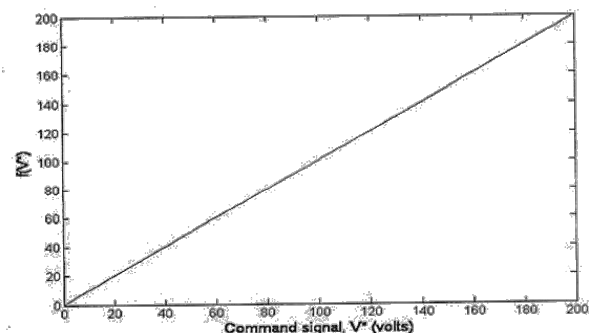


Fig.12: $f(V^*)$ - V^* relation in under modulation region
 The pulse generated by ANN for sector one , $V^* = 360KV$ and $\theta = 40^\circ$ as taken from the inverter side, is shown in figure.13.

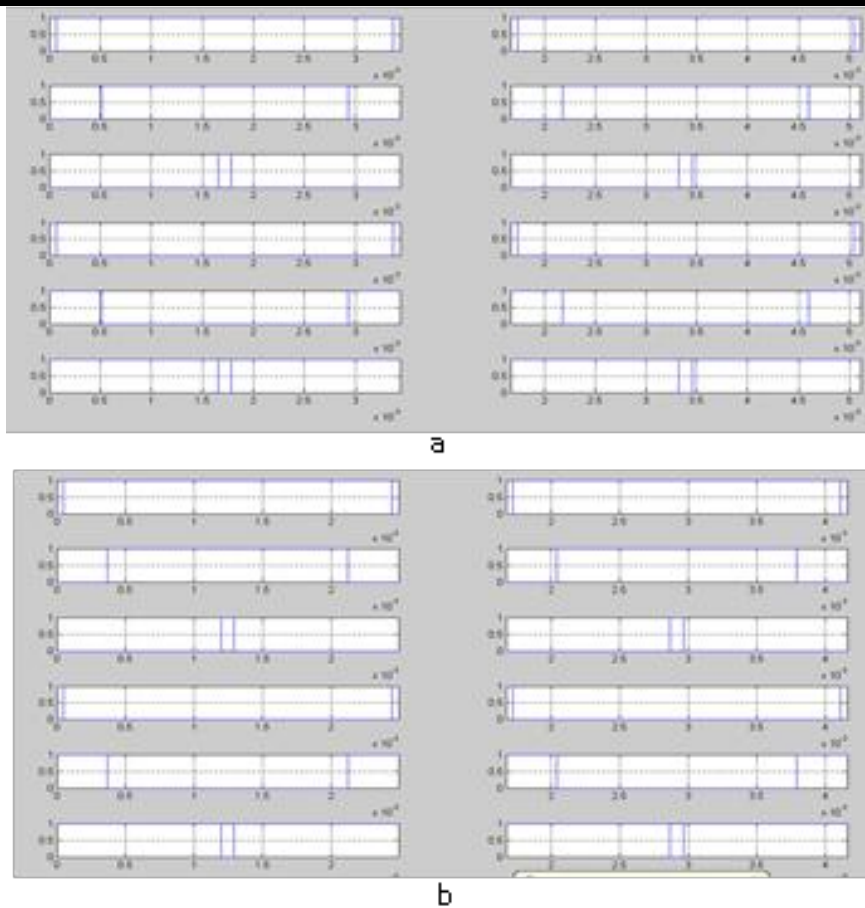


Fig.13: PWM using ANN.
 (a) at switching frequency (1050Hz).
 (b) At switching frequency (1450Hz).

VIII. SUGGESTED TOPOLOGY OF ANN BASED CONTROLLER

The ANN suggested topology has two inputs (two neurons) in the input layer, one hidden layer (N- neurons) and three outputs (three neurons) in the output layer. The input layer simply acts as a fan-out input to the hidden layer where two neurons are used and the output layer has three neurons with a sigmoidal activation function and (N) inputs (N1 from the hidden layer and one constant bias).

The input layer of the proposed ANN controller shown in figure (14) has two input variables, the first is the $V_{ref\text{vector}} \left| \bar{V}^* \right|$ and the second vector angle α . While, the output layer has two variables concerned with the on and off durations of the switching pulses. The error which represented by the target minus the actual the delta rule [9].

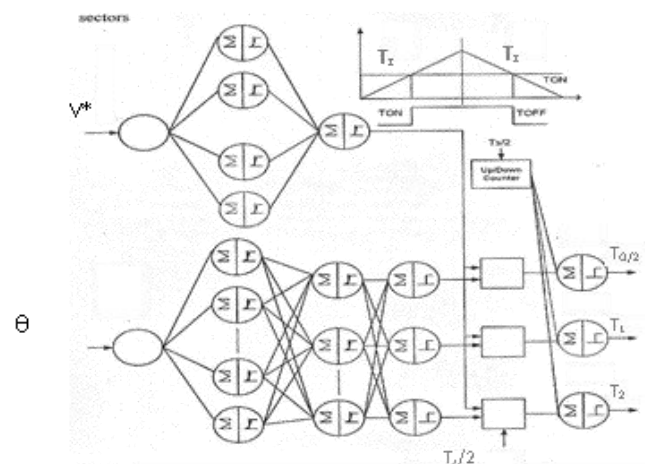


Fig. 14: ANN topology for PWM pulse generating using SVPWM.

The THD ratio of line current and line to line voltage by using NN based SVPWM is shown in table .3.

Table.3: THD ratio of line current and line to line voltage by NN based SVPWM.

Switching frequency(Hz)	Line current THD value(%)	Line-line Voltage THD value(%)
1050	4.308 %	0.4535 %
1450	2.744 %	0.4535 %

Figure. 15 represents the circuit diagram of VSI-HVDC using ANN based SVPWM.

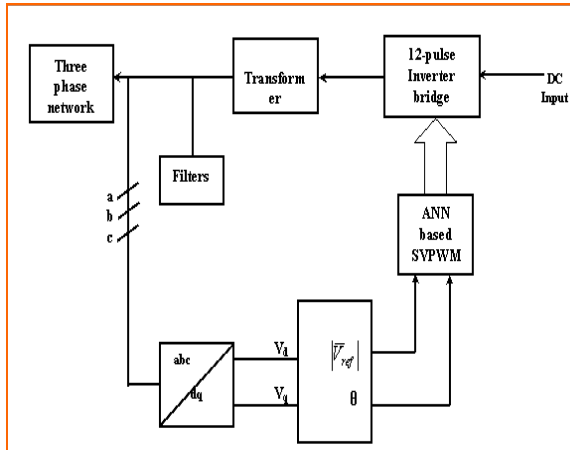


Fig.15: Block diagram represents SVPWM based on ANN with Inverter bridge.

The THD ratio of the line current for switching frequencies 1050Hz and 1450Hz after applying NN is shown in figure. 16.

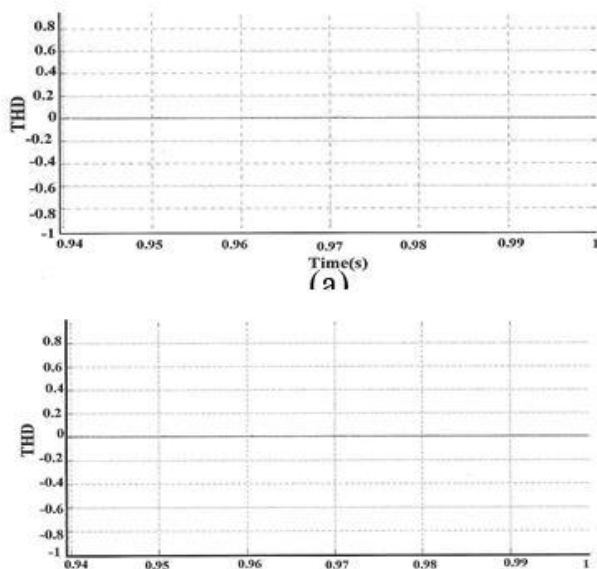


Fig.16: THD ratio of line current in time domain after applying NN based SVPWM.
 (a) at switching frequency (1050Hz).
 (b) at switching frequency (1450Hz).

The THD ratio of the line to line voltage for 1050Hz and 1450Hz switching frequencies after applying NN is shown in figure. 17.

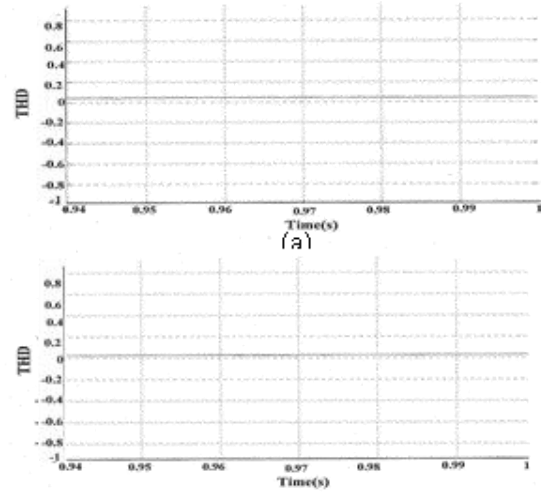


Fig.17: THD ratio of line to line voltage in time domain after applying NN based SVPWM.
 (a) at switching frequency (1050Hz).
 (b) at switching frequency (1450Hz).

IX. CONCLUSION

When using the NN controller based SVPWM the THD value of line current and line to line voltage is improved as a percentage ratio by 74.65% and 78.28% respectively as compared with SVPWM at switching frequency 1050Hz, and these value are improved as a percentage ratio by 68.1% and 65.72% respectively as compared with SVPWM and switching frequency 1450Hz.

At switching frequency 1450Hz the THD ratio is reduced as compared with the switching frequency 1050Hz but the filter losses are increased.

REFERENCES

- [1] Vijay, K. Sood "HVDC and FACTS Controllers" Kluwer power electronics and power editions series, 2004.
- [2] Michael, P., Johnson, B., and B " the ABC of HVDC Transmission Technologies" , power and energy magazine, 5, March/Aplil 2007.
- [3] Padiyar, K.R., Prabhu, N., " Modeling Control Design and Analysis of VSC Based HVDC Transmission" Paper published in POWERCOM 2004, 21-24 November, Singapore.
- [4] Guangkai, Li., et al " Research on Dynamic Characteristics of VSC-HVDC System " power Engineering Society General Meeting , IEEE, 2006.
- [5] Song, R., et al. " VSCs Based HVDC and its Control Strategy" Electric Power Research Institute, Beijing, China, IEEE/PES Transmission and Distribution Conference 2005.
- [6] Vironis, T. D., et al " Optimal Integration Fan Offshore Wind Farm to a Weak AC Grid" IEEE Transactions on Power delivery , 21,2, April 2006.

- [7] Subrata, K.,Joao,O.P.,Bimal, K.,"A Neural-Network-Based Space-Vector PWM Controller for a Three-Level Voltage-Fed Inverter Induction Motor Drive" IEEE Transactions on Industry Applications, 38,3,PP:660-669, 2002.
- [8] Vassilios, G.,A., Georgios, D., D., Nikolas, F., " Recent Advances in High-Voltage Direct-Current Power Transmission Systems",
- [9] Van, H. W., Skudelny, H.C., Stank, G., " Analysis and Realization of a Pulse Width Modulator Based on Voltage Space Vectors" IEEE Transactions Industry Applications Application, 24, 1,pp:1530-1535, 1998.
- [10] Bakhshai,A., Joos, G., Esinoza, J., "Fst Space Vector Moulation Based on a Neurocomuting Digital Signal Processor", in Proc. APEC'97,pp: 872-878, 1997.
- [11] Amitava D., Debasish L and Barnali K" Space Vector PWM Based AC Output Voltage Control of Z- Source Inverter" IEEE Transactions on Industry Applications, January 2, 2010.
- [12] "Pulse-WidthModulation(PWM)Technique"www2.ece.ohio-state.edu/ems/PowerConverter/lect25.ppt
- [13] Abdul Hamid B. and PramodA."An Artificial-Neural – Network- Based Space Vector PWM of a Three-Phase High Power Factor Converter for Power Quality Improvement" IEEE Transactions on Industry Applications, January 2, 2010.
- [14]L. Fausett, "Fundamental of Neural Networks, Architectures, Algorithms and applications", Printice Hall Int. Snc., 1994.

Quantic Analysis of Formation of a Biomaterial of Latex, Retinol, and Chitosan for Biomedical Applications

Karina García-Aguilar^{1,2}, Iliana Herrera-Cantú¹, Erick Pedraza-Gress¹, Lillhian Arely Flores-Gonzalez¹, Manuel Aparicio-Razo^{1,4}, Oscar Sánchez-Parada³, Emmanuel Vázquez-López¹, Juan Jesús García-Mar¹ and Manuel González-Pérez^{1,5}

¹Universidad Popular Autónoma del Estado de Puebla A.C. (UPAEP).

Centro Interdisciplinario De Posgrados (CIP). Posgrado en Ciencias de la Ingeniería Biomédica.

²Instituto Tecnológico Superior de Coatzacoalcos. Académica de Ingeniería Bioquímica

³Escuela de Medicina Universidad Popular Autónoma del Estado de Puebla

⁴Benemérita Universidad Autónoma de Puebla, Facultad de Ciencias de la Electrónica

⁵Sistema Nacional De Investigadores. Nivel 1.

Abstract— *The present work shows the quantum theoretical analysis and practical tests for the formation of a homogeneous mixture with Latex (Lx), Chitosan (Qn) and Retinol (Rl), which work as possible biomaterial for regeneration of epithelial tissue. Lx, Qn, and Rl compounds molecules were designed through Hyperchem to get the coefficient of electrostatic potential calculations. The amounts used to create the biomaterial are minimum depending on the quantities of molecules used in chemical design. A positive calculation was obtained for the reaction of these three compounds and the formation of the biomaterial in physical checking theory etc.*

Keywords— *Quantum analysis, Latex, Chitosan, Retinol, Biomaterial.*

I. INTRODUCTION

Latex Lx is a colloidal aqueous suspension composed of fats, waxes and gummy resins, white and milky in appearance. Rubber (CA) is a hydrocarbon that is suspended in the Lx of trees in tropical and subtropical areas. [1] The CA or rubber is inside the Lx and presents a chemical formula C_5H_8 . The chemical composition of the Lx has oils, sugars, mineral salts, proteins, terpenes, nucleic acids, hydrocarbons, waxes, resins, starch, tannins and balms. It has a neutral pH (7-7.2). Passed between twelve and twenty-four hours since removal, pH drops to 5.0, came the coagulation of the substance when it is located with a pH equal to or less than 4.2. [2]

It is characterized for being a substance insoluble in water, electric and elastic resistance. Most of the Lx is commercial use is extracted from the Syrinx (*Hevea brasiliensis*) and is dedicated to the production of rubber.

The Lx prevents the entry of pathogenic micro-organisms and promotes the healing process when there is a wound. Allergen Lx Hev 2 b with properties β -1, 3-glucanase accelerate the hydrolytic scission of polymers β -1, 3 glucans, basic component of the cell wall of fungi. This protein can prevent fungal infections to the plant through the degradation of the cell wall of fungal pathogens. The allergen in latex Hev b 11 endoquitinasa activity and could participate in the hydrolytic scission of chitin. Another protein that plays a role in defense is the hevamina. Acts by catalyzing the scission of the links β -1, 4-glucosidic linkages of chitin and the peptidoglycans of cell surface. [3]

Studies with Lx only explain their function with patients who have diabetic ulcers. The idea was to implement a template for a biomaterial (Lx) for the control of the pressure of the diabetic foot. [4]

Chitosan (QN) is a polysaccharide that is naturally in the cell walls of some fungi. The main source of production is between alkaline chitin hydrolysis. The presence of groups amines in the polymer chain has made one of the most versatile materials Chitosan by the possibility to perform a wide variety of modifications such as reactions the anchor of enzymes for applications in biomedicine. [5]

(RN) retinol or vitamin A is fat-soluble and necessary is biological processes such as the formation and maintenance of epithelial cells. This vitamin is retinol, the retinal and Retinoic acid. Formed from provitamin beta carotene and other Pro-vitamins in the tract of the large intestine. It is stored in the liver.

The most common natural polymers: silk, collagen, elastin, keratin and Chitosan are discussed as components of mixtures with artificial polymers. [6]

There are two main types of amino acids (AA) which are grouped in essential and non-essential. The essential AA can't be synthesized by the body and to obtain high-protein foods are consumed. The growth, repair and maintenance of cells depends on these amino acids. The AA is present in the body for skin regeneration: Leucine, interacting with isoleucine and valine to promote healing of muscle tissue, skin and bones.

The ETC theory.

The BG is defined as the energy difference between the valence band and the conduction band. In the BG there are no electronic states available; this means that when an electric field is applied, the electrons cannot increase their energy.

In quantum theory, it is known as HOMO and LUMO, and in the old theory they are known as E - and E +. The LUMO is defined as the range of electronic energy that allows acceleration in electrons by the presence of electrical currents and is also called conduction band; HOMO is defined as the highest energy interval that is occupied by electrons in absolute zero value and is called valence band. The HOMO is the most electron-filled orbital, while the LUMO is the orbital that lacks electrons. The HOMO equaled to zero (0 HOMO) is the last layer full of meaning that it is in the last orbital valence orbitals. The LUMO equaled to zero (0 LUMO) is the last layer that lacks electrons.

EP is defined as the total potential energy of the molecule. It is an electrostatic vector field that is defined as the potential that the electron needs to jump the Bohr radius (0.53 Armstrong) by its natural calculated electromotive force (EMF). The negative E value (E-) is the electrostatic potential with negative poles, while the positive and value (E +) is the proton-electron potential [6]. The EP, in other words, means that having 1 EP is having 1 volt for Armstrong. The EP is obtained by the absolute difference of E - and E +.

The ETC is defined as the dimensionless parameter that describes an electrochemical reaction, which is interpreted as the number of times the potential energy needs to jump to the BG. It is calculated by dividing the BG and the EP entirely. That is, if it has a BG of 10 and an etc. of 40, it means that you need 40 times the EP value in EV so that the BG of 10 jumps from the HOMO to LUMO. [7, 8]

II. MATERIALS AND METHODS

SE-PM3 is a program for molecular modeling used by scientists to analyze the composition of molecules for quantum HOMO-LUMO, BG, EP and other properties.

These data are used to form the table where are the ETC's of the interaction between the Lev and the NB.

Table.1: Parameters used for quantum computing molecular orbitals HOMO and LUMO

Parameter	Value	Parameter	Value
Total charge	0	Polarizability	Not
Spin Multiplicity	1	Geometry Optimization Algorithm	Polak-Ribière (Conjugate Gradient)
Spin Pairing	RHF	Termination condition RMS gradient of	0.1 Kcal/Amol
State Lowest Convergent Limit	0.01	Termination condition or	maximum 1000 cycles
Interaction Limit	50	Termination condition or	In vacuo
Accelerate Convergence	Yes	Screen refresh period	1 cycle

The Software Hyperchem Professional performs Molecular modeling and analysis of the Lx, Qn and, RI (Hyperchem, hypercube, Multi in for Windows, series 12-800-1501800080)The font size for heading is 11 points bold face and subsections with 10 points and not bold. Do not underline any of the headings, or add dashes, colons, etc.

Table.2: Parameters used for access the map of the electrostatic potential of the molecules

Parameter	Value	Parameter	Value
Molecular Property	Property Electrostatic Potential	Contour Grid increment	0.05
Representation	3D Mapped Isosurface	Mapped Function Options	Default
Isosurface Grid: Grid Mesh Size	Coarse	Transparency level	A criteria
Isosurface Grid: Grid Layout	Default	Isosurface Rendering: Total charge density contour value	0.015
contour Grid: Starting Value	Default	Rendering Wire Mesh	

III. RESULTS AND DISCUSSIONS

Values are obtained from the simulation of molecules of the compounds in the software HYPERCHEM. The software calculates the bandgap, potential energy and energy transfer coefficient data (for its acronym in English, BG, the EP and the ETC). When designing the molecule gets the values of e- and e+ (HOMO-LUMO) in value to zero and a density of 0.015. Cross compounds bands are taking the values of the initial calculation and swapping it with another compound interest. Under the cross-band ETC is the value of the more reactive compound.

Table.3: Distribution of values of three compounds to analyze

Su bs	HOM O	LUM O	BG	E-	E +	EP	ETC
Lx	- 9.351	0.278	9.62 9	- 0.0 03	0.1 04	0. 107	89.9 91
RI	- 8.228	- 0.483 4	7.74 46	- 0.1 1	0.1 83	0.2 93	26.4 32
QN	- 9.726	1.662	11.3 88	- 0.1 14	0.3 28	0.4 42	25.7 64

Table.4: Cross-band values

Su bs	HO MO	LU MO	BG	E-	E +	EP	ET C
Lx -RI	-951	- 0.483 4	8.86 76	- 0.0 03	0.1 83	0.186	47.6 75
RI- Lx	- 8.228	0.278	8.50 6	- 0.1 1	0.1 04	0.214	39.7 48
Lx - Qn	- 9,351	1.662	11.0 13	- 0.0 03	0.3 28	0.331	33.2 72
Qn - Lx	- 9.726	0.278	10.0 04	- 0.1 14	0.1 83	0.297	33.6 84
RI- Qn	- 8.228	1.662	9.89	- 0.1 1	0.3 28	0.438	22.5 80
Qn -RI	- 9.726	- 0.483 4	9.24 26	- 0.1 14	0.1 83	0.297 (h)	31.1 20

The compounds work together to form a mixture homogeneous. Tables 3 and 4 show individual values and cross compounds to form the desired product. Displays

the value of smaller ETC that these compounds produced the desired reaction.

Table.5: Values of pairs and trios of compounds

Subs	HO MO	LU MO	BG	E-	E +	EP	ET C
LX- RL	- 9,351	- 0.48 34	8.86 76	- 0.0 03	0.1 83	0.1 86	47.6 75
RL- LX	- 8.228	0.27 8	8.50 6	- 0.1 1	0.1 04	0.2 14	39.7 48
LX- QN	- 9,351	1.66 2	11.0 13	- 0.0 03	0.3 28	0.3 31	33.2 72
QN- LX	- 9.726	0.27 8	10.0 04	- 0.1 14	0.1 83	0.2 97	33.6 84
RL- QN	- 8.228	1.66 2	9.89	- 0.1 1	0.3 28	0.4 38	22.5 80
QN- RL	- 9.726	- 0.48 34	9.24 26	- 0.1 14	0.1 83	0.2 97	31.1 20
QN- RL/L X	- 9.726	0.27 8	10.0 04	- 0.1 14	0.1 04	0.2 18	45.8 90
LX/Q N-RL	- 9,351	- 0.48 34	8.86 76	- 0.0 03	0.1 83	0.1 86	47.6 75
RL- QN/L X	- 8.228	0.27 8	8.50 6	- 0.1 1	0.1 04	0.2 14	39.7 48
LX/R L-QN	- 9.351	1.66 2	11.0 13	- 0.0 03	0.3 28	0.3 31	33.2 72

Theoretical evidence for quantum analysis, show that the combination of compounds that interact with the AA (amino acids) that participate in the regeneration of epithelial tissue present in human skin and muscles is possible.

The Lx is the basis of this new biomaterial in combination with the substrates that held the interaction and the possible regeneration of epithelial tissue. RI and Qn compounds have lower value ETC so that it concluded a high chemical reaction between the two.

Table 5 shows combinations of three compounds (Lx, RI, Qn) for its combination with quantum chemistry obtaining a minor etc.

The Lx is the basis of this new biomaterial in combination with the substrates that held the interaction and the

possible regeneration of epithelial tissue. RI and Qn compounds have lower value ETC so that it concluded a high chemical reaction between the two.

Table.6: Interaction of reducing and oxidizing component of Lx and RI

	Reduc er	Oxidiz er	Interacti on	ETC	Limi ts
Pure Substances	LX	LX	LX - Lx	89.9 90	Top
	RL	RL	RL - RI	26.4 32	Low er
Cross band	LX	RL	LX - RI	41.6 31	
	RL	LX	RL - Lx	39.5 62	

Graphs of quantum well (figures 1) have two lines that represent the upper and lower limits (greater ETC). Black dots plotted are the percentage of probability of occurring a chemical reaction with the combination of two of the three compounds.

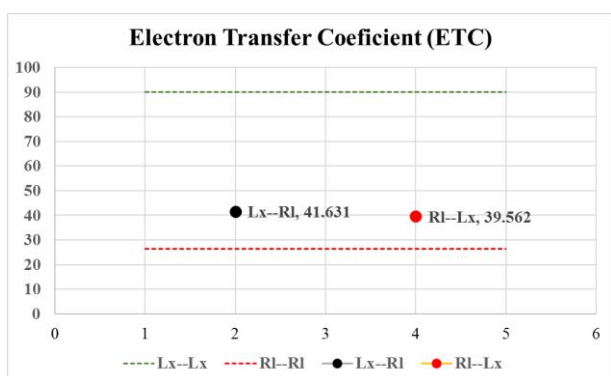


Fig.1: Quantum well, Lx-RI ETC interaction

Tables 6 and 7 show interactions between reducing and oxidizing compounds for the upper and lower limits and graphing quantum wells etc.

Table.7: Interaction of the component reducing and oxidizing of Lx and Qn

	Reduc er	Oxidiz er	Interacti on	ETC	Limi ts
Pure Substances	LX	LX	LX - Lx	89.9 9	Top
	Qn	Qn	Qn - Qn	26.4 32	Low er
Cross band	LX	Qn	LX - Qn	33.2 71	
	Qn	LX	Qn - Lx	33.6 83	

Figure 1 shows an average probability of interaction between the two compounds (50% probability). Figure 2 shows the same probability of interaction.

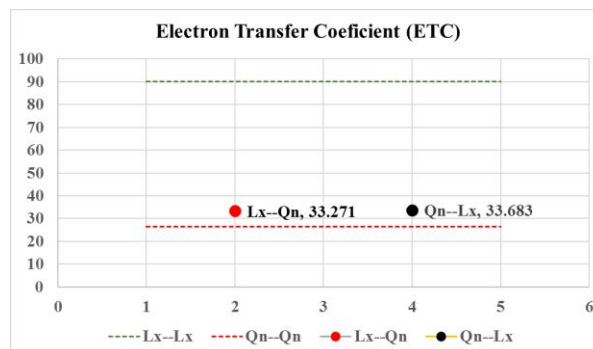


Fig.2: Quantum well, the interaction between Lx and Qn ETC



Fig.3: Emptying of Lx, Qn and RI for field testing on lab in the formation of a new biomaterial

In Figure 3 are observed practices carried out in the laboratory to check the quantum theoretical calculated previously.

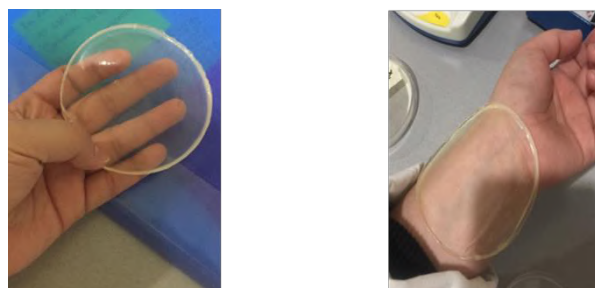


Fig.4: Form of Biomaterial with Lx, Qn, and RI

Figure 4 shows laboratory tests proving that quantum calculation (calculation of high chemical reaction between compounds) ETC is the biomaterial.

Table 8 shows the interactions of mixtures of the biomaterial the AA main compounds necessary for the regeneration of epithelial and muscle tissue. Minor interactions are likely chemical reaction between the mixtures working as oxidants and antioxidants. Obtaining ETC describes that the reaction will be likely to benefit from the growth of epithelial cells in patients who have superficial wounds.

Table.8: Pairs of AA with mixtures of Lx, Qn, and Rl

N o	Red ucer	Oxi dize r	HO MO	LU MO	B G	E -	E +	E P	E T C
1	QN- RL/ LX	LEU - GLY	- 9.73	0.9 0	10. 63	- 0. 1 1	0. 1 6	0. 2 7	38 .9
2	QN- RL/ LX	LEU - LYS	- 9.73	0.9 4	10. 67	- 0. 1 1	0. 1 9	0. 3 1	34 .5
3	LEU - LYS	QN- RL/ LX	- 9.64	0.2 7	9.9 2	- 0. 1 3	0. 1 0	0. 2 3	43 .1
4	QN- RL/ LX	ILE- GLN	- 9.73	0.7 5	10. 48	- 0. 1 1	0. 1 9	0. 3 1	34 .2
5	QN- RL/ LX	ILE- LYS	- 9.73	0.9 4	10. 67	- 0. 1 1	0. 1 9	0. 3 1	34 .5
6	QN- RL/ LX	GLY -ILE	- 9.73	0.9 7	10. 70	- 0. 1 1	0. 1 9	0. 3 0	35 .4
7	QN- RL/ LX	GLY - GLN	- 9.73	0.7 5	10. 48	- 0. 1 1	0. 1 9	0. 3 1	34 .2
8	QN- RL/ LX	LYS -ILE	- 9.73	0.9 7	10. 70	- 0. 1 1	0. 1 9	0. 3 0	35 .4
9	QN- RL/ LX	VAL - GLN	- 9.73	0.7 5	10. 48	- 0. 1 1	0. 1 9	0. 3 1	34 .2
10	QN- RL/ LX	VAL -ILE	- 9.73	0.9 7	10. 70	- 0. 1 1	0. 1 9	0. 3 0	35 .4
11	QN- RL/ LX	VAL - LYS	- 9.73	0.9 4	10. 67	- 0. 1 1	0. 1 9	0. 3 1	34 .5
12	LEU - GL N	LX/ RL- QN	- 9.64	1.6 6	11. 31	- 0. 1 3	0. 3 3	0. 4 5	24 .9

13	LEU - GL Y	LX/ RL- QN	- 9.64	1.6 6	11. 31	- 0. 1 3	0. 3 3	0. 4 5	24 .9
14	LEU - LYS	LX/ RL- QN	- 9.64	1.6 6	11. 31	- 0. 1 3	0. 3 3	0. 4 5	24 .9
15	ILE- LYS	LX/ RL- QN	- 9.87	1.6 6	11. 53	- 0. 1 3	0. 3 3	0. 4 5	25 .1
16	GL Y- ILE	LX/ RL- QN	- 9.90	1.6 6	11. 56	- 0. 1 4	0. 3 3	0. 4 6	24 .9
17	LYS - GL Y	LX/ RL- QN	- 9.52	1.6 6	11. 18	- 0. 1 3	0. 3 3	0. 4 5	24 .6
18	VA L- GL N	LX/ RL- QN	- 9.91	1.6 6	11. 58	- 0. 1 3	0. 3 3	0. 4 6	25 .2

IV. CONCLUSION

1. The Lx is highly reaccionable with compounds Qn and Rl.
2. The combination of the three compounds (Lx, Qn, Rl) is possible by low levels that present etc.
3. The highest interaction is with the Qn and Rl when working as antioxidant and oxidant respectively.
4. By combining three compounds is calculated an etc. of 33.2719033 when the Lx works as a reducing agent.
5. The compounds shown in its quantum wells High solubility and formation of striation.
6. Experiments prove the quantum chemistry calculations.
7. Forms a patch of Lx, Qn, and Rl.
8. The ETC child occur with Rl-Qn 22.57.
9. Lx, Qn, and Rl compounds interact with the AA of epithelial and muscle tissue.
10. The combination of the three main compounds for the biomaterial have high reaction with the AA.

REFERENCES

- [1] Narciso, A. R. M. (1974). The exploitation of rubber in Mexico and its use in the world.
- [2] Carreon Blaine, Emilie a. (2006). The olli in the plastic Aztec: the use of rubber in the 16th century. UNAM. ISBN 970-32-2200-5.

- [3] Fireman, Philip. Atlas of Allergy and Immunology clinic. Elsevier Mosby. p-261.
- [4] Rosa, S. D. S. R. F., do Carmo Reis, M., Rosa, M. F. F., Colon, D., dos Reis, C. A., & Balthazar, J. M. (2015). Use of Natural Latex as a Biomaterial for the Treatment of Diabetic Foot-A New Approach to Treating Symptoms of Diabetes Mellitus. In Topics in Public Health. InTech.
- [5] Velasquez, C. (2003). Some applications of chitosan in aqueous systems. *Revista Iberoamericana of polymers*, 4 (2), 91.
- [6] Sionkowska, a. (2011). Current research on the blends of natural and synthetic polymers as new biomaterials. *Progress in Polymer Science*, 36 (9): 1254-1276.
- [7] Mondragon-jimenez, Jesus Francisco, et al. interaction of methylenedioxymethamphetamine vs. neurotransmitters and the relationship by the quantum method. 2017
- [8] Gonzalez-perez, m. chemical-quantum analysis of the aggressiveness of glucose and its appeasement with ATP inside the cell and water as an excellent antioxidant, 2017.
- [9] Firmin H. Aikpo, Miriac Dimitri S. Ahouanse, Lucien Agbandji, Patrick A. Etorh, Christophe S. Houssou(2017).Assessment of contamination of soil by pesticides in Djidja's cotton area in Benin. *International Journal of Advanced Engineering Research and Science* (ISSN : 2349-6495(P) | 2456-1908(O)),4(7), 001-005.
<http://dx.doi.org/10.22161/ijaers.4.7.1>
- [10] Perfect, T. J., & Schwartz, B. L. (Eds.) (2002). *Applied metacognition* Retrieved from <http://www.questia.com/read/107598848>
- [11] Myers, D. G. (2007). *Psychology*(1st Canadian ed.). New York, NY: Worth.
- [12] Cognition.(2008). In *Oxford reference online premium dictionary*. Retrieved from <http://www.oxfordreference.com>
- [13] Blue, L. (2008, March 12).Is our happiness preordained? [Online exclusive]. *Time*. Retrieved from <http://www.time.com/time/health>
- [14] J. Clerk Maxwell, *A Treatise on Electricity and Magnetism*, 3rd ed., vol. 2. Oxford: Clarendon, 1892, pp.68–73.
- [15] I. S. Jacobs and C. P. Bean, "Fine particles, thin films and exchange anisotropy," in *Magnetism*, vol. III, G. T. Rado and H. Suhl, Eds. New York: Academic, 1963, pp. 271–350.
- [16] K. Elissa, "Title of paper if known," unpublished.
- [17] R. Nicole, "Title of paper with only first word capitalized," *J. Name Stand. Abbrev.*, in press.